List of Participants

Alvarez Marcelo	Kavli, Stanford University (USA) malvarez@slac.stanford.edu
Ames Susan	Oxford University (UK) sames@astro.ox.ac.uk
Barkana Rennan	Tel Aviv University (Israel) barkana@wise.tau.ac.il
Becker George	Carnegie Observatories (USA) gdb@ociw.edu
Begum Ayesha	IoA, Cambridge (UK) ayesha@ast.cam.ac.uk
Bekki Kenji	UNSW (Australia) bekki@phys.unsw.edu.au
Bianchi Simone	INAF/IRA, Firenze (Italy) sbianchi@arcetri.astro.it
Blitz Leo	UC Berkeley (USA) blitz@berkeley.edu
Bolatto Alberto	UC Berkeley (USA) bolatto@berkeley.edu
Bolton James	MPA, Garching (Germany) jsb@mpa-garching.mpg.de
Braine Jonathan	Observatoire de Bordeaux (France) braine@obs.u-bordeaux1.fr
Braun Robert	CSIRO-ATNF (Australia) robert.braun@csiro.au
Briggs Frank	Mount Stromlo Observatory (Australia) fbriggs@mso.anu.edu.au
Bruscoli Marialuce	INAF/IRA, Firenze (Italy) bruscoli@arcetri.astro.it
Burkert Andreas	University of Munich (Germany) burkert@usm.uni-muenchen.de
Cantalupo Sebastiano	ETH Zurich (Switzerland) cantalupo@phys.ethz.ch
Carilli Chris	NRAO (USA) ccarilli@nrao.edu

Choudhury Tirthankar	IoA, Cambridge (UK) chou@ast.cam.ac.uk
Chung Aeree	NRAO/UMass achung@astro.umass.edu
Ciardi Benedetta	MPA, Garching (Germany) ciardi@mpa-garching.mpg.edu
Combes Francoise	Observatoire de Paris (France) francoise.combes@obspm.fr
Cooke Jeff	UC Irvine (USA) cooke@uci.edu
Corbelli Edvige	INAF/Arcetri Astrophysical Observatory (Italy) edvige@arcetri.astro.it
Cristiani Stefano	INAF/Trieste Astronomical Observatory (Italy) cristiani@oats.inaf.it
Crociani Daniela	University of Bologna (Italy) daniela.crociani2@studio.unibo.it
Dall'Aglio Aldo	AIP (Germany) adaglio@aip.de
de Bruyn Ger	ASTRON & Kapteyn Institute (The Netherlands) ger@astron.nl
di Serego Alighieri Sperello	INAF/Arcetri Astrophysical Observatory (Italy) sperello@arcetri.astro.it
Disney Michael	Cardiff University (UK) mjdisney@gmail.com
D'Odorico Valentina	INAF/Trieste Astronomical Observatory dodorico@oats.inaf.it
Ellis Richard	Caltech (USA) rse@astro.caltech.edu
Ellison Sara	University of Victoria (Canada) sarae@uvic.edu
Fan Xiaohui	University of Arizona (USA) fan@as.arizona.edu
Ferrara Andrea	SISSA/ISAS (Italy) ferrara@sissa.it
Fox Andrew	IAP (France) fox@iap.fr
Fraternali Filippo	University of Bologna (Italy) filippo.fraternali@unibo.it

Gallerani Simona	SISSA/ISAS (Italy) galleran@sissa.it
Garcia-Appadoo Diego	AIfA, Bonn (Germany) dgarcia@astro.unibonn.de
Giovanelli Riccardo	Cornell University (USA) rg39@cornell.edu
Grossi Marco	INAF/Arcetri Astrophysical Observatory marco.grossi@arcetri.astro.it
Haiman Zoltan	Columbia University (USA) zoltan@astro.columbia.edu
Heitsch Fabian	University of Michigan (USA) fheitsch@umich.edu
Hennebelle Patrick	Observatoire de Paris (France) patrick.hennebelle@ens.fr
Hoeft Matthias	International University of Bremen (Germany) m.hoeft@iu-bremen.de
Hunter Deidre	Lowell Observatory (USA) dah@lowell.edu
Inutsuka Shu-ichiro	Kyoto University (Japan) inutsuka@tap.scphys.kyoto-u.ac.jp
Kanekar Nissim	NRAO (USA) nkanekar@aoc.nrao.edu
Kilborn Virginia	Swinburne University (Australia) vkilborn@swin.edu.au
Klein Uli	AIfA, Bonn (Germany) uklein@astro.unibonn.de
Koribalski Baerbel	CSIRO-ATNF (Australia) baerbel.koribalski@csiro.au
Lah Philip	Mount Stromlo Observatory (Australia) plah@mso.anu.edu.au
Leroy Adam	MPIA Heidelberg (Germany) leroy@mpia-hd.mpg.de
Lonsdale Colin	MIT Haystack Observatory (USA) cjl@haystack.mit.edu
Malhotra Sangeeta	Arizona State University (USA) sangeeta.malhotra@asu.edu
Maselli Antonella	MPA Garching (Germany) maselli@mpa-garching.mpg.de

Mesinger Andrei	Yale University (USA) andrei.mesinger@yale.edu
Meurer Gerhardt	Johns Hopkins University (USA) meurer@pha.jhu.edu
Naoz Smadar	Tel Aviv University (Israel) smadar@wise.tau.ac.il
Nestor Daniel	IoA, Cambridge (UK) dbn@ast.cam.ac.uk
Noterdaeme Pasquier	ESO (Chile) pnoterda@eso.org
Oh Peng	UC Santa Barbara (USA) peng@physics.ucsb.edu
Omar Amitesh	Leiden University (The Netherlands) aomar@strw.leidenuniv.nl
Omukai Kazuyuki	NAO (Japan) omukai@th.nao.ac.jp
Oosterloo Tom	ASTRON (The Netherlands) oosterloo@astron.nl
Palla Francesco	INAF/Arcetri Astrophysical Observatory (Italy) palla@arcetri.astro.it
Pen Ue-Li	CITA (Canada) pen@cita.utoronto.ca
Peroux Celine	Observatoire de Marseilles (France) celine.peroux@oamp.fr
Peterson Jeff	Carnegie Mellon University (USA) jbp@cmu.edu
Petitjean Patrick	IAP (France) petitjean@iap.fr
Petrovic Nada	UC Santa Barbara (USA) petrovic@physics.ucsb.edu
Pillepich Annalisa	ETH Zurich (Switzerland) annalisa.pillepich@phys.ethz.ch
Popping Attila	Kapteyn Astronomical Institute (The Netherlands) popping@astro.rug.nl
Prochaska Jason X.	UCO/Lick Observatory (USA) xavier@ucolick.org
Putman Mary	University of Michigan (USA) mputman@umich.edu

Rakic Olivera	Leiden University (The Netherlands) rakic@strw.leidenuniv.nl
Rao Sandhya	University of Pittsburgh (USA) rao@everest.phyast.pitt.edu
Razoumov Alexei	Saint Mary's University (Canada) razoumov@ap.smu.ca
Rhoads James	Arizona State University (USA) James.Rhoads@asu.edu
Ricotti Massimo	University of Maryland (USA) ricotti@astro.umd.edu
Rosolowsky Erik	CfA Harvard (USA) erosolow@cfa.harvard.edu
Ryan-Weber Emma	IoA Cambridge (UK) eryan@ast.cam.ac.uk
Sabatini Sabina	INAF/Rome Astronomical Observatory (Italy) sabina.sabatini@oa-roma.inaf.it
Salpeter Edwin	Cornell University (USA) ees12@cornell.edu
Salvadori Stefania	SISSA/ISAS (Italy) salvas@sissa.it
Salvati Marco	INAF/Arcetri Astrophysical Observatory (Italy) salvati@arcetri.astro.it
Sancisi Renzo	INAF/Bologna Astronomical Observatory (Italy) sancisi@bo.astro.it
Scaramella Roberto	INAF/Rome Astronomical Observatory (Italy) kosmobob@oa-roma.inaf.it
Schaye Joop	Leiden Observatory (The Netherlands) schaye@strw.leidenuniv.nl
Schneider Raffaella	INAF/Arcetri Astrophysical Observatory (Italy) raffa@arcetri.astro.it
Schneider Steve	University of Massachusetts (USA) schneider@astro.umass.edu
Semelin Benoit	Observatoire de Paris (France) benoit.semelin@obspm.fr
Shapiro Paul	University of Texas (USA) shapiro@astro.as.utexas.edu
Siana Brian	Spitzer Science Center (USA) bsiana@ipac.caltech.edu

Simon Josh	Caltech (USA) jsimon@astro.caltech.edu
Staveley-Smith Lister	University of Western Australia (Australia) lister.staveley-smith@uwa.edu.au
Susa Hajime	Rikkyo University (Japan) susa@rikkyo.ac.jp
Thilker David	Johns Hopkins University (USA) dthilker@pha.jhu.edu
Tripp Todd	University of Massachusetts (USA) tripp@astro.umass.edu
Turnshek David	University of Pittsburgh (USA) turnshek@pitt.edu
Valdes Marco	SISSA/ISAS (Italy) valdes@sissa.it
van Gorkom Jacqueline	Columbia University (USA) jvangork@astro.columbia.edu
van Woerden Hugo	Kapteyn Astronomical Institute (The Netherlands) hugo@astro.rug.nl
Verheijen Marc	Kapteyn Astronomical Institute (The Netherlands) verheyen@astro.rug.nl
Viel Matteo	INAF/Trieste Astronomical Observatory (Italy) viel@oats.inaf.it
Vladilo Giovanni	INAF/Trieste Astronomical Observatory (Italy) vladilo@oats.inaf.it
Wakker Bart	University of Wisconsin (USA) wakker@astro.wisc.edu
Wolfe Arthur	UC San Diego (USA) awolfe@ucsd.edu
Worseck Gabor	AIP (Germany) gworseck@aip.de
Wyithe Stuart	University of Melbourne (Australia) swyithe@physics.unimelb.edu.au
Zaroubi Saleem	Kapteyn Astronomical Institute (The Netherlands) saleem@astro.rug.nl
Zibetti Stefano	MPE-Garching (Germany) szibetti@mpe.mpg.de
Zwaan Martin	ESO (Germany) mzwaan@eso.org

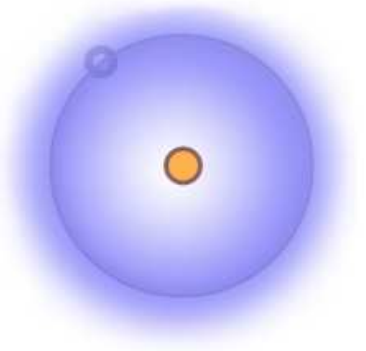

The hydrogen atom is the main constituent of baryonic matter in our Universe and cosmic evolution largely relies on its ability to absorb/emit radiation and to form heavier elements and molecules. From the epoch of recombination to today's galaxies, hydrogen atoms had gone through several thermal phases as bound structures developed and stars began to shine. The aim of the Conference is to bring together scientists to discuss at various epochs and in various structures the dominance of the ionized, neutral and molecular hydrogen and the interplay between these phases and light. In view of Future Instrumentation, capable to enlight our knowledge of HI Survival Through Cosmic Times it is important to outline the current state of art.

The meeting takes place in one of the most beautiful spots of the Tuscan countryside, far from the noise and haste of everyday life. Located south of Siena, the Abbazia di Spineto and its rural environs is still one of the few unspoiled venues in Tuscany, ideal for a few days of retreat and discussion. The central Abbey is surrounded by several old houses and the whole complex provides lodging facilities for all the participants. Common areas in the rural houses and in the Abbey definetely favour the interaction among subgroups and at the same time offer a variety of stimulating enviroments.

The Conference starts on the evening of June 10^{th} and ends on June 15^{th} 2007. This book summarizes the scientific goals of each talk or poster presented at the HI Survival Conference, related to one or more of the following main topics of the programme:

- HI in the dark ages
  - 21-cm line absorption/emission
  - imprints of reionization process on the 21-cm signal
  - 21-cm experiments

- Reionization epoch
  - nature of ionizing sources
  - the physics of reionization
  - detecting the epoch of reionization

- Radiative feedback
  - H_2 photodissociation
  - photoionization/photoevaporation
  - preheating

- Gas at intermediate redshifts
  - cosmic evolution with the ultraviolet background
  - from WHIM to molecular gas
  - correlation between absorbers and galaxies

- Dwarf satellites and dark galaxies
  - theoretical predictions and observational census
  - gas survival in small potential wells at various epochs
  - the HI mass function

- Local galaxies and the IGM connection
  - dark and visible matter in outer disks
  - where do galaxies end
  - gas accretion and outflows

- Driving molecule formation
  - HII/HI/H_2 mass budget along the Hubble sequence and the star-gas cycle
  - rotation & turbulence: triggering molecular clouds formation
  - large and small scale properties of molecular clouds

- Future instruments

We are very grateful to all of you who made possible the printout of this book before the Conference opening. We hope it will stimulate discussions and interactions among all participants who made the effort to come to Spineto from all over the World.

Simone Bianchi, Edvige Corbelli, Raffaella Schneider

The Scales and Topology of Reionization

Marcelo Alvarez[1], Paul Shapiro[2], Ilian Iliev[3], Garrelt Mellema[4], and Ue-Li Pen[3]

[1]Kavli Institute for Particle Astrophysics and Cosmology, Stanford University, USA
[2]Department of Astronomy, University of Texas at Austin, USA
[3]CITA, University of Toronto, Canada
[4]Department of Astronomy, Stockholm University, Sweden

Context: Cosmic reionization is closely related to the earliest structure and galaxy formation. Much progress has been made recently both observationally and theoretically. In the future, 21-cm surveys such as LOFAR, MWA, and SKA, as well as very high-redshift galaxy surveys carried out using planned and existing observational facilities promise to open new windows into the reionization epoch. The prospect of observing the topology of reionization on large scales serves as the primary motivation for the development of a theory of its large scale structure, and numerical simulations can play a vital complementary role to analytical models.

Aims: We use large-scale N-body and radiative transfer simulations of reionization to calculate its characteristic scales and topology. Our aim is to investigate their dependence on some basic properties of the sources of reionization and the intergalactic medium, such as the halo mass-to-light ratio, susceptibility of haloes to positive and negative feedback, and the clumping factor. We characterize the scales and topology of reionization using the size distribution of H II regions, the power spectrum of ionized gas, and genus statistics of the ionization field.

Results: We find a characteristic size of order comoving Mpc for ionized regions near the half-ionized epoch, roughly consistent with previous analytical models, although ambiguities remain in how to define the size of an H II region. Suppression of ionizing sources within ionized regions, as well as clumping, reduce the size and increase the number of H II regions, although the effect is modest, reducing the typical radii of H II regions by factors of a

few. The ionization power spectrum is found to exhibit a peak at wavenumbers which correspond to a spatial scale of order comoving Mpc, consistent with the typical size of H II regions. We also find that density and ionized fraction are correlated on large scales, regardless of the degree of clumping and suppression, validating the "inside-out" picture of reionization. Finally, the genus of the ionization field proves to be much more sensitive to source suppression and clumping than the size distributions or power spectra.

21-cm Emission from the Era of the First Galaxies

Rennan Barkana[1], Smadar Naoz[1], Avi Loeb[2]

[1] School of Physics and Astronomy, The Raymond and Beverly Sackler Faculty of Exact Sciences, Tel Aviv University, Tel Aviv 69978, ISRAEL
[2] Astronomy Department, Harvard University, 60 Garden Street, Cambridge, MA 02138, USA

Context: A new generation of radio telescopes is being built that is expected to measure the cosmic distribution of atomic hydrogen using the 21-cm line of hydrogen. The best prospects are to measure the substantial large-scale fluctuations caused by ionization fluctuations during cosmic reionization. Since detailed maps will be difficult to extract due to noise and foreground emission, efforts have focused on a statistical detection of the 21-cm fluctuations. The two-point correlation function is usually considered, since it is the most natural statistic both to predict and to measure. Due to the limitations on current numerical simulations, it is useful to develop analytical calculations of 21-cm statistics that capture the main physics and allow a thorough investigation of the dependence of the observables on the various input parameters.

During cosmic reionization, the 21-cm fluctuations are driven by ionization fluctuations which are highly non-Gaussian, and thus more information can be extracted than just the correlation function. The one-point probability distribution function (PDF) of the 21-cm brightness temperature T_b at a point has been previously suggested and explored.

Aims: Our aim was first to develop a self-consistent analytical model for the correlated distribution of ionization and density at two points, as a function of their separation. We then applied this model to calculate two-point statistics. In particular, we produced the first self-consistent analytical expression for the two-point correlation function, which had previously been calculated more schematically. In addition to the two-point correlation function, which is a 1-D function of separation, and the PDF, which is a 1-D function of T_b, we looked for a two-dimensional function that would generalize both and yield additional information. We considered the PDF of

the difference of the 21-cm brightness temperature between two points, as a function of their separation. While the usual correlation function is determined by a complicated mixture of contributions from density and ionization fluctuations, we found that the difference PDF holds the key to separately measuring statistics of the ionization distribution.

21-cm fluctuations are driven by radiation from galaxies, not only during reionization but also much earlier, when fluctuations in the Lyman-α radiation emitted by the galaxies produced 21-cm fluctuations. Thus, we first investigated halo formation at high redshift, which differs from the usual redshift range due to the aftereffects of the baryon-photon coupling prior to recombination, and due to the ongoing influence of baryonic pressure from the Compton-heated gas. In the linear regime we investigated the relation between the baryon and the dark matter fluctuations, and in the non-linear regime we investigated the effect on the formation times of various halos. In the context of Lyman-α fluctuations, we also investigated previously neglected physical effects on the radiation, which should make it easier for future observations to detect the signal from these early galaxies.

Results: Regarding the suppression of baryon density fluctuations compared to the dark matter at high redshifts, we found that it occurs on significantly lower mass scales than suggested by previous calculations. This reduction in the characteristic mass scale is a result of including the fact that the baryons have smoother initial conditions than the dark matter, due to the aftereffects of the coupling with the radiation before recombination. In particular, this implies that the fraction of the cosmic gas that is in minihalos is significantly higher than previously expected.

Figure 1 shows the 21-cm power spectrum from the analytical model of Barkana (2007, MNRAS, 376, 1784). This model also allowed an analytical calculation of the 21-cm difference PDF. We explored the dependence of the difference PDF on a number of the input parameters (including the redshift and the observational resolution). We also considered robust ways to extract information from the difference PDF without requiring an accurate measurement of the full PDF. We found that even a rough measurement of the difference PDF should suffice for measuring some quantities that depend directly only on ionization statistics, not mixed in with the value of the density as in the 21-cm correlation function.

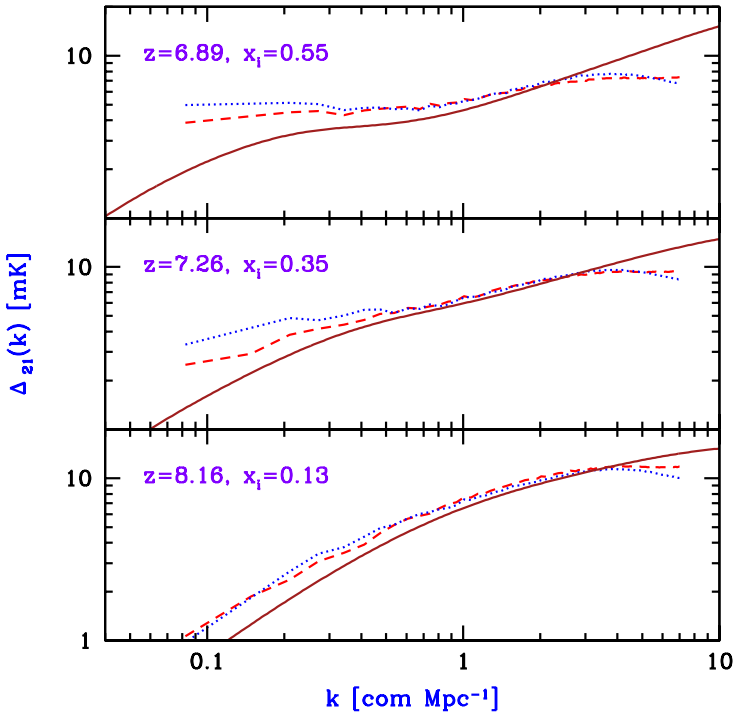

Figure 1: 21-cm power spectrum, comparing the analytical model of Barkana (2007, MNRAS, 376, 1784) (solid curves) to those from the simulation of Zahn et al. (2007, ApJ, 654, 12) (dashed curves) and from their numerical scheme based on the final ionizing sources (dotted curves). The results are shown at several different redshifts, as indicated in each panel. At each redshift z, the value of the efficiency in the analytical model is adjusted in order to match the mean global ionized fraction x_i from the simulation. While the model and the numerical scheme include some approximations and the simulation has resolution and size limitations, they all show the same overall trend: as reionization advances, the power spectrum flattens, with the increased power on large scales ($k \sim 0.1$ Mpc^{-1}) reflecting the increasing size of bubbles that are due to clustered groups of galaxies.

The High-Resolution Case Against Late Reionization (and for Radiative Transfer)

George Becker[1], Michael Rauch[1], Wallace Sargent[2]

[1] Observatories of the Carnegie Institute of Washington; Pasadena, CA, USA
[2] California Institute of Technology; Pasadena, CA, USA

Context: The timing and mechanisms of cosmic hydrogen reionization remain an open issue. Rapid evolution in the mean transmitted Lyα flux at $z > 5.7$, culminating in the appearance of extended Gunn-Peterson troughs in the spectra of the highest-redshift QSOs, has been interpreted as an indication that reionization may have ended as late as $z \sim 6$ (Becker et al. 2001; White et al. 2003; Fan et al. 2006). In contrast, isolated Lyα and Lyβ transmission spikes in the spectrum of the highest-redshift QSO indicate that at least some regions of the $z \sim 6$ IGM are already highly ionized (White et al. 2005; Oh & Furlanetto 2005). Even complete absorption of Lyman-series photons can at best constrain the IGM neutral fraction to $\chi_{\rm H\ I} > 10^{-3}$ (Fan et al. 2002). A large drop in the observed number of Lyα-emitting galaxies (LAEs) at $z > 6$ would more strongly suggest that the IGM was becoming significantly neutral. The luminosity function of LAEs remains constant from $z \sim 5.7$ to 6.5, however, or may at most decline slightly (Malhotra & Rhoads 2004; Stern et al. 2005; Kashikawa et al. 2006). Additional arguments can been made about the thermal history of the IGM (Theuns et al. 2002; Hui & Haiman 2003) or the apparent size of the transmission regions around $z \sim 6$ QSOs (e.g., Mesinger & Haiman 2004; Wyithe & Loeb 2004). The evolution of the Lyα forest, however, remains the strongest evidence for late reionization.

Aims: An important check on the Lyα forest results is whether the simulations being used to convert Lyα fluxes into H I ionization rates produce not only the correct *mean* flux, but the correct *distribution* of fluxes. At $z \sim 6$, the little remaining transmitted flux in the forest samples only the low-end tail of the optical depth distribution, which corresponds to voids in the IGM. Computing the hydrogen ionization state in large cosmological simulations often requires making assumptions about the distributions of gas temperatures and ionization rates. Any errors in these assumptions may have

potentially large effects on the transmissivity of the voids, and hence on the ionization rates inferred from the mean transmitted flux at high redshift.

We use the full Lyα flux distribution to test whether a commonly-used cosmological simulation (along with the associated assumptions about the IGM temperature) is accurate enough to use the mean transmitted flux alone to infer an end to reionization at $z \sim 6$. The observed flux distributions in a large set of high-resolution QSO spectra spanning $2 < z < 6$ are compared to predictions from the theoretical optical depth distribution based on the gas *density* distribution of Miralda-Escudé et al. (2000; MHR00), assuming an isothermal IGM and a uniform UV background. These are the same assumptions used in previous studies where the evolution of the mean flux was used to infer a late end to reionization.

Results: We find that the MHR00 model does not reproduce the observed flux distribution at redshifts where the transmitted flux best samples the full range of underlying optical depths. Most of the disagreement occurs at high transmitted fluxes (low optical depths), and the fit improves if we allow large adjustments to the quasar continua. These adjustments are disfavored by the high-resolution spectra of a $z \sim 4$ GRB, however, for which the continuum is known to be a simple power law that can be fixed from the red end of the spectrum. In contrast, a lognormal distribution of optical depths gives the correct flux distribution at all redshifts without large continuum corrections. The best-fit parameter of the lognormal distribution evolve in a simple way with redshift, and extrapolating this evolution out to $z > 6$ predicts that the transmitted flux in the Lyα forest should completely disappear by $z \sim 6.2$. At least empirically, therefore, the appearance of "Gunn-Peterson troughs" at $z \sim 6$ is consistent with the slow evolution of the Lyα forest over $2 < z < 5$ (Figure 1), and does require a sudden change due to late reionization. This is consistent with the WMAP 3-year $\tau_{\rm e}$ value, which requires substantial reionization by $z \sim 10$ (Spergel et al. 2006).

Several modifications to the MHR00 model may potentially improve the fit to the flux distribution, including the use of a non-isothermal temperature-density relation. We find that an inverse temperature temperature-density relation greatly improves our fits by allowing the voids to be more transparent for a given H I ionization rate. While an inverse $T - \rho$ relation is contrary to the usual predictions for photoionization heating and adiabatic cooling of the IGM (e.g., Hui et al. 1997), it may reflect the complex thermodynamic state created by radiative transfer effects (Bolton et al. 2004).

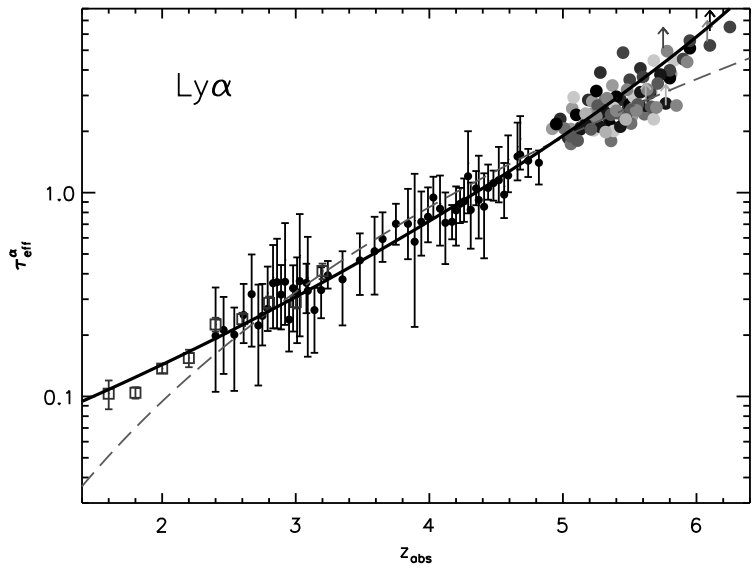

Figure 1: The evolution of Lyα effective optical depth with redshift, where $\tau_{\rm eff} = -\ln\langle F\rangle$. Data points are from Kirkman et al. (2005) (open squares), Songaila (2004) (small circles), and Fan et al. (2006) (large circles and arrows). The dashed line shows the best-fit power-law to $\tau^{\alpha}_{\rm eff}$ at $3 < z < 5.5$. The solid line shows $\tau^{\alpha}_{\rm eff}$ calculated from the lognormal distribution of Lyα optical depths, for which the parameters were fit at $z < 5.4$. A simple evolution in the lognormal τ distribution predicts the rise in $\tau^{\alpha}_{\rm eff}$ at $z > 5.5$ while producing an excellent fit to the observed $\tau^{\alpha}_{\rm eff}$ at all redshifts. In this empirical sense, the evolution of the Lyα forest at $z \sim 6$ is consistent with observed trends at lower redshift. If the evolution of the forest at $z < 5$ reflects a slowly-evolving density field, temperature, and UV background, then no sudden change in the IGM, such as one due to late reionization, appears necessary to explain the disappearance of transmitted flux at $z \sim 6$.

FIGGS: Faint Irregular Galaxies GMRT Survey

Ayesha Begum[1], Jayaram N. Chengalur[2], Igor D. Karachentsev[3], Margarita Sharina[3] & Serafim Kaisin[3]

[1] Institute of Astronomy, Cambridge, UK
[2] National Center for Radio Astrophysics, Pune, India
[3]Special Astrophysical Observatory, Nizhnii Arkhys, Russia

Context: I will present results from the Faint Irregular Galaxies GMRT Survey (FIGGS), an observing program to observe a large ($\sim$ 65) number of faint ($M_B < -15.0$), nearby, dwarf irregular galaxies in HI, at high velocity resolution (1.6 kms^{-1}) with the Giant Metrewave Radio Telescope (GMRT). The GMRT HI images obtained at a variety of spatial resolutions viz $40''$, $20''$ and $10''$ are supplemented by V and I band HST images, as well as the H-alpha images from the 6-m BTA telescope. In addition distances accurate to $\sim$10% are available from several of the galaxies in our sample. Our study is, by far, the most detailed multi-wavelength study of such faint galaxies. The FIGGS survey has uncovered galaxies like NGC 3741 and AndIV which have very extended HI disks and thus provide an unique opportunity to trace the extended distribution of dark matter around faint galaxies.

Aims: I will report on studies examining the correlations between dark and luminous matter (e.g. the Baryonic Tully Fisher relation), and star formation and the gas distribution and kinematics in the FIGGS sample.

Results: We find that most of the FIGGS galaxies show systematic large scale velocity gradients, unlike earlier studies which found chaotic velocity fields for such faint galaxies. For many sample galaxies the velocity fields are completely consistent with ordered rotation, though, in some cases, the peak circular velocities are comparable to the observed random motions. These are the faintest known galaxies with such regular kinematics.

We examine the trends between the derived HI and optical properties of FIGGS galaxies and their local environment. Except for a trend in M_{HI}/L_B, we do not find any correlation between the observed properties of FIGGS galaxies and the local environment.

We investigate the Tully-Fisher and Baryonic Tully-Fisher relation for a subsample of FIGGS galaxies with extended HI rotation curves and accurate distances. Our FIGGS galaxies not only allows us to study these relations to much fainter magnitudes (reaching globular cluster mass scales), than has been done previously, but is also the first sample for which distances accurate to $\sim 10\%$ are available.

For some of our galaxies we construct maps of the HI column density at a constant linear resolution of $\sim$ 300 pc; this forms an excellent data set to check for the presence of a threshold column density for star formation. We find that while current star formation (as traced by Hα emission) is confined to regions with relatively large [$N_{HI} > (0.4 - 1.7) \times 10^{21} cm^{-2}$] HI column density, the morphology of the Hα emission is in general not correlated with that of the high HI column density gas. Thus, while high column density gas may be necessary for star formation, in this sample at least, it is not sufficient to ensure that star formation does in fact occur. Finally, we examine the very fine scale ($\sim$ 20-100 pc) distribution of the HI gas in some of the faintest galaxies in FIGGS, and find that at these scales the emission exhibits a variety of shell-like, clumpy and filamentary features. The Hα emission is sometimes associated with high-density HI clumps, sometimes the Hα emission lies inside a high-density shell, and sometimes there is no correspondence between the Hα emission and the HI clumps. In summary, the interplay between star formation and gas density in these faint galaxies does not seem to show the simple large-scale patterns observed in brighter galaxies.

Formation and evolution of isolated HI clouds

Kenji Bekki

School of Physics, University of New South Wales, Sydney 2052, Australia

Context: A number of possible candidates of isolated massive HI clouds with no optical counterparts have been discovered by latest observations (e.g., HIPASS). Optical observations have also found that some of these clouds show emission lines, which implies that new stars are now being formed in the clouds. Formation and evolution processes of these objects however remain unclear.

Aims: Based on gas dynamical simulations of gas-rich galaxies interacting with galaxies and group and cluster environments, we investigate whether the observed isolated HI clouds can be tidal debris from interacting galaxies in different environments.

Results: We show that the isolated HI clouds can be tidal debris formed from very outer parts of HI gas disks in galaxies interacting with group and cluster environments. We also show that in some models, gas density in the clouds exceeds a threshold gas density of star star formation so that new stars and star clusters can be formed in the clouds. Furthermore we discuss the impact of dark matter subhalos on outer gas disks in galaxies ("dark impact"). The dark impact is demonstrated to form HI holes and possible star-forming regions in the very outer parts of gas disks in galaxies.

Radial Gas Distributions and Gas Depletion Time Problem

Leo Blitz[1], Andrew West[1], Erik Rosolowsky[3]

[1] University of California, Berkeley, USA
[2] Harvard-Smithsonian Center for Astrophysics, USA

We review the problem of gas depletion times in spiral galaxies: the molecular gas must be replaced in about 10^9 years if we are not in the last throes of star formation. We show that the radial gas distributions in spiral galaxies are sufficiently similar to one another, that the gas is probably being resupplied in some manner. Infall from High Velocity Clouds and their extragalactic analogues, as well as the failure to detect inflows through the disk, suggest that some other mechanism is likely to be responsible for gas redistribution. We speculate what this mechanism might be and propose some observational tests.

Molecular Gas and Molecular Clouds at the Low Mass End of the Galaxy Spectrum: Lessons from the Local Universe

Alberto D. Bolatto[1], Adam K. Leroy[1,2], Fabian Walter[2]

[1] University of California, Berkeley, USA
[2] Max-Planck Institute for Astronomy, Heidelberg, Germany

Context: In a bottom-up CDM cosmology, local low-mass systems are the best analogues of distant primitive galaxies amenable to detailed study. Many of these small galaxies exhibit low metallicities, low dust-to-gas ratios, and substantial star formation activities for their sizes. Molecular clouds in these objects provide the boundary conditions for star formation, thus they are a link that we would like to understand. However, there is a dearth of data on molecular content and molecular cloud properties in small galaxies. These systems are faint in molecular lines, and the available sensitivity is only enough to detect the nearest galaxies.

Aims: What is the star formation efficiency in low-mass, low-metallicity galaxies? Observations show scant molecular gas emitting in CO. Yet many of these systems show star formation rates normalized by galaxy mass that are above that of the Milky Way, and unexpectedly high when their CO emission is considered. Is their faintness in molecules a problem with CO as a tracer of H_2, or is there evidence for unusually high efficiencies in converting H_2 into stars? Do the observations match the predictions from the theory?

Results: Systematic analysis of interferometric and single dish CO data shows that the properties of GMCs in these systems are very similar to those of GMCs in the Milky Way. A few of these galaxies show molecular clouds that fall under the size-linewidth relation, suggesting lower than Galactic volume densities (if they are in virial equilibrium) or lower than Galactic turbulent energy densities (if they are out of virial equilibrium).

Analysis and modeling of the dust continuum data in the case of one of the most extreme objects (SMC, the Small Magellanic Cloud), however, shows that there is a wealth of H_2 gas extending beyond the CO clouds. When this gas is taken into account, the star formation rate observed in the

SMC is as predicted by extrapolation of the molecular Schmidt Law observed in larger galaxies.

One of the most attractive theoretical scenarios to understand how GMC properties tie into star formation is that presented by photoionization - regulated star formation theory. In this context we expect larger column densities of molecular gas in low-metallicity systems, which have lower than Galactic dust-to-gas ratios. We find no such behavior: the H_2 column densities observed in GMCs in these systems are not radically different from Galactic column densities. Furthermore, as mentioned in a previous paragraph, apparently not all the gas that partakes in star formation has large-enough column densities to tbe observed in CO. Thus some of the predictions of photoionization-regulated star formation theory do not appear to be entirely supported by the observations.

Exploring the neutral hydrogen content of the IGM with quasar absorption spectra

James S. Bolton[1], Martin G. Haehnelt[2]

[1] Max Planck Institut für Astrophysik, Karl-Schwarzschild Str. 1, 85748 Garching, Germany
[2] Institute of Astronomy, University of Cambridge, Madingley Road, Cambridge, CB3 0HA, UK

Context: Quasar absorption spectra are currently the premier observational probe of the hydrogen reionization epoch. The average amount of Lyman series absorption observed in quasar spectra is consistent with an intergalactic medium (IGM) with a volume weighted neutral hydrogen fraction in excess of $\langle f_{\rm HI} \rangle_{\rm V} \sim 10^{-3.5}$ at $z \simeq 6$. However, obtaining more stringent constraints on the IGM neutral hydrogen fraction using this technique at $z > 6$ is extremely difficult; larger neutral fractions produce saturated Lyman series absorption over substantial regions in the spectra of these quasars.

Aims: Several techniques which may be sensitive to larger values of $\langle f_{\rm HI} \rangle_{\rm V}$ have been proposed. The sizes of transparent regions observed immediately blueward of the Lyα emission line of $z > 6$ quasars, if equivalent to the size of the H II regions surrounding the quasars, should be proportional to the surrounding IGM neutral fraction when adopting assumptions for the quasar age and ionizing luminosity. A critical analysis of the accuracy of the constraints on $\langle f_{\rm HI} \rangle_{\rm V}$ from these highly ionized near-zones will be presented using state of the art hydrodynamical simulations combined with a radiative transfer implementation.

Accurate measurements of the metagalactic hydrogen photoionization rate, $\Gamma_{\rm HI}$, approaching the tail end of H I reionization at $z \simeq 6$ can also provide interesting constraints on the types of sources responsible for reionizing the IGM. Robust estimates for $\Gamma_{\rm HI}$ at $z = 5$ and 6 derived from recent measurements of the Lyα opacity of the IGM will be presented. Attention is given to the issue of whether known sources can provide enough ionizing photons to maintain the hydrogen in the IGM in an ionized state at this epoch. The implications for the reionization history at $z > 6$ based on the

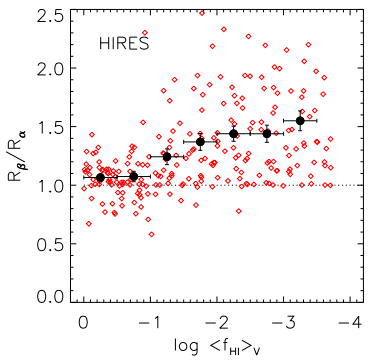

Figure 1: The ratio of Lyβ to Lyα near-zone sizes as a function of the volume weighted neutral hydrogen fraction, measured from synthetic HIRES spectra. The red diamonds show the individual measurements and the filled black circles with 1σ error bars correspond to the averages in bins of width $\Delta[\log\langle f_{\rm HI}\rangle_{\rm V}] = 0.5$.

ionizing emissivity derived from recent constraints on the star formation rate at $z > 6$ will also be discussed.

Results: The sizes of Lyα near-zones alone are consistent with both a substantially neutral and highly ionized IGM. Stronger constraints may be possible by considering the Lyα and Lyβ near-zone sizes in tandem. Under standard assumptions for quasar ages and ionizing luminosities, a future sample of several tens of high resolution Lyα and Lyβ near-zone spectra should be capable of distinguishing between a volume weighted neutral hydrogen fraction which is greater or less than 10 per cent (Fig. 1).

The number of hydrogen ionizing photons emitted by known sources at $z = 5$ and 6 are in reasonable agreement with measured photoionization rates. In comoving units the inferred ionizing emissivity is found to be nearly constant over the redshift range $2 - 6$ and corresponds to $1.5 - 3$ photons emitted per hydrogen atom over a time interval corresponding to the age of the Universe at $z = 6$ (Fig. 2). Completion of reionization at or before $z = 6$ requires either an emissivity which rises towards higher redshifts or one which remains constant but is dominated by sources with a rather hard spectral index. Therefore, unless the ionizing emissivity rises dramatically at $z > 6$, the hydrogen in the IGM may well be substantially neutral by $z = 7$.

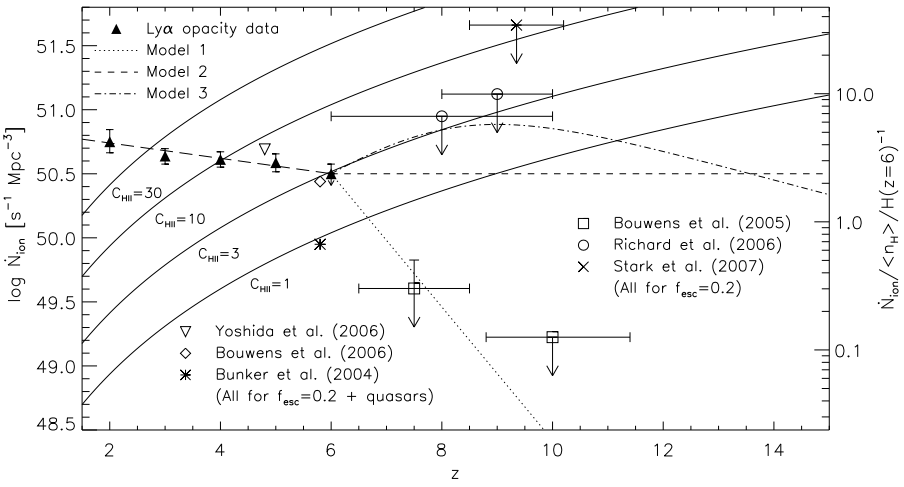

Figure 2: Observational constraints on the emission rate of ionizing photons per comoving Mpc, $\dot{N}_{\rm ion}$, as a function of redshift. The scale on the right-hand vertical axis corresponds to the number of ionizing photons emitted per hydrogen atom over the Hubble time at $z = 6$. The filled triangles give an estimate of $\dot{N}_{\rm ion}$ based on measurements of $\Gamma_{\rm HI}$. The inverted triangle at $z = 5$ and the diamond and star at $z = 6$ correspond to estimates of $\dot{N}_{\rm ion}$ based on the emissivities of LBGs and quasars. At $z > 6$, the open squares and circles are derived from the upper limits on the comoving star formation rate per unit volume, and the cross is derived from the number density of Lyα emitters. Three simple models for the evolution of $\dot{N}_{\rm ion}$ are also shown as the dotted, short dashed and dot-dashed lines. The solid lines correspond to the emission rate of ionizing photons per unit comoving volume, $\dot{N}_{\rm rec}$, needed to balance recombinations for various H II clumping factors. For an H II clumping factor of $C_{\rm HII} = 2$ and an ionizing background spectral index of $\alpha_{\rm b} = 3$, only model 3 will reionize the IGM by $z = 6$.

The phases and mass budget of the interstellar medium in outer disks

Jonathan Braine & Erwan Gardan

Observatoire de Bordeaux, Université Bordeaux 1, B.P. 89, 33270 Floirac, France

Context: It is generally accepted that the Star Formation Rate (SFR) increases very sharply in galaxies up to a redshift of about $z = 1$. Since stars form from H_2, and not directly from HI (with the possible exception of the so-called Pop. III, or first generation stars), this suggests that either large amounts of molecular hydrogen were available or that for some reason the efficiency of star formation (SFE, defined as the SFR per unit H_2) was particularly high back then. In fact, the SFRs proposed (e.g. Madau et al. 1996, MNRAS 283, 1388 and many other more recent articles) are so much higher than the SFR today that both possibilities may be required. While more galaxies existed, the bulk of the change is in the individual objects rather than having 15 – 20 times more galaxies at $z = 1$. Because at least 10% of the baryons in galaxies are thought to be in neutral gas (and more than 10% in many cases), an SFR a factor 15 – 20 higher must result at least partially from a higher SFE. While there may not be a 100% consensus, it is widely believed that the fraction of molecular gas (with respect to atomic) decreases going to later types and smaller objects. Moderate to high redshift galaxies are typically smaller and more gas-rich than today's spirals and most likely have a slightly subsolar metallicity. They thus resemble todays small spirals such as M33 in the Local Group and could be expected to have a low H_2/HI mass ratio. If so, this would make the SFE in these objects even more extreme.

The first step is to learn more about the molecular cloud content of galaxies with these properties. Recently we (Braine, Herpin, Ferguson, Gardan ...2004-2007) have shown that significant quantities of molecular gas were detectable far out in spiral disks but that long integration times were required to detect it. The outskirts of spirals share the subsolar metallicities and low mass surface densities of small and/or medium/high redshift spirals but not the level of star formation. This first step has revealed that molecular gas

forms very far out in at least NGC 4414, NGC 6946, and M33 despite the low metallicity and very low ambient pressure (Gardan et al. 2007, submitted).

I will often refer to "outer disks" and the definition is not entirely clear. Probably for any definition, the fraction of a galaxy which is "outer disk" increases with redshift because the optical sizes of galaxies are substantially smaller at intermediate redshift. A convenient definition, in order not to be too biased by galaxy colors, might be to define the outer disk as where the gaseous surface density exceeds the stellar surface density. This is usually around the R_{25} radius for big spirals and further in for small spirals like M33.

The talk: We would like to determine how much of each of the gas phases – molecular, atomic, and ionized – is present in the outer disks of todays spirals *and understand why*. Since it is clear that in spiral galaxies the neutral interstellar medium (ISM) dominates in mass although it is in fact difficult to measure that of the ionized gas, I will focus on the neutral ISM. Star formation takes place in the neutral interstellar medium so the properties of the atomic and molecular gas must be an important part of understanding whether and why star formation is different at higher redshift.

The ratio of atomic to molecular gas is much higher in the outer disk than in the inner parts, even at equivalent H column density. Why? The atomic component has long been observed in outer disks and the atomic gas column density can be reasonably reliably derived from the 21cm HI line. Only recently, however, has it been possible to observe the molecular gas far out in disks. It is clearly associated with the atomic component yet for a given galaxy the HI column density does not provide a reliable prediction of the molecular gas content. I will present unpublished data on the molecular components of several nearby spiral galaxies in order to better understand the relationship between the atomic and molecular gas and star formation in the outer disks of spirals and what the differences are with respect to inner disks.

The long term goal is to test whether some local galaxies share the high starforming efficiencies of intermediate redshift galaxies, determine which local galaxies, and understand what is different about their molecular ISM that results in a high SFE.

HI in the M31 Sub-group

Robert Braun[1], David Thilker[2], Edvige Corbelli[3] & René Walterbos[4]

[1] CSIRO – ATNF, PO Box 76, Epping, NSW 2121, Australia
[2] Johns Hopkins University, 3400 N. Charles St., Baltimore MD 21218, USA
[3] Arcetri, INAF, Largo E. Fermi, 5, 50125, Firenze, Italy
[4] New Mexico State University, PO Box 30001, Las Cruces, NM 88003, USA

Context: Galaxies often appear to be "Island Universes" when their neutral gas content is imaged with only the modest column density sensitivity, of about 10^{19}cm^{-2}, which is typical of current programs. This column density is near the threshold where HI can become self-shielding to the intergalactic ionizing radiation field and marks the transition from essentially fully neutral HI within galaxy disks to an almost fully ionized medium without. Galaxy disks display an exponential decline in HI column density to mark this transition from the optically thick to the optically thin regime. However, if one can push beyond this "HI desert" into the tail of residual neutral gas in the optically thin regime, the sky once again opens up with additional detectable structures. Although such gas has a moderately high ionization fraction (99% or more) the trace neutral constituent can permit it's kinematic and morphological study. Achieving the requisite brightness sensitivity is at the limits of what can be achieved with today's instrumentation, but is just accessible to long integrations with (almost) filled apertures.

Aims: We have undertaken a series of very sensitive HI surveys of the M31 Sub-group to detect and study the trace neutral components which approach the optically thin regime to ionizing intergalactic radiation.

Results: Our sensitive wide-field survey using the 14 telescopes of the Westerbork Array (WSRT) in total power mode of the M31 sub-group has revealed a filament of very diffuse neutral gas joining the systemic velocities of M31 and M33, with peak column densities of only 4×10^{17}cm^{-2} as shown in Figure 1. Pointed Green Bank Telescope (GBT) observations (with ten times smaller beam area) have confirmed these very low peak values and

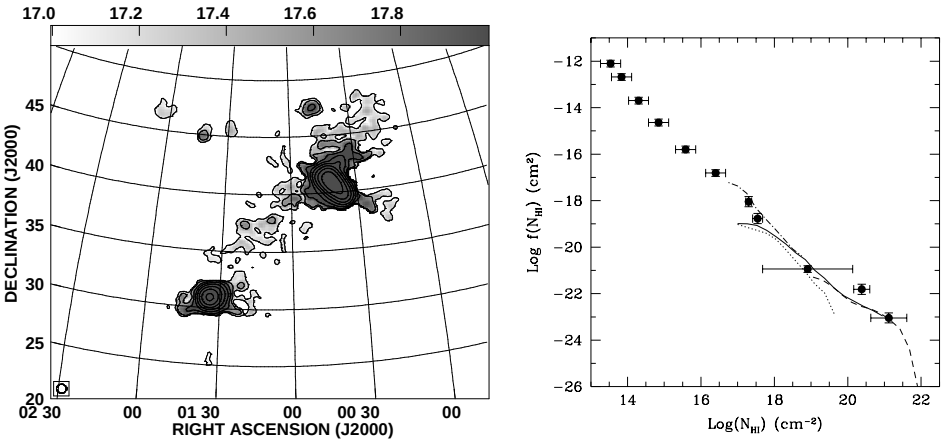

Figure 1: Left: Integrated HI emission from the subset of features seen in our wide-field total power survey which are kinematically associated with M31 and M33. The grey-scale varies between $\log(N_{HI}) = 17 - 18$. Right: The corresponding HI distribution function. The curves are the HI data, while the filled points represent QSO optical absorption line data.

have excluded resolution effects as their cause. The filament is likely to be a fossil of an ancient interaction between M31 and M33 that may have occurred some 5 Gyr ago, according to a recent orbit model of the system. The HI distribution function of this feature together with the high column density disk of M31 agrees well with the distribution function determined from QSO absorption line systems at low red-shift as also shown in Figure 1. The expected increase in surface covering factor of about 30 when going down from 10^{19} to $10^{17}\mathrm{cm}^{-2}$ is directly observed.

One end of the filament terminates near the minor axis of M31 (and extends beyond in the anti-M33 direction) where it can just be detected in our higher resolution imaging (shown in Figure 2). The other end of the filament joins M33 at it's north-western extremity. Our deep mosaic of M33 displays the strongly warped outer disk of this galaxy in this region where filament infall may well be fueling the complex outer disk structures. Kinematic modeling of the outer disk distribution is now underway to better constrain the galaxy potential and interaction history.

Additional results from these surveys will be presented.

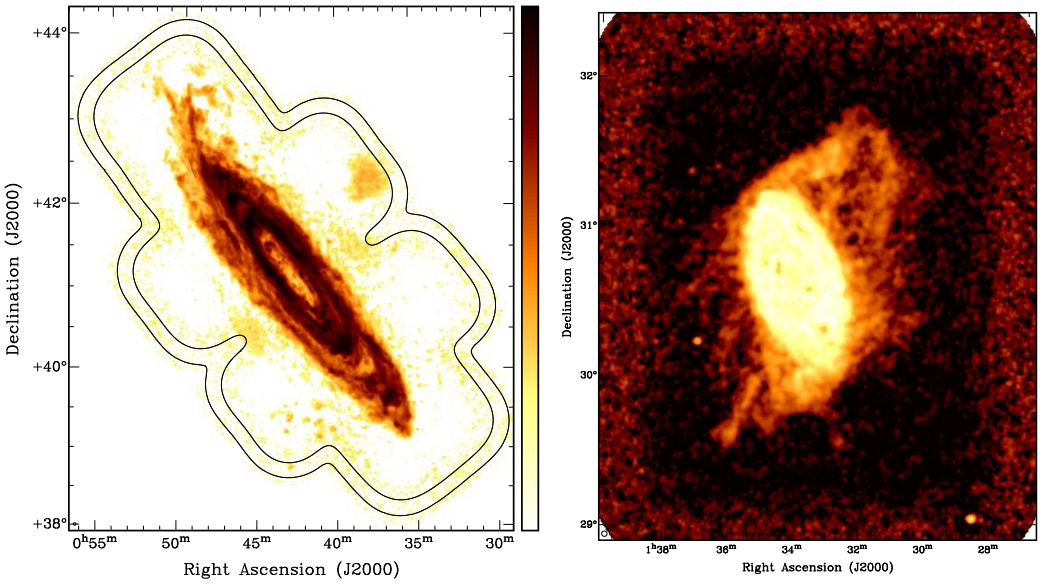

Figure 2: Left: Peak brightness of HI emission in M31 determined at 120 arcsec and 10 km/s resolution is overlaid with the combined sensitivity pattern of the 163 pointings in the combined WSRT mosaic and GBT total power observations. Contours are drawn at 10 and 50% of the peak sensitivity. Peak brightness is shown on a logarithmic scale which saturates at 60 K. The beam size is indicated in the lower left corner. The RMS column density sensitivity is about $10^{18}\mathrm{cm}^{-2}$ over 20 km/s. The "lobes" on either side of the minor axis are at the systemic velocity and are the diffuse termination points of the filament in Figure 1. Right: Peak brightness of HI emission in M33 determined at 130 arcsec and 20 km/s resolution is shown, based on our combined 200 pointing VLA mosaic and GBT total power observations. Peak brightness is shown on a logarithmic scale which saturates at 20 K. The beam size is indicated in the lower left corner. Several unresolved sources in the field are residual continuum artifacts. The RMS column density sensitivity is about $6{\times}10^{17}\mathrm{cm}^{-2}$. The filament terminates in the north-western extremity of the disk, where it may be feeding the warped and distorted structure.

The nature of Giant LSB Galaxies and their relationship to QSO absorption-line gas

F.H. Briggs, M.B. Pracy, H. Jerjen

RSAA, Mount Stromlo Observatory, The Australian National University

Context: Giant Low Surface Brightness galaxies form a morphological class that is typified by high integrated optical luminosity, faint blue emission of very large disk scale-length extending far outside the size of more normal spiral galaxies, and large HI mass content. These galaxies individually present large gaseous cross sections that could account for some of the interception probability for absorption lines against background QSOs, provided the GLSBs are sufficiently numerous, and they could provide insight into the nature of the intervenors, especially the MgII/LLS and DLα systems.

The GLSB Malin 1 has served as the prototype for the class, continuing to uphold its reputation as "an extreme object" in many parameters, as well as being one of the galactic systems containing the largest concentrations of HI known. However it has remained difficult to study in detail due to its large redshift $z \sim 0.083$.

Aims: New observational data provides the framework for a reassessment of the nature of Malin 1 and for the GLSB class as a whole. In this framework, the GLSBs are related to the wealth of information on nearby, well-characterized galactic systems - such as extended, gas-rich, warped disks and tidally interacting groups. The GLSBs take a natural place in the study of the exchange of both neutral and ionized gas between central host and extended halo.

Results: High resolution HST imaging reveals the nature of the Malin 1 host galaxy to be *"a typical SB0/a galaxy. The remarkably extended, faint outer structure detected out to* $r \sim 100$ *kpc appears to be a photometrically distinct component and not a simple extension of the inner disk,"* according to Barth (2007, AJ, 133, 1085). Moore and Parker (2006, PASA, 23,165) have created an ultra-deep image of the diffuse outer emission from a stack of 63 scanned, R-band films to reveal a large-scale spiral structure encircling the SB0/a host.

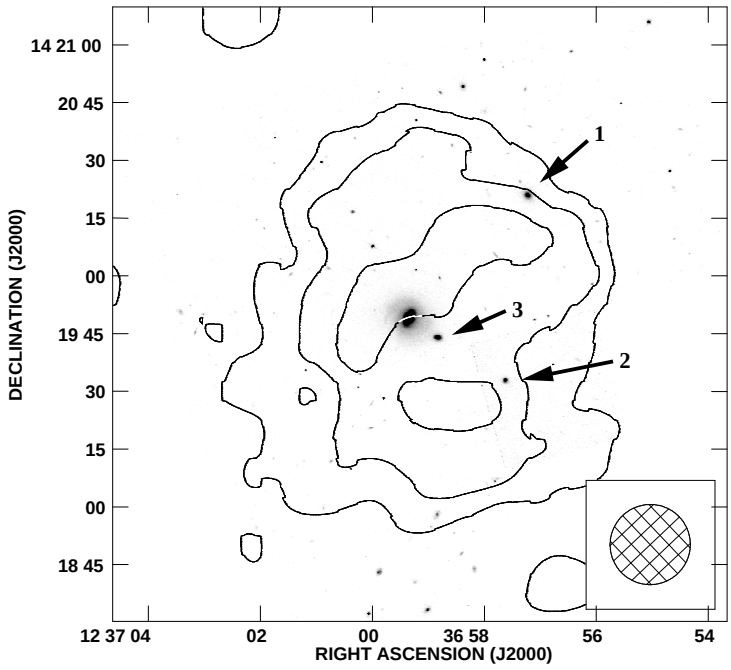

Figure 1: Image of Malin 1 field: HI 21cm line emission contours from the VLA dataset of Pickering et al (1997) are overlaid on the archival HST I-band image. The $20''$ resolution of the radio data is indicated in the lower right corner. The central stellar body of Malin 1 lies at the center of the image, and three smaller galaxies are labeled numerically. HI column density contours at 1.2, 2.5, 3.7 $\times 10^{20}$ cm^{-2}.

Here, we form a unified interpretation of the new optical results, together with the radio cube of Pickering et al (1997, AJ, 114, 1858) to specify both gas distribution and kinematics. The archival HST images also suggest the presence of companion galaxies to Malin 1, which appear together form a group of mildly interacting galaxies embedded in a common HI structure. Spectroscopy with the Siding Spring Observatory 2.3m Telescope indicates that redshifts for galaxies 2 and 3 in Figure 1 are consistent within 200 km s^{-1} of the Malin 1 redshift.

The emergent picture is that the invisible, extended HI disks that are known to envelop at least 10% of nearby isolated galaxies (such as NGC 628, Kamphuis & Briggs 1992, A&A, 253, 335) will "light up" when they expe-

rience the mild tidal disturbance of an unequal mass interaction with additional (one or more) galaxies. The weak interaction is adequate to stimulate weak star formation in the low column density gas, creating a diffuse blue light, without driving massive arms or intense nuclear bursts. In some sense, the extended disks can be considered "old and quiescent" - a conventional interpretation of LSB disk (Sprayberry et al 1993, ApJ, 417, 114) in that the neutral HI envelope may have been present for a long time, hovering in outlying orbits around a central host (c.f., van Driel & van Woerden 1991, A&A, 243, 71). On the other hand, the blue stellar population must result from the recent triggering of the system. An important question is whether the outer HI disks and rings are residuals left in place after the main assembly of the galaxy hosts or whether they signify the ongoing entrapment of gas that is being attracted into the galaxian potential well.

The gentle interactions now observed in these systems are mild forms of the more vigorous redistributions of matter in galaxies that occurred much earlier, during galaxy assembly, when galaxy halos are polluted with metal enriched gas. The re-accretion of the halo material on ballistic trajectories (which retain some memory of the original formation) will occur in a distinct fashion from the accretion of primordial material with no previous dynamical association with the system. Fukugita & Peebles (2004, ApJ, 616, 643) find that approximately half of the universal baryon budget is located in "virialized regions of galaxies" at the present epoch, and it is this reservoir that is thought to give rise to the some classes of QSO absorption lines; this reservoir of baryonic material is a likely source of re-accretion and replenishment of galactic disks.

The QSO proximity effect and the estimate of the UV ionizing background

M. Bruscoli[1,2], V. D'Odorico[3], F. Saitta[4,1], S. Cristiani[3], M. Viel[3], P. Monaco[1] & F. Fontanot[5]

[1] Dipartimento di Astronomia, Universitá degli Studi di Trieste, Via Tiepolo 11, 34131 Trieste, Italy
[2] INAF-IRA, sezione di Firenze, Largo E.Fermi 5, 50125 Firenze, Italy
[3] INAF-OATS, Via Tiepolo 11, 34131 Trieste, Italy
[4] European Southern Observatory, Karl-Schwarzschild-Str. 2, D-85748 Garching bei München, Germany
[5]Max-Planck-Institute for Astronomy, Königstuhl 17, D-69117, Heidelberg, Germany

Context: Motivated by the high quality of recent observational quasar spectra, we investigate the proximity effect around 19 high redshift quasars ($2.13 < z_{em} < 3.27$) with the aim of giving an accurate estimate of the intensity of the ionizing ultraviolet background. This study, based on the Large Program high resolution absorption quasars spectra and on improved numerical SPH simulations implementing, in addition to standard processes, a new scheme for outflow physics description, leads to the following results.

Aims: In previous works, authors derived the proximity effect from the number density of the Lyα absorption lines obtained from their QSOs sample: this number depends on how the Voigt profile fitting is executed. Problems arise principally in the fitting analysis of the complex absorption lines where the decomposition in Voigt profiles is not univocally determined. In this work, we adopt a new method based on the fact that the sum of the neutral hydrogen column density (NHI) of the velocity components in the complex absorption lines is conserved indipendently of the number of Voigt profiles used for the decomposition (for more details Saitta et al. 2007 in preparation). We therefore convert the observed NHI, in the optical thin approximation ($NHI < 10^{17}$ cm^{-2}), in observed hydrogen number density (n_H) and then we compare it with synthetic hydrogen number density $n_{H,syn}$

obtained from cosmological simulations. The accurate study of n_H and $n_{H,syn}$ behaviours as a function of the QSOs distance, allow us to draw important conclusions on the mutual interplay of clustering and QSOs ionizing flux in giving origin to the proximity effect. As direct consequence, we infer the correction for J_ν estimate.

Results: As a first approximation we have not take into account the effect of the QSOs ionizing flux on their environments, deriving the standard proximity effect. We then exploit the case where also the QSOs ionizing flux is considered. In Fig.1 we present, for the 19 QSOs of the sample the comparison between the standard proximity effect and the one computed with the contribution of the QSOs ionizing radiation. As the plot clearly shows, Γ_{QSO} begins to dominate at distances less than 20 proper Mpc from the QSOs where the values of the overdensity starts to grow. The result obtained with the introduction of Γ_{QSO} support the information, already known from other studies, that QSOs reside in overdense regions. Near the QSOs, where the effect of the QSOs ionizing radiation is dominant, to obtain the observed values of NHI, there must be, respect to the mean IGM, higher values of the total hydrogen number density.

We exploit also the effects of the variation of the IGM temperature, Γ_{12} and QSOs emission redshift on the proximity effect.

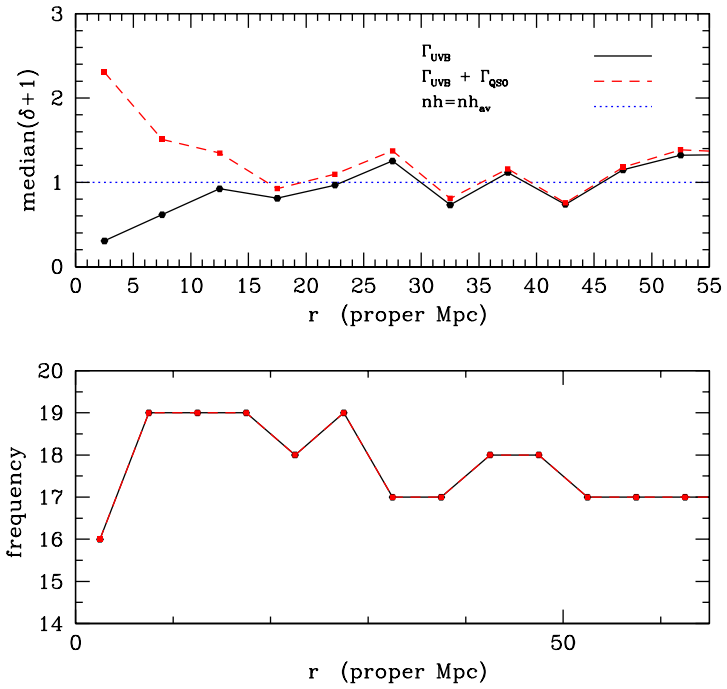

Figure 1: Proximity effect for the 19 QSOs of the sample: Γ_{UVB} only (solid line) and $\Gamma_{UVB} + \Gamma_{QSO}$ (dashed line). In the bottom panel the number counting falled in each bin are shown.

The Formation of Dense Stellar Clusters and their Affect on the Ionisation and Disruption of Turbulent Molecular Clouds

Andreas Burkert

University of Munich, University Observatory, Germany

I would like to summarize recent numerical simulations on the formation of stellar clusters in turbulent molecular clouds including energetic feedback through ionising radiation that allow us to estimate star formation efficiencies and provide detailed insight into the the physics of molecular cloud disruption by young massive stars.

The Bright Lyα Side of the High-Redshift Intergalactic Medium

Sebastiano Cantalupo, Cristiano Porciani, Simon J. Lilly

Institute for Astronomy, ETH Zürich, CH-8093 Zürich, Switzerland

Context: The analysis of absorption systems in the spectra of high-redshift quasars has represented for several decades the only practical way to obtain information about the properties of the Intergalactic Medium (IGM). Unfortunately this information is almost always one-dimensional. An interesting alternative to absorption studies is to try to detect the IGM in emission rather than in absorption. Optically thick clouds to the cosmic ionizing background are expected to emit fluorescent Lyα photons produced in hydrogen recombinations at a rate that is set by the impinging ionizing flux (Gould & Weinberg, 1996, ApJ, 468, 462). Positive fluctuations in the ionizing background can be used to increase the signal. For instance, clouds lying close to a bright quasar are exposed to a stronger UV flux (with respect to an *average* cloud) and are then expected to be brighter in fluorescent Lyα.

The emission is typically concentrated in the outer parts of the clouds where hydrogen is significantly ionized. However, Lyα photons cannot directly escape the clouds because of the large optical depth in the center of the line. Each photon thus suffers a large number of resonant scatterings (more precisely: absorptions and re-emissions) by neutral hydrogen atoms in the ground state. Monte Carlo simulation is the most popular method for addressing the radiative transfer problem. Analytical solutions only exist for highly symmetric systems, like a plane-parallel and static homogeneous slab. Previous Monte Carlo codes are based on rather crude approximations, e.g. highly symmetric semi-analytical models for the gas distribution (e.g., Zheng & Miralda-Escudé, 2002, ApJ, 578, 33).

Aims: Our method is based on a new approach: we start from the gas density and velocity distributions given by high-resolution hydro-simulations of the ΛCDM cosmology. A simplified radiative transfer scheme is then used

to propagate ionizing radiation through the computational box and to derive the distribution of neutral hydrogen. Finally, the transport of Lyα photons generated by hydrogen recombinations is followed using a three-dimensional Monte Carlo code. In the first radiative transfer scheme, the computational box is adaptively refined in correspondence of the cloud shielding layer, where the original unrefined cells become optically thick. This is fundamental to avoid that the spatial distribution of recombinations and the escape probabilities of Lyα photons along different directions are spuriously altered. As ionizing radiation, we first considered the smooth UV background generated by galaxies and quasars. Then, as a second case, we superimposed to the background the UV flux produced by a quasar lying in the vicinity of the simulation box.

Results: Our results show that simple models (e.g. Gould & Weinberg 1996) tend to overpredict the Lyα flux emitted from optically thick clouds. In fact, we identified two effects that reduce the fluorescent Lyα flux and modify the spectral energy distribution with respect to the widespread static and plane-parallel model. The importance of these effects depends on the intensity of the impinging radiation. For this reason, we provided a fitting function for the maximum Lyα brightness and for the number density of optically thick sources as a function of the incident ionizing flux (Cantalupo et al., 2005, ApJ, 628, 61).

Based on our model, we carried out a spectroscopic survey in the field surrounding the z=3.1 quasar QSO0420-388 using the FORS2 instrument on the VLT (Cantalupo, Lilly, & Porciani, C. 2007, ApJ, 657, 135). We used a "multi-slit plus filter" technique to sparsely sample a volume of $\sim$ 14000 comoving Mpc^3 around the quasar (directly sampling $\sim$ 1700 comoving Mpc^3). We found 13 emission line sources which are likely to be Lyα at a redshift close to the quasar. In order to try to distinguish fluorescent objects from internally ionized clouds, we measured three possible signatures of fluorescence: i) the line equivalent width, ii) the line profile, iii) the surface brightness. We also calculated the expected number of fluorescent and non-fluorescent sources from theoretical models and recent Lyα surveys. The properties of the detected sources and their number density both suggest that about half of them are plausibly fluorescent. The distance of most of the candidates from the ionizing source would imply that the quasar has been active for at least 30 Myr, with a UV luminosity similar (within a factor of a few) to the present day value. In particular, one of the best candidates for

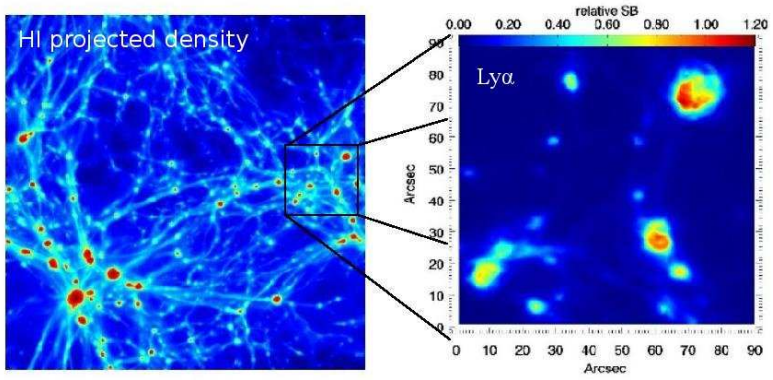

Figure 1: Simulated distribution of neutral hydrogen in our 10 Mpc/h computational box (left panel) illuminated by the UV background at $z = 3$ and fluorescent Lyα surface brightness for a selected region (right panel). Notice that in the HI distribution, self-shielded clouds are indicated by the red color.

fluorescence is sufficiently far behind the quasar to imply a life-time of (at least) 60 Myr.

We also used an improved version of our radiative-transfer model to study the epoch of reionization (Cantalupo et al., 2007, submitted to ApJ). We present here our recent results that show how the Lyα emission from the IGM around the ionizing sources at $z > 6$ can be used to constrain the epoch and topology of the reionization process.

High-z galaxies & ALMA

Chris Carilli

NRAO, USA

I will discuss observations of the first galaxies at centimeter and millimeter wavelengths. I will start with a summary of current mm and cm observations of the host galaxies of the most distant QSOs ($z \sim 6$). These observations reveal the atomic and molecular gas, dust, and star formation in the host galaxies on kpc-scales. These data imply an enriched ISM in the QSO host galaxies within 1 Gyr of the big bang, and are consistent with models of coeval supermassive black hole and spheroidal galaxy formation in major mergers at high redshift. Current instruments are limited to studying pathologic objects at these redshifts ($L_{FIR} \sim 10^{13}$ $L_\odot$). ALMA will provide the nearly two orders of magnitude improvement in sensitivity required to study normal star forming galaxies (eg. Ly-α emitters) at $z \geq 6$, including sub-kpc resolution imaging of line emission from molecular gas, and fine structure line emission from atomic gas. ALMA will reveal the thermal gas and dust – the fundamental fuel for star formation – in galaxies into cosmic reionization.

Observational Constraints on Reionization History

T. Roy Choudhury[1] **& A. Ferrara**[2]

[1] Institute of Astronomy, Madingley Road, Cambridge CB3 0HA, UK
[2] SISSA/ISAS, via Beirut 2-4, 34014 Trieste, Italy

Context: The study of reionization received a big boost due to availability of a variety of observational data accumulated over the past few years. These observations suggest that the reionization occurred somewhere between $z \sim 6 - 15$, and that the nature of this process is quite complex. We are about to enter the most exciting phase in the study of reionization as new ground-based (LOFAR, MWA, PAST, SKA, ALMA) and space-born (JWST, PLANCK, GLAST) experiments will soon settle the long-standing question on when and how the Universe was reionized. It is thereby important to develop detailed analytical and numerical models to extract the maximum information about the physical processes relevant for reionization out of the expected large and complex data sets.

Aims: Our present aim is to build up self-consistent models that can reconcile with a wide variety of observations concerning the thermal and ionization history of the IGM. The main features of the semi-analytical model used in this work[1] could be summarized along the following points. The model accounts for IGM inhomogeneities by adopting a lognormal distribution; reionization is said to be complete once all the low-density regions (say, with overdensities $\Delta < \Delta_{\rm crit} \sim 60$) are ionized. The mean free path of photons is thus determined essentially by the distribution of high density regions. We follow the ionization and thermal histories of neutral, HII and HeIII regions simultaneously and self-consistently, treating the IGM as a multi-phase medium.

Three types of reionization sources have been assumed: (i) metal-free (i.e. PopIII) stars having a Salpeter IMF in the mass range $1 - 100 M_{\odot}$; (ii) PopII stars with sub-solar metallicities also having a Salpeter IMF in the mass

[1]Throughout the paper, we use the best-fit cosmological parameters from the 3-year WMAP data, i.e., a flat universe with $\Omega_m = 0.24$, $\Omega_\Lambda = 0.76$, and $\Omega_b h^2 = 0.022$, and $h = 0.73$. The parameters defining the linear dark matter power spectrum are $\sigma_8 = 0.74$, $n_s = 0.95$, $dn_s/d\ln k = 0$.

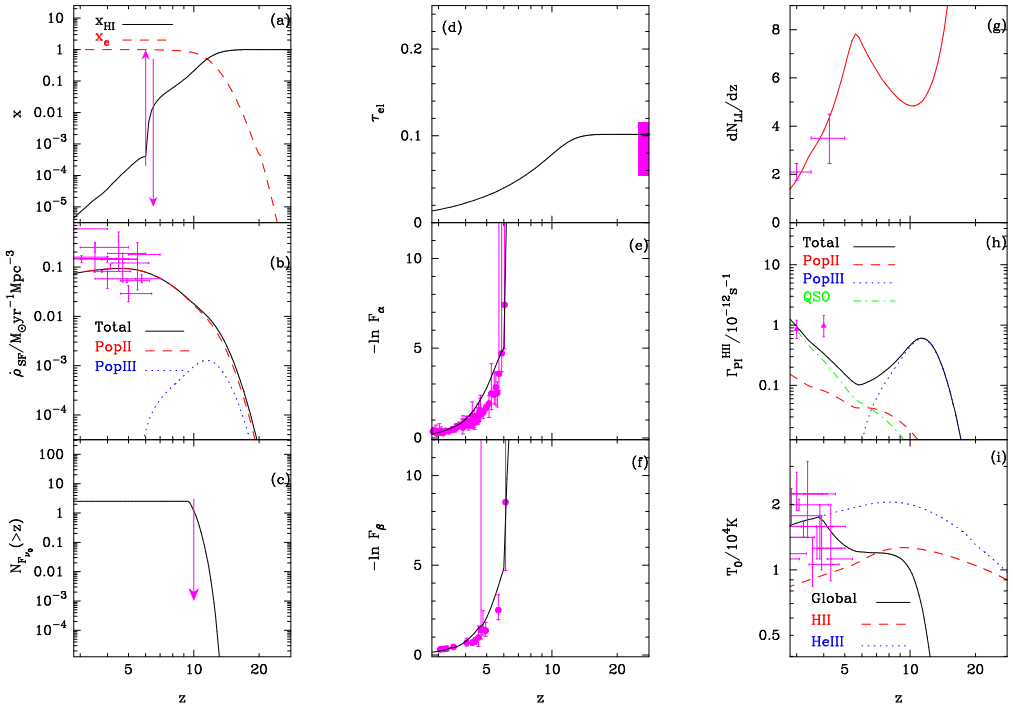

Figure 1: Comparison of model predictions with observations for the best-fit model. The different panels indicate: (a) The volume-averaged neutral hydrogen fraction $x_{\rm HI}$, with observational lower limit from QSO absorption lines at $z = 6$ and upper limit from Lyα emitters at $z = 6.5$ (shown with arrows). In addition, the ionized fraction x_e is shown by the dashed line. (b) SFR for different stellar populations. (c) The number of source counts above a given redshift, with the observational upper limit from NICMOS HUDF shown by the arrow. (d) Electron scattering optical depth, with observational constraint from WMAP 3-year data release. (e) Lyα effective optical depth. (f) Lyβ effective optical depth. (g) Evolution of Lyman-limit systems. (h) Photoionization rates for hydrogen. (i) Temperature of the mean density IGM

range $1 - 100 M_{\odot}$; (iii) QSOs, which are significant sources of hard photons at $z < 6$.

Reionization by UV sources is accompanied by photo-heating of the gas, which can result in a suppression of star formation in low-mass haloes. We compute such (radiative) feedback self-consistently from the evolution of the thermal properties of the IGM. Furthermore, the chemical feedback inducing the PopIII $\rightarrow$ PopII transition is implemented in which a merger-tree "genetic" approach is used to determine the termination of PopIII star formation in a metal-enriched halo.

Results: The predictions of the model are compared with a wide range of observational data sets, namely, (i) IGM Lyα and Lyβ optical depths, (ii) electron scattering optical depth, (iii) cosmic star formation history, (iv) source number counts at $z \approx 10$ from NICMOS HUDF, (v) redshift evolution of Lyman-limit absorption systems and (vi) temperature of the mean intergalactic gas.

The best-fit reionization model is characterized by a PopII (PopIII) star-forming efficiency $\epsilon_{*,\mathrm{II}} = 0.1 (\epsilon_{*,\mathrm{III}} = 0.03)$ and escape fraction $f_{\mathrm{esc,II}} = 0.01 (f_{\mathrm{esc,III}} = 0.68)$ (keeping in mind that $f_{\mathrm{esc,II}}$ and $f_{\mathrm{esc,III}}$ are not independent). The data constrain the reionization scenario quite tightly. We find that metal-free (PopIII) stars within the lower mass 10^7-$10^8 M_{\odot}$ haloes dominate the photon production rate at early redshifts ($z > 10$) and the reionization is 90 per cent complete by $z \approx 8$. At $z < 8$, the contribution from PopIII haloes decreases because their formation is hampered by the heating associated with radiative feedback. As a result, the progress of ionization fronts relies on photons emitted by more massive haloes with $M > 10^9 M_{\odot}$. Such high mass haloes do not host PopIII stars as they form from the merging of already polluted progenitors, a result of the "genetic" transmission of chemical feedback. This combination of radiative and chemical feedback makes the reionization process quite extended and its completion has to wait until $z \approx 6$ when the PopII stars and QSOs dominate the photoionization rate.

Our model can be used for predicting the observable properties of the sources responsible for cosmic reionization. J-band detection of sources contributing to 50% (90%) of the ionizing power at $z \sim 7.5$ requires to reach a magnitude $J_{110,\mathrm{AB}} = 31.2(31.7)$, where $\sim 15(30)$ (PopIII) sources/arcmin^2 are predicted. We conclude that $z > 7$ sources tentatively identified in broad-band surveys are relatively massive ($M \approx 10^9 M_{\odot}$) and rare objects which are only marginally ($\approx 1\%$) adding to the reionization photon budget.

VIVA (VLA Imaging of Virgo in Atomic gas): HI Stripping in Virgo Galaxies

Aeree Chung[1], J. H. van Gorkom[2], Hugh Crowl[3], Jeffrey D. P. Kenney[3], Bernd Vollmer[4]

[1]NRAO/UMass, USA
[2]Columbia University, USA
[3]Yale University, USA
[4]Observatoire astronomique de Strasbourg, France

We present results of a new Very Large Array survey of 53 Virgo galaxies (48 spirals and 5 dwarf/irregular systems). The goal is to study how the HI gas properties get affected by the cluster environment. The survey covers galaxies in a wide range of densities from the center of the cluster to more than 3 Mpc from M87. The gas is imaged down to a column density sensitivity of a few times 10^{19}cm^{-2}. We find examples of gas stripping at all stages. Within $\sim$0.5 Mpc distance from M87, most galaxies are severely HI stripped. The HI disks are truncated to well within the optical disks. While the HI looks asymmetric, the outer stellar disks look undisturbed. The fact that only the gas and not the stars has been stripped suggests that those galaxies have been affected by the hot and dense cluster gas. Interestingly we also find a few truncated disks at large projected distances from the center. Although some of these may have been stripped while crossing the cluster core, a detailed population synthesis study of the outer disk of one of these shows that star formation was terminated recently. The time since stripping is too short for the galaxy to have traveled from the core to its current location. So at least one galaxy has lost its gas from the outer disk by another mechanism than ram pressure stripping in the dense cluster core.

At intermediate to low density regions (>0.6 Mpc) we find HI tails with various lengths. We find seven galaxies with long one sided HI tails pointing away from M87. The galaxies are at 0.6-1 Mpc from M87. Since these galaxies are only midly HI deficient and the tails point away from M87 these galaxies are probably falling into the cluster for the first time on highly radial orbits. For all but two of the galaxies the estimated ram pressure at their location in the cluster would be sufficient to pull out the HI in the very outer

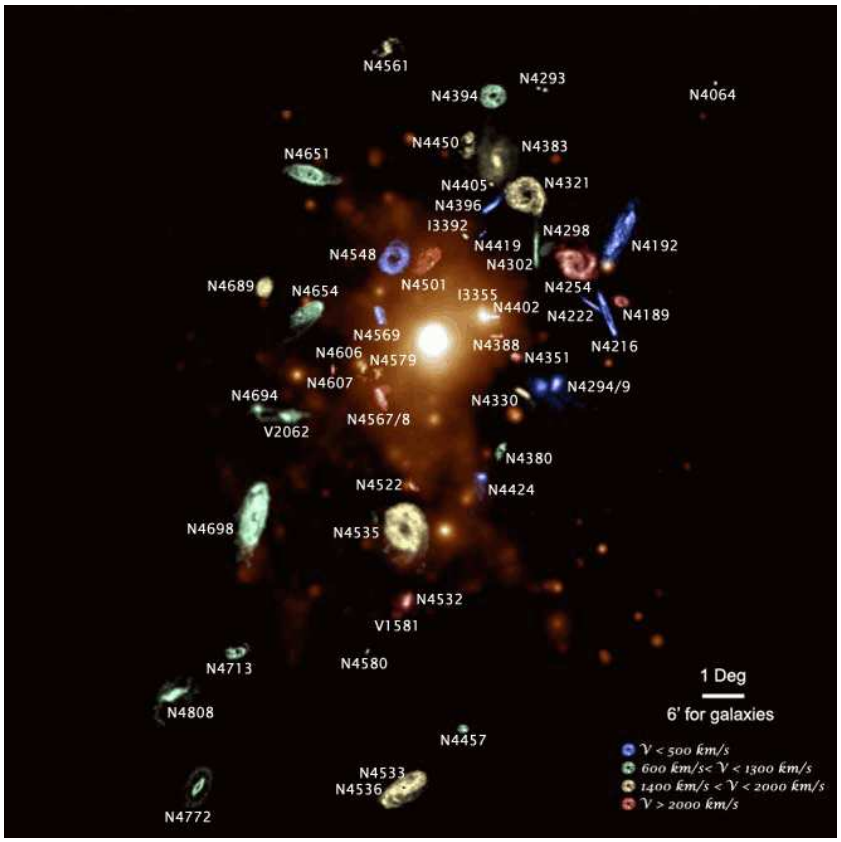

Figure 1: The image shows the distribution of HI gas of 53 galaxies in the Virgo cluster overlaid on the X-ray emission from the hot intracluster gas (ROSAT). The field is 20×20 deg^2 size and centered at $\alpha = 12^h32^m0^s$, $\delta = 10°30'$. The galaxies are placed at their proper positions. We have blown up the HI images by a factor 10 and they are color coded based on velocity as indicated in the bottom-right corner.

disks. One galaxy also looks optically disturbed and a simulations suggests that a combination of rampressure plus a tidal interaction has pulled out the tail.

In the outskirts of the cluster we find several examples of tidally interacting galaxies. We possibly see evidence for some accresion of gas as well. Lastly the merging of subclusters with Virgo can cause bulk motions of the ICM. We see one example of a galaxy far out that appears to be ram pressure stripped by a dynamic ICM.

In summary our results show that galaxies already get affected in the low density outer regions of the cluster through ram pressure stripping and tidal interactions or a combination of both.

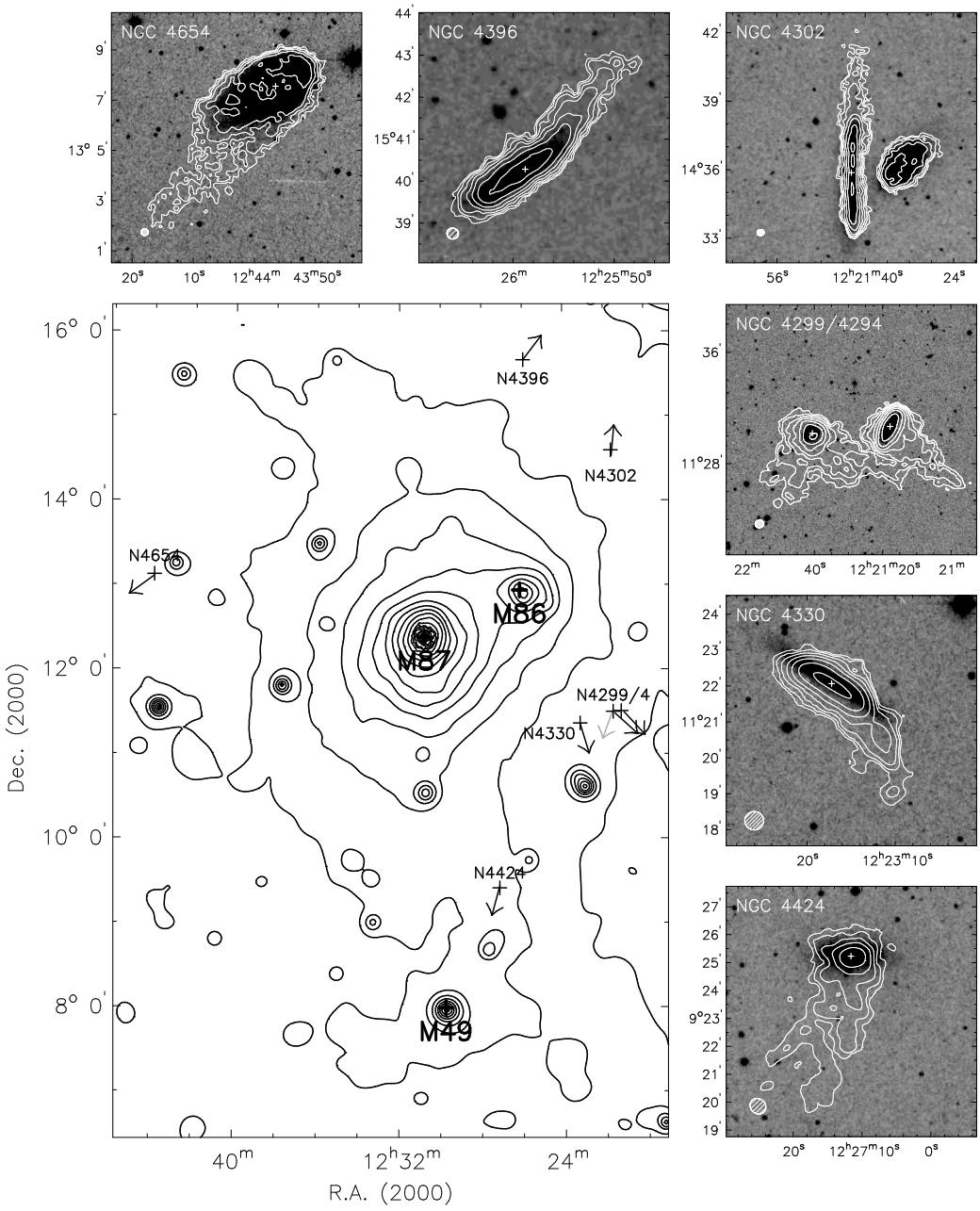

Figure 2: bottom-left) The locations of the HI tail galaxies are shown with the cross on the X-ray background of the Virgo region (0.5−2.0 keV, ROSAT). The directions of the tails are indicated with the arrow. The second tail of NGC 4299 (E tail) is shown in lightgray. Seven figures on the top and on the right, we show zoomed views of individual galaxies. The HI contours (white) are shown overlaid on the Digitized Sky Survey (DSS) image in grayscale. The galaxy name and the synthesized beam size appear in the upper-left and the bottom-left corner in each box. The white crosses indicate the optical center. The HI contours are 2.8 (NGC 4294/9), 6.7 (NGC 4302), 2.2 (NGC 4330), 4.3 (NGC 4396), 1.9 (NGC 4424), 13.0 (NGC4654)×1, 2, 4, 8, 16, ... in 10^{19} cm^{-2}.

21cm views of IGM reionization

Benedetta Ciardi

MPA, Garching, Germany

In the standard cosmological scenario, the diffuse gas (IGM), initially in a highly ionized state, is expected to recombine 450 thousand years after the Big Bang and to remain neutral until the first objects form and their UV radiation reionized the surrounding gas. This epoch marks the beginning of the reionization process, which is complete by $z \sim 6$.
The actual contraint on such process come mainly from observations of high-z QSOs spectra (which give information on the latest stages of reionization) and from cosmic microwave background (CMB) anisotropies (which provide an estimate of the global amount of electrons produced during reionization), but no information is available on the history of reionization and its sources. The most promising tool for observation of the reionization process is the 21cm line emission from neutral hydrogen in the IGM, which will map the temporal evolution of cosmic reionization. It has long been known that HI in the IGM and gravitationally collapsed systems may be directly detectable in emission or absorption against the CMB at the frequency corresponding to the redshifted HI 21cm line (associated with the spin-flip transition from the triplet to the singlet ground state). Nevertheless, only the planned generation of low frequency radio telescopes will allow its detection in the redshift range of interest. Among these new facilities, LOFAR (observing in the frequency range 30-90 MHz and 115-240 MHz) is presently being built in Holland and other European countries.
In this talk I will give a general introduction on reionization and 21cm line. I will then present predictions of 21cm line emission from different reionization histories discussing their observability, the possibility of using such measurements in combination with observations of CMB, the contamination of the signal by foreground sources, the physical conditions under which emission of the line is to be expected.

The work presented is done in collaboration with T. Di Matteo (CMU), A. Ferrara (SISSA), I. Iliev (CITA), P. Madau (UCSC), F. Miniati (ETH), I. Pelupessy (CMU), E. Scannapieco (UCSB), R. Salvaterra (U Insubria), P. Shapiro (UA Texas), F. Stoehr (ESO), M. Valdes (SISSA), S. White (MPA)

Barions and Dark Matter in outer disks

Francoise Combes

Observatoire de Paris, LERMA, 61 Av. de l'Observatoire, F-75014, Paris, France

Context: In the concordance model, the density of baryons in the Universe is now well known (Ω_b =0.045), and an essential problem remains, to identify where and under which form are the dark baryons which are missing. Visible baryons in stars and gas in galaxies and galaxy clusters represent only about 10% of them. At low redshifts another 30% of the baryons can be found in the photoionized Ly-α forest (gas at T$\sim$ 10^4 K) (Shull et al. 2005, Lehner et al. 2006). Other baryons are hiding in the warm/hot IGM (WHIM), gas that has been shock-heated to temperatures $> 10^5$ K (Cen & Ostriker 1999; Nicastro et al 2005); their fraction is the most uncertain, but they could account for another 10%.

Thus, about 50% of the baryons are not yet identified. Where are they? A small fraction could reside within galactic disks, but the HI rotation curves limit their amount to about 10%, doubling the visible baryons there. Most of them should be in the intergalactic medium, along matter filaments, that connect to and include galaxies.

Baryons in filaments will be hard to identify, since they are widely diluted; it appears more easy to tackle their mass in the outer parts of galaxies, which could be as large as that visible inside galaxies. A likely location for the missing baryons is in molecular clouds in the external parts of galaxies, that are numerous (10^{11}), small (AU size), very cold (10 K), and massive (10^{-3} to one solar mass) (Valentijn 1991, Lequeux et al. 1993, Pfenniger & Combes 1994). Indirect evidences for such a cold molecular component comes from the fact that the rotation curves of many galaxies can roughly be modelled by assuming a component that is about 5–10 times more massive as the neutral hydrogen (HI), with the same radial distribution (Hoekstra et al. 2001, Combes 2002). Many authors have tried to constrain the amount of dark matter residing in galactic planes (e.g. Kalberla et al 2007).

Tracers: The tracer of molecular gas that is most easily observed is CO. In the inner regions of galaxies, it is probably a good tracer, as the

metallicity is high and the gas is relatively warm (although even in the solar neighborhood, evidence of dark gas has been found, Grenier et al 2005). In the outer regions of galaxies, CO emission disappears, and Hα emission becomes too faint. However, there is indirect evidence for molecular gas not traced by CO. Thilker et al (2005) have shown with GALEX FUV emission that ionised gas and star formation are present well outside the optical disk, far from the Hα truncation, and traced by the HI gas. Deep search of CO emission in the outer parts of galaxies have succeeded to find weak emission, revealing that molecular gas can form far from the optical disk (Braine & Herpin, 2004).

If there is sufficient H_2 that is warmed to temperatures above 80 K, observable emission in the infrared can be generated. This H_2 emission is the best (because most direct) tracer of the very cold molecular gas – the emission only depends on the amount of H_2 and its temperature (which are derived from the observation), but not on the unknown metallicity of the gas. Tantalizing evidence for the presence of warm H_2 in the outer parts of galaxies comes from the detection of H_2 S(0) and S(1) emission in the outer disk of NGC 891 (Valentijn & van der Werf 1999).

Pure rotation lines of H_2 have been detected with ISO and Spitzer, in many different environments, and sometimes serendipitously. They are quite easy to detect in ULIRGs, as shown by the survey in 77 starbursts between z=0.02 and 0.93 (Higdon et al 2006), where the deduced warm H_2 mass corresponds to about 1% of all the molecular hydrogen, deduced from the CO emission. They are more surprising in the intergalactic space within the Stephan's quintet, where they are excited by a large-scale shock (Appleton et al 2006); they are coexistent there with very low excitation ionized gas, with no PAH features. They are also detected in the nascent starburst NGC1377 (Roussel et al 2006), and very intense in cooling flow filaments (Egami et al 2006).

In some circumstances, although its metallicity is low, a possible tracer of the cold gas could be cold dust emission. This is true in external galaxies, where the CO emission is poorly excited, and where the ISM emission is dominated by the HI (e.g. NGC 4565, Neininger et al 1996). The cold dust emitting in the millimeter domain is more extended radially than the CO line emission, and follows the HI. Similarly, Miville-Deschênes et al (2005) report the first detection of dust emission in a high velocity cloud (HVC), although no CO has yet been detected (e.g. Dessauges-Zavadsky et al. 2007). HVC are a possible manifestation of gas infall in our Galaxy.

Gas infall: Several observations at the galaxy scale require some level of external gas infall onto galaxies: these come from stellar populations, their metallicity distribution and the well known G-dwarf problem (e.g. Rocha-Pinto & Maciel 1996), and also from the almost constant star formation rate (SFR) inferred for spiral galaxies in the middle of the Hubble sequence (e.g. Kennicutt et al 1994). The high frequency of HI warps observed in galaxies is only accounted for by external gas and dark matter accretion. The amount of matter accretion required, with an angular momentum misaligned with that of the inner parts, can re-orient the whole system in 7-10 Gyr, (Jiang & Binney 1999). The same order of magnitude of accretion is required to explain the bar frequency (Block et al 2002).

Cosmological simulations begin to shed light on how matter is assembled in galaxies, and in particular about cold and hot gas. Until recently, the spatial resolution and density dynamical range was insufficient to take into account the cool gas phase. But cold accretion is now emphasized, in parallel to hot gas accretion, after shock heating to the Virial temperature of the structures (e.g. Keres et al 2005). The possibility of cold gas flowing along filaments would explain the difference between the sequence of massive red galaxies, and the blue light ones (Dekel & Birnboim 2006). The angular momentum problem, and the size of spiral disks require also recent accretion of gas (D'Onghia et al 2006).

The challenge of this contribution is to try to build a coherent scenario including all these recent results, on how gas is accreted in galaxies, and how stability, star formation can be accounted for in spiral disks. The various remaining problems will be discussed.

The Clustering of Damped Ly-a Absorbers with $2.5 < z < 5.0$ Lyman Break Galaxies

Jeff Cooke[1], Arthur M. Wolfe[2], Jason X. Prochaska[3], Eric Gawiser[4]

[1] Center for Cosmology and the Department of Physics and Astronomy, University of California, Irvine, Irvine, CA, 92697-4575
[2] Department of Physics and Center for Astrophysics and Space Sciences, University of California, San Diego, La Jolla, CA, 92093-0424
[3] Department of Astronomy and Astrophysics, UCO/Lick Observatory; University of California, 1156 High Street, Santa Cruz, CA, 95064
[4] Yale Astronomy Department and Yale Center for Astronomy and Astrophysics, New Haven, CT, 06520

Context: The damped Ly-α absorbers (DLAs) are the highest column density QSO absorption-line systems, defined as having N(HI) $> 2 \times 10^{20}$ atoms cm^{-1} (Wolfe et al. 1986,2005). DLAs are large reservoirs of neutral gas, containing $\sim 80\%$ of the HI content of the universe (Prochaska et al. 2005). The belief that DLAs are capable of evolving into present-day galaxies like the Milky Way (Kauffmann 1996) follows from several lines of evidence that include the high-resolution analysis of DLA gas kinematics (Prochaska & Wolfe 1997,1998 and Wolfe & Prochaska 2000) and the agreement between the comoving neutral gas density at $z > 2$ and the mass density of visible stars in local disks (Wolfe et al. 1995). Over the last two decades, DLAs in the sightlines to bright QSOs have allowed high-resolution analysis of their properties. However, the glare of background QSOs has prevented the measurement of the luminosity and morphology of nearly all DLAs and has kept the fundamental properties of mass and luminosity elusive. The measurement of the DLA mass at high redshift can discriminate between various morphological models and provide an important step toward understanding the nature of these systems that cover one-third of the sky out to $z \sim 4$.

Aims: The mass of high redshift galaxies can be inferred by their spatial distribution in the context of the ΛCDM model. In the early universe, high-mass galaxies formed clustered near peaks of overdense regions whereas low-mass galaxies formed more uniformly throughout the universe. Measurement of the spatial distribution of galaxies via the correlation function

$\xi(r)$ has been successful in determining the typical mass of the Lyman break galaxies (LBGs) at high redshift (e.g., Steidel et al. 1998, Adelberger et al. 1998). Because of the sparse distribution of DLAs in QSO sightlines, the DLA correlation function is much more difficult to obtain. However, the mass of DLAs can be inferred from the cross-correlation of DLAs with another known population. We use the distribution of DLAs with LBGs in a narrow-field survey of galaxies at $z \sim 3$ and a wide-field survey of galaxies at $z \sim 4$ to make the first measurement of the DLA-LBG cross-correlation function. From this, we calculate the DLA galaxy bias (e.g., Mo et al. 1998) and infer the typical mass of high redshift DLAs.

Results: We obtained the spectra of ∼250 LBGs at $z \sim 3$ and used their spatial distribution with 11 DLAs to successfully measure the 3-D LBG auto-correlation function and make the first measurement of the 3-D DLA-LBG cross-correlation function. We measured the correlation functions via conventional binning and a maximum likelihood analysis and found the results from both methods agree within the uncertainties. Here we report the values from the maximum likelihood method. Using the fiducial model of the correlation function $\xi(r) = (r/r_0)^{-\gamma}$ we found best fit values and 1σ confidence levels of $r_0 = 2.91^{+1.0}_{-1.0}$, $\gamma = 1.21^{+0.6}_{-0.3}$ ($r_0 = 3.32^{+0.6}_{-0.6}$, for a fixed $\gamma = 1.6$) for the LBG auto-correlation and $r_0 = 2.81^{+1.4}_{-2.0}$, $\gamma = 2.11^{+1.3}_{-1.4}$ ($r_0 = 2.93^{+1.4}_{-1.5}$, for a fixed $\gamma = 1.6$) for the DLA-LBG cross-correlation function (Figure 1). Our results for the LBG auto-correlation are lower than Adelberger et al. (1998,2003) but agree within the uncertainties. We derive galaxy bias for both populations and calculate a typical mass of $10^{9.7} < \langle M_{LBG} \rangle < 10^{11.6}\ M_\odot$ for LBGs and $10^9 < \langle M_{LBG} \rangle < 10^{12}\ M_\odot$ for DLAs at $z \sim 3$. From all measurements and tests (see Cooke et al. 2006), we find strong evidence for an overdensity of LBGs near DLAs, equivalent to that of LBGs near other LBGs, and conclude that DLAs likely reside in the same regions that harbor LBGs.

To refine these results, we obtained the spectra of ~ 500 LBGs at $z \sim 4$ from a deep wide-field survey (one square degree) to correlate with four DLAs. We find additional field DLAs in the sightlines to $I < 23$ LBGs and QSOs and use these to improve the correlation statistics. Nearly complete, the results from this analysis will improve the DLA-LBG cross-correlation to $\sim 3\sigma$. Finally, two of the six QSOs discovered in the $z \sim 3$ survey were found within $\Delta z = 0.0125$ of two survey DLAs (Figure 2). We estimate a 1 in 940 probability of this occurring by chance. We find a similar QSO-DLA distribution in the $z \sim 4$ survey data. This suggests an interesting relationship between the distribution of QSOs and DLAs at high redshift.

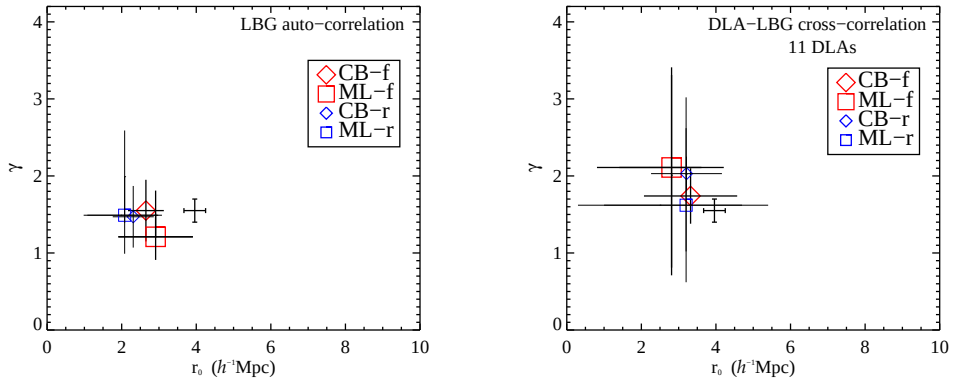

Figure 1: Best fit values and 1σ errors for the LBG auto-correlation *(right)* and the DLA-LBG cross-correlation *(left)*. In both plots, the best-fit values are determined by conventional binning *(CB)* and maximum likelihood *(ML)* methods. We test the results using fixed *(f)* and random *(r)* angular values *(see Cooke et al. 2006)*.

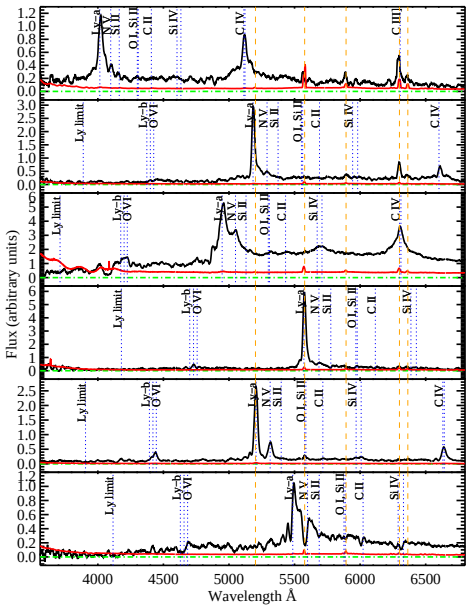

Figure 2: Six faint $21 < R < 25$*)* QSOs discovered in the $z \sim 3$ survey. The third and fifth QSO from the top are within $\Delta z = 0.0125$ of 2 survey DLAs.

The CODEX@ELT and ESPRESSO@VLT experiment

Stefano Cristiani

INAF-Osservatorio Astronomico di Trieste, via G.B. Tiepolo 11, I-34131 Trieste, Italy

The COsmic Dynamics EXperiment (CODEX) at the E-ELT and its precursor, the Echelle Spectrograph for PREcision Super Stable Observations (ESPRESSO) at the VLT, will open new horizons in the study of the IGM and, more in general, in cosmology.

The Proximity Effect along single lines of sight

Aldo Dall'Aglio[1], Lutz Wisotzki[1], Nick Gnedin[2], Gabor Worseck[1]

[1] Astrophysikalisches Institut Potsdam, An der Sternwarte 16, D-14482 Potsdam, Germany,
[2] Fermi National Accelerator Laboratory, Batavia IL 60510

Context: The surrounding regions of strong UV sources such as bright quasars are characterised by a local enhancement of the HI photoionization rate leading to a reduction of the neutral hydrogen fraction. This enhances the transparency of the intergalactic medium and should become observable as a weakening of the Lyman forest absorption near such sources. This is the so-called proximity effect detectable on the blue wing of the Lyα emission line of the ionising source.

Aims: We exploit a set of high signal-to-noise (~ 70), low-resolution ($R \sim 800$) quasar spectra to search for the signature of the enhanced UV radiation field in the HI Lyα forest. Our sample consists of 17 bright quasars in the redshift range $2.7 < z < 4.1$. We also perform extensive Monte-Carlo simulations to understand systematic and statistical effects involved in our analysis. To further develop a theoretical framework indispensable to interpret our results, we additionally conduct hydro 3D simulations.

Results: Analysing the spectra with the flux transmission technique, we detect the proximity effect in the combined sample at high significance. We use this to estimate the average intensity of the metagalactic UV background, assuming it to be constant over the observed redshift range. We obtain a value of $J = (9.5 \pm 4.5) \times 10^{-22}$ erg cm^{-2} s^{-1} Hz^{-1} sr^{-1}, in good agreement with previous measurements at similar z. We then apply the same procedure to individual lines of sight, finding a significant decrease of the optical depth close to the emission redshift in every single object except one (which by a different line of evidence does nevertheless show a noticeable proximity effect).

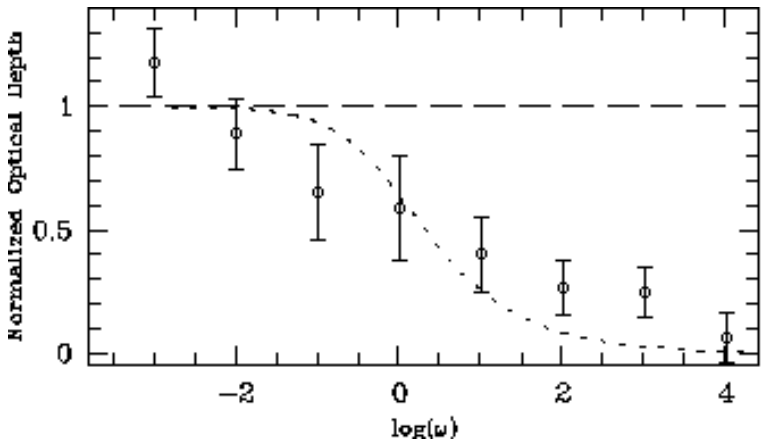

Figure 1: Optical depth versus ω profile for the combined sample of 17 quasars, binned in steps of $\Delta \log \omega = 1$. The signature of the proximity effect is clearly visible. The dotted line is the best fit of the simple photoionisation model to the data, corresponding to a UV background of $\log(J_\nu) = -21.02$. The dashed line refers to the case of no proximity effect.

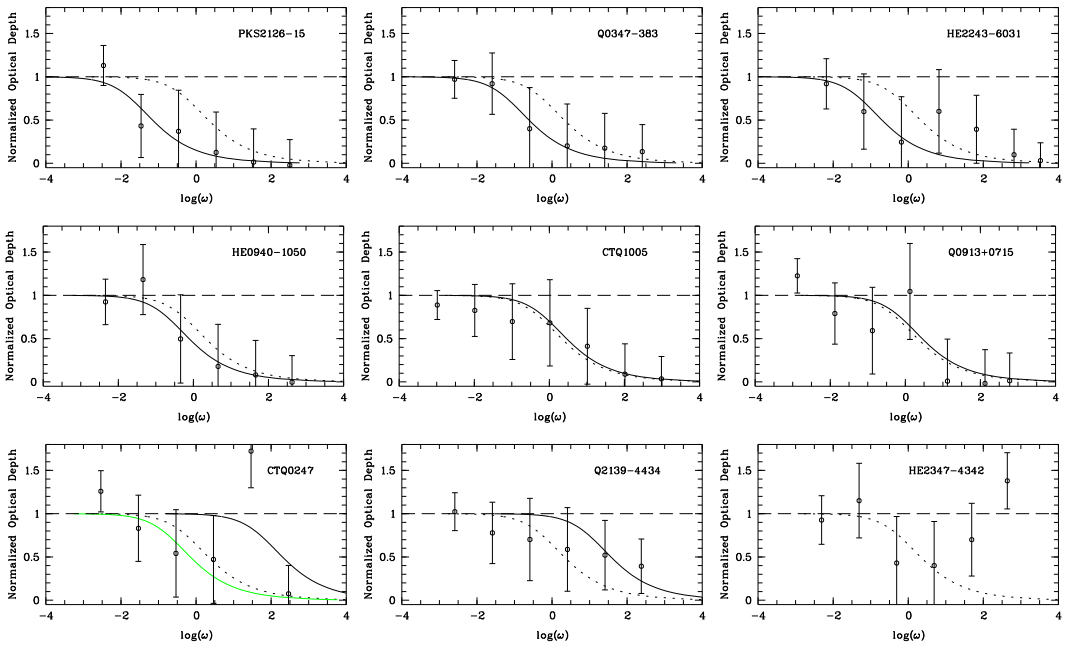

Figure 2: Search for proximity effect signatures in individual lines of sight, for all 17 QSO spectra. Each panel shows the normalized optical depth ξ versus ω in the same way as Fig. 1, with the best-fit model of the combined analysis superimposed as dotted lines. The solid lines delineate the best fit to each individual QSO as described in the text. For CTQ 0247 we also plot the best fit excluding the strong absorption at $z \sim 3.014$ (green curve). The panels are sorted in order of decreasing strength of the proximity effect (horizontal displacement of solid and dotted lines). HE 2347−4342 has no detectable proximity effect in HI.

LOFAR and the search for HI at z=6-11.5

A.G. de Bruyn[1,2] for the LOFAR EoR core team[1,2]

[1] ASTRON, Dwingeloo, The Netherlands,
[2] Kapteyn Institute, University of Groningen, The Netherlands

Context: LOFAR is a next generation radio telescope working in the frequency bands from 10-80 and 115-240 MHz. We will review the LOFAR EoR Key Science Project.

Aims: Simulations constrained by WMAP3 results suggest that LOFAR will be able to probe an important part of the HI evolution in the Universe during the era of reionization; the frequency range covered by LOFAR will cover redshifts from z = 11.5 to z = 5. Several hundred hours of integration time will be required to detect the feeble statistical HI signals at the expected 5 - 10 mK brightness temperature levels.
The observing strategy and the most important technical and astronomical issues facing the project will be discussed. Among these are wide-field ionospheric phase calibration, station beam calibration, (polarized) Galactic foreground contamination, chromatic confusion due to the global sky and the signal extraction methodology. We will also briefly discuss some simulations of the end-to-end signal processing.

Results: The first station of LOFAR (core station 1 or CS-1) was completed in the spring of 2007. It has taken data in both the 10 - 80 and 115 - 240 MHz bands. Some images will be shown. The first observations for the EoR project are scheduled for the autumn of 2008. The hardware of LOFAR is scheduled to be completed by mid 2009.

The HI Content of Early-Type Galaxies

Sperello di Serego Alighieri[1], Giuseppe Gavazzi[2], Carlo Giovanardi[1], Riccardo Giovanelli[3], Marco Grossi[1], Ginevra Trinchieri[4]

[1] INAF – Osservatorio Astrofisico di Arcetri, Largo E. Fermi 5, Firenze, Italy,
[2] Università di Milano–Bicocca, Piazza delle Scienze 3, Milano, Italy,
[3] Cornell University, Ithaca, NY 14853, U.S.A.,
[4] INAF – Osservatorio Astronomico di Brera, Via Brera 28, Milano, Italy

Context: Early-Type galaxies (ETG), in particular the massive ones, contain large quantities of hot gas ($T \geq 10^6 K$), which has been well studied from its X–ray emission. Some of them also have ionized gas ($T \sim 10^4 K$), as documented with emission–line surveys. On the other hand the cold gas ($T \leq 10^3 K$) content of ETG is poorly known: only a few objects have been looked at for HI and an unbiased survey of the whole class of ETG is still lacking.

The Arecibo Legacy Fast ALFA HI survey (ALFALFA), initiated in 2005 using the new multi–beam Arecibo L–band Feed Array (ALFA), provides a unique opportunity to fill this gap, since it is surveying in an unbiased way about 7000 deg^2 of high galactic latitude sky to $cz \sim 15000$ km/s and it is designed to detect objects with an HI mass of $\sim 2 \times 10^7 M_\odot$ at the Virgo cluster distance.

Aims: We are using the ALFALFA survey to study the HI content of ETG in an unbiased way. The aim is to get a complete picture of the hot, warm and cold ISM of ETG, as a function of galaxy mass and environment, and to relate it to the formation and evolution history of these objects.

Results: We have correlated the catalogue of HI sources obtained from the ALFALFA survey for the 8-16 deg. declination strip on the Virgo cluster (Giovanelli et al. 2007, astro–ph/0702316) with the 939 ETG contained in the same declination strip in the Virgo Cluster Catalog of Binggeli et al. (1995, AJ 90, 1681), and found a total of only 10 sources in common. We will present a preliminary analysis of these sources.

Frozen HI: HIPASS finds no dark HI clouds?

Michael Disney

Cardiff University, UK

As HI detectors become ever more sensitive one has to worry about 21-cm excitation mechanisms, and in particular Spin Temperature. The fact that HIPASS never finds HI unassociated with stars is disturbing. Is there no HI out there in intergalactic space? Can its lack always be attributed to ionisation? What is going on? Why didn't the dog bark in the night?

The HI picture from the Lyman-α forest at $z \sim 2-3$

Valentina D'Odorico[1], Marialuce Bruscoli[2], Francesco Saitta[3,5], Stefano Cristiani[1], Fabio Fontanot[4], Pierluigi Monaco[5], Matteo Viel[1]

[1]INAF - Osservatorio Astronomico di Trieste, Via Tiepolo 11, I-34143 Trieste, Italy
[2]INAF - Istituto di Radioastronomia, Sezione di Firenze, Largo E. Fermi 5, Firenze I-50125, Italy
[3]European Southern Observatory, Karl-Schwarzschild-Str. 2, D-85748 Garching bei München, Germany
[4]Max-Planck-Institute for Astronomy, Königstuhl 17, D-69117, Heidelberg, Germany
[5]Dipartimento di Astronomia, Università degli Studi di Trieste, Via Tiepolo 11, I-34143 Trieste, Italy

Context: The study of QSO absorption lines has undergone in the last decade a major improvement thanks mainly to three complementary factors: the advent of 8-10m class telescopes coupled with high-efficiency, high-resolution spectrographs, the compilation of incredibly extended QSO and galaxy surveys, and the development of complex semi-analytical and hydrodynamical simulations reproducing the formation and evolution of structures in cosmological volumes. In this framework, the so called Lyman-α forest, i.e. the large number of HI Lyman-α absorption lines observed in the optical spectra of QSOs at redshifts larger than $\simeq 2$, has gained a great relevance in cosmology. Indeed, simulations have shown (e.g. Cen et al. 1994; Bi & Davidsen 1997) that this plethora of lines is principally due to the fluctuations of the intermediate to low density intergalactic medium (IGM), following the hierarchical process of structure formation. This low density gas is governed by the Hubble expansion and by gravitational instabilities, as a consequence the physics involved is quite simple and mildly linear.

The ESO Large Programme 'The Cosmic Evolution of the IGM' (LP; Bergeron et al. 2004, ESO The Messenger, 118, 40) has gathered the UVES spectra of 18 QSOs with emission redshifts in the range $\sim 2.1-3.3$ at very

high resolution, ($R \simeq 45000$, corresponding to a FWHM ~ 6.7 km s^{-1}), and high signal-to-noise ratio (typically SNR ~ 35 and 70 per pixel at $\lambda\,3500$ and 6000 Å, respectively).

In this talk, I will briefly review the latest analysis we have carried out on the LP QSO spectra regarding in particular, the clustering properties of the IGM gas, the estimate of the UV background intensity from the proximity effect, and the distribution of metals in the low density gas. I would also like to present the serendipitous discovery of a peculiar metal absorption system showing, for the first time in a QSO spectra, associated absorption lines due to Si I, Ca I, and Fe I.

Preliminary results: We carried out the classical statistical studies with Lyman-α lines (see Figs. 1 and 2).

However, one of the main goal of our study was to identify a new statistical indicator overcoming the drawbacks characterizing both the analysis based on the fitting and counting of absorption lines and those based on the transmitted flux, and keeping, at the same time, the advantages of both approaches. We developed a new algorithm to transform the lists of HI column densities of absorption lines into a smooth H density field and tested it against numerical simulations. The redshift evolution and clustering properties of the density field are determined and the proximity effect due to QSOs is clearly detected.

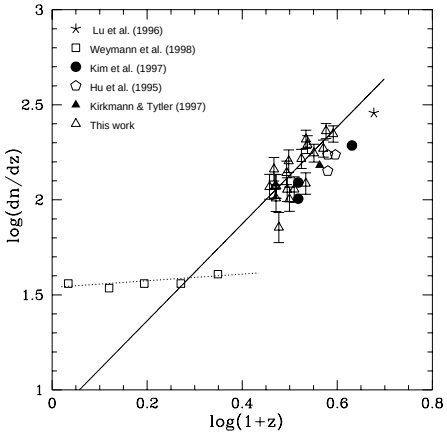

Figure 1: Number density evolution of the Lyman-α forest lines in the column density range $13.64 < \log N(\mathrm{HI}) < 17$ cm^{-2} for the QSOs in our sample (open triangles). For comparison we report also previous measurements at high redshit and the result of the low redshift HST campaign.

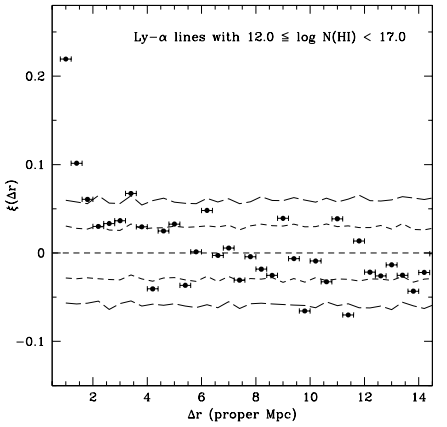

Figure 2: Two-point correlation function vs proper spatial separation for the Lyman-α forest lines in the column density range $12.0 \leq \log N(\mathrm{HI}) < 17$ cm^{-2} for the QSOs in our sample. The short and long-dashed lines indicate the 1 and $2\,\sigma$ confidence intervals, respectively.

Evidence for a Significant Population of Feeble Star-forming Sources at z∼8 and Beyond

Richard Ellis

Caltech, USA

I review recent attempts to constrain the abundance of star forming sources at epochs where cosmic reionization is now thought to occur. Both direct searches, using deep HST/Spitzer imaging and surveys conducted through powerful foreground gravitational lenses, are providing interesting constraints. Additional information is available from measures of the assembled stellar mass at lower redshifts (z∼5-6); this provides a valuable integral constraint on the earlier activity. Uncertainties abound but an emerging picture consistent with the data is an abundant population of low luminosity sources which may have dominated the reionization process at z∼10.

Galaxy sizes and environments probed by binary QSOs

Sara L. Ellison[1], Joe Hennawi[2], Crystal Martin[3],Jesper Sommer-Larsen[4]

[1] University of Victoria, Canada
[2] University of California, Berkeley, USA
[3] University of California, Santa Barbara, USA
[4] DARK Cosmology Centre, Denmark

Context: Damped Lyman alpha (DLA) systems provide detailed information on the neutral gas content and chemical abundances of galaxies from low to high redshifts. However, other simple parameters such as sizes, luminosities and environments remain largely unknown. One technique which can address the first of these unknowns is the use of binary and lensed QSOs to search for coincident absorption on kpc scales and build-up a statistical picture of DLA size. Measurements of DLA sizes from lensed QSOs are currently limited by the very small number (4) of DLAs that have been detected in lensed sightlines and by the small transverse scales that they probe. Two out of the four cases (Churchill et al. 2003, ApJ, 593, 203; Kobayashi et al. 2002, ApJ, 569, 676) probe very small scales (< 250 pc), leaving only two measurements on kpc scales ($d \sim 5$ kpc by Lopez et al. 2005, ApJ, 626, 767 and $d \sim 10$ kpc by Smette et al. 1995, A&AS, 113, 199). A few indirect limits of DLA sizes also exist, for example lower limits based on extended background radio emission (e.g. Foltz et al. 1988, Proceedings of the QSO Absorption Line Meeting; Briggs et al. 1989, ApJ, 341, 650) or on the unique case of transverse Lyα fluorescence discovered by Adelberger et al. (2006, ApJ, 637, 74).

Aims: We present observations of a close binary QSO, SDSS 1116+4118 AB, hereafter QSO A/B, with an angular separation between the two components (both at $z \sim 3$) of 13.8 arcseconds There are DLAs/sub-DLAs at three intervening redshifts: $z_{\rm abs} = 2.47, 2.66, 2.94$. The transverse physical separation of the two lines of sight corresponds to ~ 100 kpc at the redshifts of these absorbers. Despite the large separation, 2/3 of the intervening DLAs is seen as a DLA/sub-DLA in both lines of sight. We obtain Keck ESI spectra

with S/N $\sim$ 50 and spectral resolution of $\sim$ 60 km/s in order to determine N(HI) and metal column densities for the five intervening absorbers. We use cosmological hydrodynamic simulations and a clustering analysis to interpret this result in terms of galaxy sizes and environments.

Results: In Figure 1 we show the intervening DLAs and sub-DLAs with best-fit HI profiles as determined from our ESI spectra. Although metals are detected for all five absorbers, due to the potential of ionization corrections in sub-DLAs, we only determine element abundances for the 3 absorbers with log N(HI)>20. The $z_{\rm abs}$ = 2.66 DLA towards QSO A has [Zn/H]=$-$0.71, whereas only an upper limit of [Zn/H]=< $-$0.51 can be determined for the sub-DLA at the same redshift towards QSO B. For the DLA at $z_{\rm abs}$ = 2.94 towards QSO A we determine abundances of S, Si and Zn that are all approximately 1/3 solar (see Ellison et al. 2007, MNRAS in press, arXiv:0704.1816v1 for more details). We also derive an upper limit for the molecular H_2 fraction < -5.5 for this DLA, i.e. this DLA is poor in molecules, despite its relatively high metallicity.

In order to determine whether the coincident absorption across $\sim$ 100 kpc is likely to be due to single extended galaxies at $z_{\rm abs}$ = 2.66 and 2.94, we use high resolution SPH simulations taken from Sommer-Larsen, Götz & Portinari (2003, ApJ, 596, 46). We focus on two galaxies which have, at z=0, characteristic circular speeds of V_c=245 and 180 km/s. The galaxies bracket typical disk galaxy formation histories: the formation of the larger disk is merger induced, with the disk growing strongly between z=1 and 0, whereas the smaller galaxy starts developing a disk by $z \sim 2.5$, which subsequently grows gradually to the present epoch. We analyse the model galaxies by passing sightlines through the simulation box and integrating the HI volume density along the line of sight. We find that the probability of two coincidences, such as we see in our data, is $< 10^{-5}$ and therefore conclude that it is unlikely that we are observing single galaxies with a transverse dimension in excess of 100 kpc.

Having rejected a large single system, and a galaxy plus satellite structure (since satellites are included in the simulation boxes) as the reason for coincident absorption towards SDSS 1116+4118 AB, we now consider the possibility that we are observing a structure that contains multiple galaxies. We can estimate the likelihood of a multiple galaxy coincidence by considering the clustering scale of DLA galaxies and their column density distribution (e.g. Hennawi & Prochaska 2007, ApJ, 655, 735). Assuming that DLAs

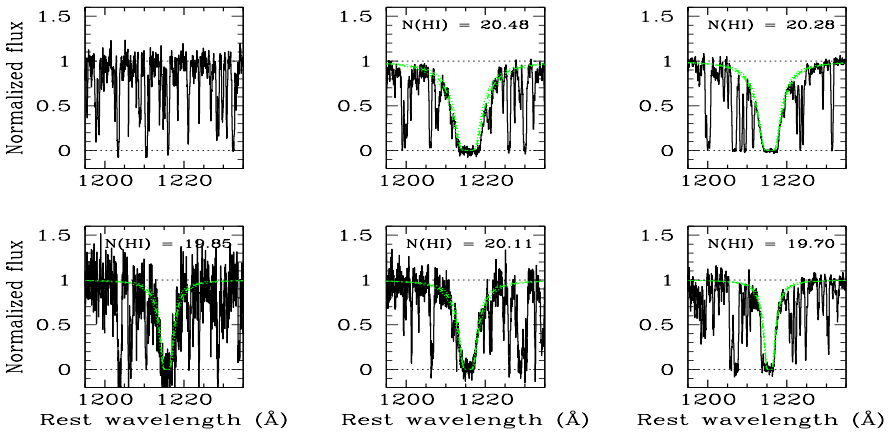

Figure 1: DLAs and sub-DLAs in the line of sight to SDSS1116+4118A (top panels) and SDSS1116+4118B (bottom panels). The redshifts are, from left to right, $z_{\rm abs} = 2.47, 2.66, 2.94$. Green lines show the best fit HI profile with errors in dashed green lines. See Ellison et al. (2007) for more details.

cluster like LBGs (Cooke et al. 2006, ApJ, 636, L9) we determine that the probability of finding coincident sub-DLA absorption (both absorbers N(HI) > 19.5) in the SDSS 1116+4118 AB binary within a $\pm$400 km/s window is 3–8%, depending on clustering parameters (see Ellison et al. 2007 for more details). Although the probabilities that we determine from the clustering analysis are not large ($< 10\%$ for a single coincident pair), they are more than an order of magnitude more likely than the probability of absorption from a single large galaxy. We therefore conclude that the coincident absorption is most likely to be probing a group environment.

The correlated absorption has interesting ramifications for single line of sight observations. The most simplistic extrapolation of the three intervening absorbers towards this one binary system indicates that $\sim 2/3$ of DLAs in single lines of sight are not simple systems. Since the superposition of DLAs with velocity differences < 1000 km/s will not be resolved in Lyα, such line of sight blending may often go unnoticed. Blending two absorbers with different N(HI) and metallicities can impact the abundances derived for the integrated system by several tenths of a dex and complicate the interpretation of kinematics.

Reionization constraints from high-z quasars

Xiaohui Fan

Univerisity of Arizona, USA

I will update the results on constraining reionization epoch using high-redshift quasars. I will first summarize the recent and ongoing high-z quasars surveys, then discuss using quasar absorption spectra to measure IGM neutral fraction at z$\sim$6. In addition to the classic Gunn-Peterson trough measurement, I will emphasize the ongoing efforts of using dark gap statisitcs and HII region size to constrain neutral fraction.

Ionized Gas in DLAs and sub-DLAs: Hidden Metal Reservoirs

Andrew J. Fox[1], Patrick Petitjean[1], Cédric Ledoux[2], Raghunathan Srianand[3]

[1] Institut d'Astrophysique de Paris, Paris, France
[2] European Southern Observatory, Santiago, Chile
[3] Inter-University Centre for Astronomy and Astrophysics, Pune, India

Context: Gaseous galactic halos can be traced using quasar absorption line spectroscopy. These halos can be detected in the form of damped and sub-damped Lyman-alpha (DLA/sub-DLA) systems, defined as QSO absorbers with log N(H I)$>$ 20.3 and with 19.0$<$log N(H I)$<$ 20.3, respectively. By studying the highly ionized lines Si IV, C IV, N V, and O VI in absorption in DLAs, one can trace the warm ionized and hot ionized components of the host galaxy's interstellar medium.

Aims: We have assembled a sample of high-resolution, high signal-to-noise quasar spectra provided by the Ultraviolet and Visible Echelle Spectrograph (UVES) on the VLT, in order to carry out a quantitative study of ionized halos in the young ($z > 2$) Universe. Our goals are to characterize the kinematics of the O VI and C IV profiles, to diagnose the origin of the ionized gas, and to measure the contribution of the ionized plasma in DLAs to the high-redshift baryon and metal budgets.

Results: O VI absorption is detected in 12 DLAs out of 35 cases with coverage of the O VI wavelength (Fox et al. 2007a, A&A, 465, 171). In the other cases the blending is to severe to make a statement about the presence of O VI. In three of these twelve N V is also detected. One sub-DLA from the UVES sample also shows a strong O VI detection. C IV absorption is detected in all DLAs and sub-DLAs where data is available (Wolfe & Prochaska 2000, ApJ, 545, 591; Fox et al. 2007b, A&A, submitted). The typical high-ion column densities in DLAs are of the same order as those in the Milky Way, despite the low metallicities in these systems (median [Z/H] in the C IV sample is -1.36, Ledoux et al. 2006, A&A, 457, 71).

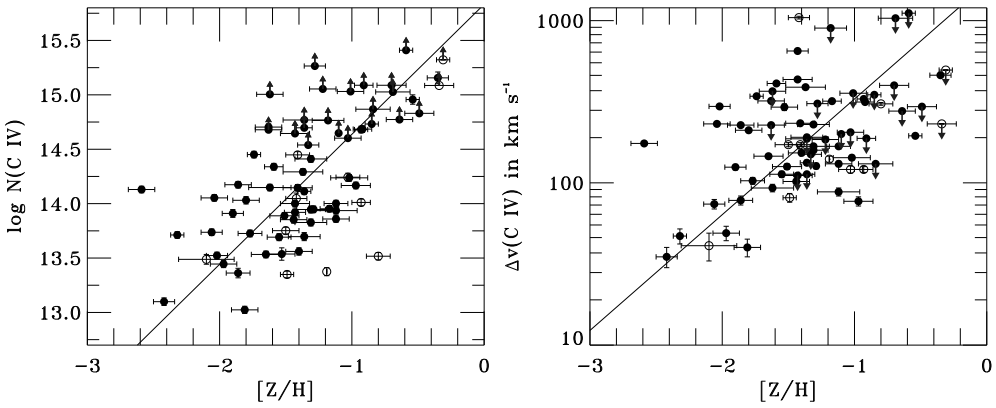

Figure 1: Observed correlations between metallicity and C IV column density (left) and line width (right). DLAs: filled circles, sub-DLAs: open.

The component structure of the C IV and O VI profiles suggests that both warm ionized and hot ionized plasma phases are present in DLA host galaxies. The warm ionized gas is seen in narrow ($b < 10$ km s^{-1}) components of C IV (and Si IV), and is likely photoionized, either by photons in the extragalactic ionizing background, or from local sources of UV radiation. The hot ionized gas is traced by broad ($b \approx 30$ km s^{-1}) components of O VI and C IV. This gas is collisionally ionized and could result from supernova-driven processes that follow star formation in the DLA host galaxies, or from the accretion and shock-heating of infalling intergalactic gas.

We find that the strength and line width of the C IV absorption are each strongly correlated to the DLA metallicity, which is measured in the neutral phase of the gas. These correlations, shown in Figure 1, are also found independently in the lower- and upper- redshift halves of the sample.

Based on the 12 DLAs with O VI detections, we determine that the column density ratio N(Hot H II)/N(H I) in DLAs is >0.4. Based on 73 DLAs and sub-DLAs with C IV detections, we determine that the ratio N(Warm H II)/N(H I) in DLAs is >0.1. Adopting the value of Ω(H I) from Prochaska et al. 2005 (ApJ, 635, 123), and the maximum allowed O VI ionization fraction, we find that the O VI DLAs represent >1% of the metal budget at $z \approx 2.5$. However, if the temperature in the hot ionized gas were much higher than 300 000 K, the O VI ionization fraction would be much lower, and the contribution of ionized gas in DLAs to the metal budget would

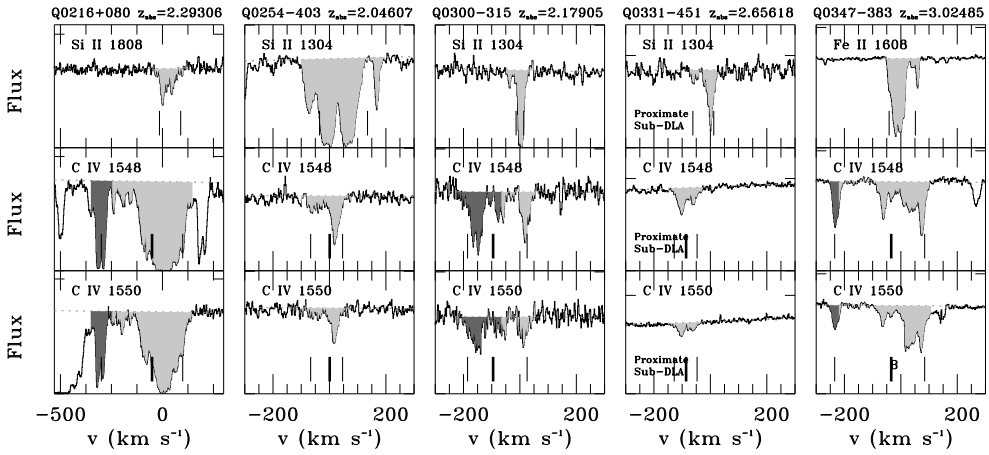

Figure 2: C IV and neutral gas profiles in four DLAs and one sub-DLA from the UVES sample. Candidate winds are shaded in dark.

consequently be much higher. Sutherland & Dopita (1993, ApJS, 88, 253) report an O VI ionization fraction of 0.004 for gas in collisional ionization equilibrium at 10^6 K. If the gas were this hot, the O VI would represent the tip of the iceberg, with the majority of the oxygen atoms ionized up to O VII and O VIII.

We are able to estimate the escape velocity in each DLA system using the relation $v_{\rm circ} = 0.6\Delta v_{\rm Neut}$, found in CDM simulations by Haehnelt et al. (1998, ApJ, 595, 647). $\Delta v_{\rm Neut}$, the line width of the neutral species, is directly measured in the data. In 30 of 73 systems, we observe C IV absorption above the escape velocity $v_{\rm esc} = \sqrt{2}v_{\rm circ}$, i.e. wind candidate absorbers are seen in $\approx$40% of the systems; the spectra of several are shown in Figure 2. If the C IV-absorbing gas lies far from the bottom of the potential well, the local escape speed will be lower. The derived mass flow rates in these winds have a median value of $8\,{\rm M}_\odot\,{\rm yr}^{-1}$, assuming a characteristic C IV radius of 40 kpc. These high-velocity C IV components are unlikely to trace satellite galaxies, since there is no neutral gas absorption at these velocities. Instead, the components are more analogous to the highly ionized high-velocity clouds seen in the vicinity of the Milky Way (Collins et al. 2005, ApJ, 623, 196; Fox et al. 2006, ApJS, 165, 229).

The Gaseous Haloes of Spiral Galaxies

Filippo Fraternali

Department of Astronomy, University of Bologna, Italy

Context: Recent observations show that the discs of nearby spiral galaxies are surrounded by massive haloes of both neutral and ionized gas. Such haloes extend to large distances (tens of kpc) and have a low angular momentum with respect to their discs. They are probably analogous to the Intermediate and High Velocity Clouds of the Milky Way.

Aims: The origin of the gaseous haloes is still a matter of debate. They may be generated by supernova outflows from the disc (galactic fountain) and/or by gas accretion from the intergalactic space. If the latter is the case their study may provide a way to quantify the gas accretion rate onto galaxies.

Results: Both theory and observations show that a large fraction of the halo gas is produced by galactic fountain flows. However, it appears that such processes alone cannot explain the observed kinematics and that gas accretion must play an important role.

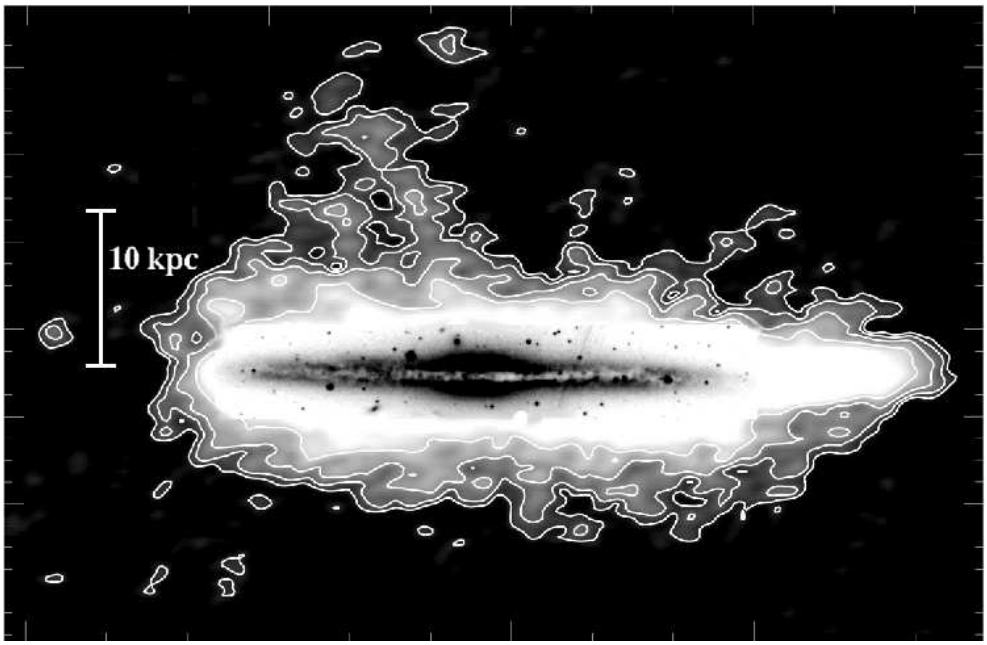

Figure 1: The edge-on spiral galaxy NGC891: optical (grayscale) + neutral hydrogen (white shade + contours). The neutral gas forms an extended halo surrounding the disc with a filament reaching more than 20 kpc from the plane.

Was the Universe neutral beyond redshift six?

Simona Gallerani[1], Andrea Ferrara[1], Xiaohui Fan[2], Tithankar Roy Choudhury[3]

[1] SISSA/International School for Advanced Studies, via Beirut 2-4, 34014 Trieste, Italy
[2] Steward Observatory, The University of Arizona, Tucson, AZ85721, USA
[3] Institute of Astronomy, Madingley Road, Cambridge CB3 OHA, UK

Context: Although observations of cosmic epochs closer to the present have indisputably shown that the InterGalactic Medium (IGM) is in an ionized state, it is yet unclear when the phase transition from the neutral state to the ionized one started. Thus, the redshift of reionization, z_{rei}, is still very uncertain.
Quasar absorption spectra contain a huge amount of informations concerning the neutral hydrogen distribution in the Universe. After the detection of the first Gunn-Peterson trough in the spectrum of SDSS J1030+0524 (Becker et al. 2001), the reionization was supposed to end by redshift 6. However some residual flux has been observed along the LOS to the most distant quasar SDSS J1148+5251 (Fan et al. 2003), suggesting an highly ionized IGM at $z \approx 6$, at odd with the previous claim.

Aims: Spectroscopy of the Lyman Alpha forest for QSOs at $z > 6$ seems to indicate that the IGM ionization state might be very different along different LOS. For this reason, Gallerani et al. 2006, hereafter GCF06, have tried to clarify if the SDSS data effectively require that the IGM was reionized as late as $z \approx 6$, finding that QSO observational data currently available are compatible with a highly ionized Universe at that redshift.
Moreover, GCF06 have shown that a statistical analysis of the transmission windows (peaks) and of the dark portions (gaps) in the absorption spectra are very promising for discriminating between an early ($z_{rei} > 6$) and a late ($z_{rei} \approx 6$) reionization scenario.
In this work, we apply these statistics to a sample of 17 observed QSOs spectra at $5.74 \leq z_{em} \leq 6.42$ (Fan et al. 2006). We compare the obtained results with Lyα forest simulations, with the aim to put tighter constraints on the volume-averaged neutral hydrogen fraction, $x_{\rm HI}$, at $z \approx 6$.

Results: We use a semi-analytical approach to simulate absorption spectra of QSOs at high redshifts. We consider two physically motivated and detailed reionization histories: (i) an Early Reionization Model (ERM) in which the IGM is reionized at $z \sim 7$, and (ii) a Late Reionization Model (LRM) in which overlapping occurs at $z \sim 6$ (Choudhury & Ferrara 2006).
For what concerns observations, we divide the observed sample into two redshift-selected sub-samples: the "Low-Redshift" (LR) sample (emission redshifts $5.7 < z_{em} < 6$), and the "High-Redshift" (HR) one ($6 < z_{em} < 6.4$).
In Fig. 1, on the top, the LGW[2] distribution is plotted for the LR (HR) sample on the left (right). Filled circles denote observations, while the solid red and the blue dotted lines represent the ERM and the LRM, respectively.
We exploit the agreement between the simulated and observed LGW distributions to derive an estimate of $x_{\rm HI}$. According to the predictions of our models, we find that $x_{\rm HI}$ evolves smoothly from $10^{-4.4}$ at $z = 5.3$ to $10^{-4.2}$ at $z = 5.6$.
Although the predicted LGW distributions are quite similar for the two models considered, yet some differences can be pointed out. Both for the LR and HR cases the early reionization LGW distribution provides a very good match to the observed points, thus suggesting $z_{rei} >\sim 7$. The agreement is satisfactory also for the LRM, but it is important to notice that a neutral hydrogen fraction at $z \approx 6$ higher than that one predicted by the LRM would imply an even worst agreement with observations. Thus, this study suggests $x_{\rm HI} < 0.36$ at $z = 6.32$.
From Fig. 1, on the bottom, by comparing the simulated LPW[1] distribution with the observed one, it is evident that simulations predict peak widths that are much smaller than the observed ones both for LR (on the left) and HR (on the right) cases. The possible reasons for this puzzling discrepancy are discussed in Gallerani et al. 2007.

References

Becker R. H. et al., 2001, AJ, 122, 2850
Choudhury T. R. & Ferrara A., 2006, MNRAS, 371, L55
Fan X. et al., 2003, AJ, 125, 1649
Fan X. et al., 2006, AJ, 132, 117
Gallerani S., Choudhury T. R., Ferrara A., 2006, MNRAS, 370, 1401
Gallerani S., Ferrara A., Fan X., Choudhury T. R., 2007, submitted

[2]The Largest Gap (Peak) Width distribution, called LGW (LPW), quantifies the fraction of LOS which are characterized by the largest gap (peak) of a given width.

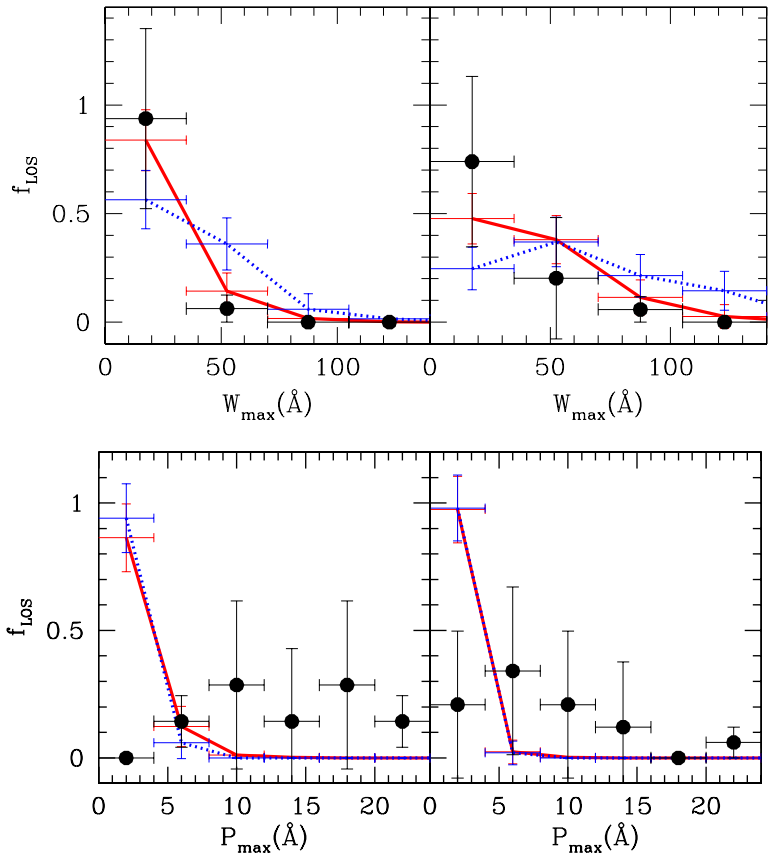

Figure 1: *Top*: Largest Gap Width distribution for the LR and the HR cases (left and right, respectively). Filled circles represent observational data obtained by analyzing the observed spectra of the 17 QSOs considered. Solid red (dotted blue) lines show the results obtained by the semi-analytical modeling implemented for the ERM (LRM). Vertical error bars measure poissonian noise, horizontal errors define the bin for the peak widths. *Bottom*: Same as on the top but for the Largest Peak Width distribution.

Properties of HI-selected galaxies - Contribution of gas-rich, LSB galaxies to the local Universe.

Diego A. Garcia-Appadoo[1,4], Andrew A. West[2], Julianne J. Dalcanton[3] & Mike J. Disney[4]

[1]Argelander-Institut für Astronomie, Bonn Universität, Bonn, Germany
[2]Astronomy Department, University of California, Berkeley, USA
[3]Department of Astronomy, University of Washington, Seattle, USA
[4]Astronomy Department, Cardiff University, Cardiff, UK

Context: Understanding the relationship between neutral hydrogen (HI) and stars in the interstellar medium of galaxies is integral to the study of galaxy evolution. Because stellar populations in galaxies form from collapsed clouds of hydrogen, we can naively claim that galaxies with few stars and large quantities of gas must be less evolved than those with little gas and many stars and that galaxies evolve by converting their gas into stars. To first order this description is valid; we know that galaxies with large stellar populations must have once had fewer stars and more gas. However, how a galaxy follows this evolutionary path is presumably much more complicated. Factors such as mass, metal content, gas fraction, internal motions, and other environmental conditions play an important role in determining how quickly HI gets converted into stars (e.g. van Zee et al. 1998; Kennicutt 1998).

Aims: The Equatorial Strip is a unique sample which comprises 1077 galaxies selected purely by their HI signature. This sample covers a large area of sky, is free from optical selection effects and has complete, very high quality, optical data (SDSS) for a subsample of 195 galaxies. The combination of the HI data with optical data allows us to make a comprehensive analysis of the properties of HI selected extragalactic sources and investigate vital global correlations which improves our understanding of gas-rich and Low Surface Brightness galaxies. The Equatorial Strip runs along the celestial equator from $-6^\circ < \delta < +10^\circ$ and through all R.A.s out to a distance of $\sim$ 170 Mpc. The Equatorial Strip sample represents $\sim$ 14% of the whole sky, covering an area of 5738 deg^2 and a total volume of $\sim 2.76 \times 10^6$ Mpc^{-3}.

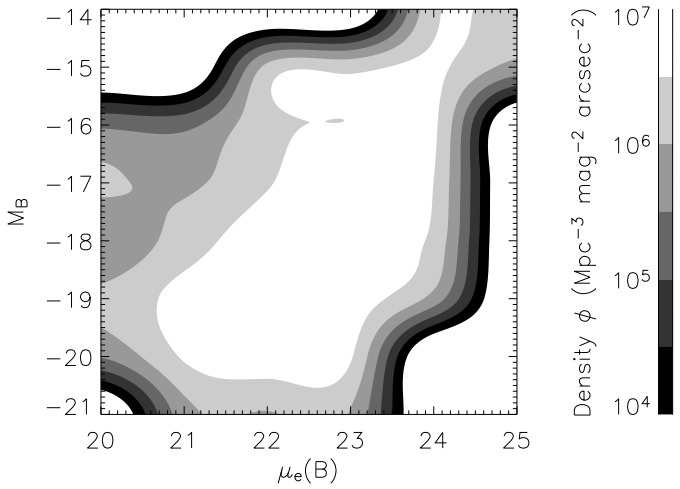

Figure 1: HI mass density-surface brightness distribution. The distribution is not peaked and the contribution is provided and shared by a wide variety of galaxies, from bright, high luminosity galaxies (bottom left) to low surface brightness, low luminosity galaxies (top right).

Results: LSB galaxies make up 12% of the sample, however, no high luminosity or high HI mass LSB galaxies have been found. Consequently, LSB galaxies make up no more than 6% of the high luminosity, gas-rich population, and massive LSB galaxies contribute no more than 13% of the population, at the 95% confidence level.

The Bivariate Brightness Distribution (see Fig. 1) and the Luminosity Function for the sample have been calculated and relationships found between surface brightness and optical luminosity, HI, baryonic and dynamical mass. From these results I find that LSB galaxies contribute 35^{+29}_{-20}% to the number density of gas-rich galaxies in the Universe but only 7^{+3}_{-2}% to the luminosity density. They also contribute 21^{+7}_{-6}% and 12 ± 3% respectively to the neutral hydrogen (HI) and baryon density of gas-rich galaxies in the Universe.

The Equatorial Strip sample has unveiled many objects not found in optical surveys, ranging from very low surface brightness, very blue galaxies to extremely gas-rich galaxies.

ALFALFA: the Arecibo Legacy Extragalactic HI Survey

Giovanelli, Riccardo

Cornell University, Ithaca, NY 14853, USA

Context: ALFALFA is an ongoing legacy survey at the Arecibo Observatory. It will cover 7000 square degrees of sky, in the 21cm HI line covering the frequency range 1330-1430 MHz. ALFALFA has eight times the sensitivity, four times the angular resolution, three times the spectral resolution, and 1.6 times the total bandwidth of HIPASS. The survey area is intended to map, with complete 2-pass coverage, the region from 0° to +36° in declination and from $22^h < R.A. < 3^h$ (the "fall sky") and $7^h30^m < R.A. < 16^h30^m$ (the "spring sky"). Started in Feb. 2005, ALFALFA observations have so far covered about 1/3 of the proposed area. The first source catalog has been released. Preliminary results of the survey will be presented.

Aims: A list of usual suspects: (i) Determination of the faint end of the HI mass function and the cosmic abundance of low mass halos; (ii) The environmental variations in the HIMF; (iii) making light on the LSS of HI sources and the "void problem"; (iv) A blind survey for tidal remnants; (v) Determining the HI Diameter function; (vi) Inspecting the low N_{HI} environments of galaxies, statistics of HI absorbers and their link to DLAs; (vii)Doubling the number of known OH Megamasers at intermediate redshifts; (viii) Cross-correlating gas and optical properties of HI-rich systems.

Results: The characteristics of the first set of 2700 ALFALFA sources will be discussed, with particular emphasis on a number of mostly extended, optically inert features discovered in the Virgo cluster region. 69% of ALFALFA detections are new . The figure below shows a comparison of ALFALFA and HIPASS.

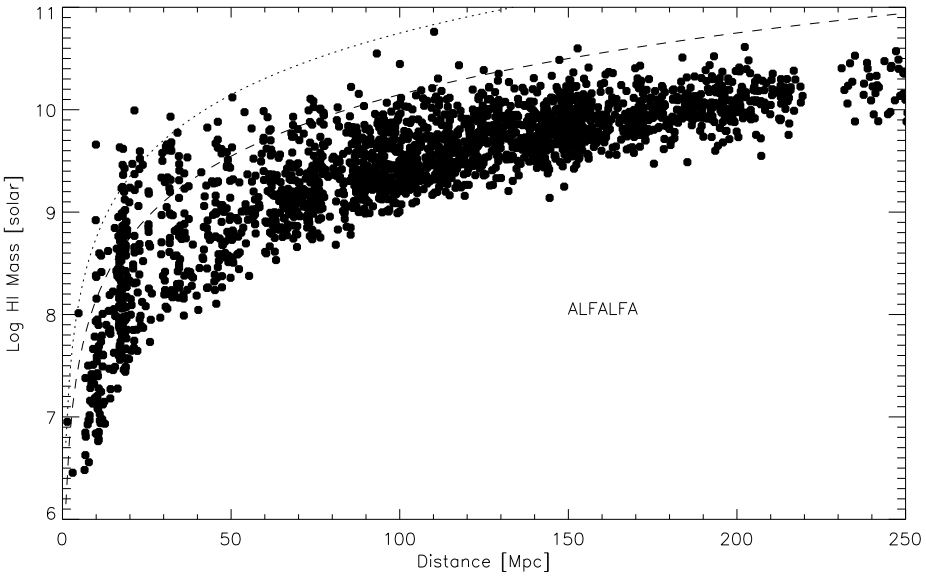

Figure 1: HI mass of 2700 ALFALFA HI detections in the region $7.5^h < RA < 16.5^h$, $12^\circ < Dec < 16^\circ$. The dotted line indicates thee HIPASS completeness limit, while the dashed line is the HIPASS survey limit. The gap in the data near 220 Mpc is due to rfi.

Stellar population of nearby gas-rich galaxies

M. Grossi[1] , M.J. Disney[2], B.J. Pritzl[3], P.M. Knezek[4], J.S. Gallagher[5], R.F. Minchin[6], K.C. Freeman[7]

[1] INAF − Osservatorio Astrofisico di Arcetri, Florence, Italy
[2] School of Physics and Astronomy, Cardiff University, UK
[3] Macalester College, Saint Paul, MN, USA
[4] National Optical Astronomy Observatory, Tucson, AZ, USA
[5] Dep. of Astronomy, University of Wisconsin, Madison, WI, USA
[6] Arecibo Observatory, PR, USA
[7] Research School of Astronomy and Astrophysics, Mount Stromlo Observatory, Australia

Context: Nearby dwarf galaxies are one of the best environments in which to study in detail how stellar evolution proceeds. Particularly the analysis of the resolved stellar population of objects within 10 Mpc allows to infer their star formation histories (SFHs) over long look-back times (see Tosi 2007 for a short review). All dwarf galaxies in the Local Group (LG) show varied and very complex SFHs and it is difficult to identify a common pattern in their evolution. However not all type of galaxies can be found in the LG and in order to get a complete overview of the evolution of dwarfs one needs to extend the same analysis to nearby environments.

The Centaurus A/M83 group is, after Sculptor, the second nearest cluster outside the LG. Blind 21-cm surveys of the group (Banks et al. 1999, Minchin et al. 2003) have found a number of gas-rich systems ($M_{HI} \sim 10^7$ $M_\odot$) which appear in the optical as low luminosity, low surface brightness dwarf spheroidals. Their gas-to-stellar ratios (M_{HI}/L_B) range from 1.4 to 5 in solar units which means they have no similar counterparts in the LG. Here we present HST/WFPC2-ACS images of such gas-rich galaxies. For three of them, high resolution maps of their HI content have also been obtained.

Aims: In principle, these galaxies represent an ideal environment for SF, given their large gas fractions and their location in a fairly populated group such as Centaurus A. Yet their gas fractions indicate that these dwarfs are 'underevolved' since a large part of the galactic gas reservoir has not been

converted into stars yet. To understand the evolution of these systems we have constructed colour-magnitude diagrams (CMDs) of their stellar population and we have derived their star formation history (SFH) from the comparison with synthetic CMDs (Harris & Zaritsky 2001).

Results: The gas-rich dwarfs in the Centaurus A group with their large gas fractions, their low masses, surface brightnesses and faint luminosities, give an insight into a different evolutionary environment, where galaxies can evolve in a smooth and more quiescent way. Our analysis of the resolved stellar populations allows us to estimate the timescale of the main evolutionary episodes of the history of these galaxies. We do find evidence of an intermediate-age population, showing that SF occurred several Gyr ago, most likely with modest episodes of SF activity alternating with periods of very low production of stars or even quiescence. Much deeper data is needed to verify that the SF activity started in these galaxies at the same time as in the LG dwarfs. Understanding the characteristics of the ISM and the conditions of the local environment is crucial in order to infer why SF is inefficient in these dwarfs. A low density neutral medium and the relative isolation within the group seem to be the main factors responsible for their observed underevolved evolution (see also Grossi et al. 2007). If the SF process were to proceed at the same average rate that they have experienced so far, it will take at least another Hubble time to consume all their gas.

References

Banks G.D., et al., 1999, ApJ, 524, 612
Grossi, M., et al., 2007, MNRAS, 374, 107
Harris J., & Zaritsky D., 2001, ApJS, 136, 25
Minchin R.F., et al., 2003, MNRAS, 346, 787
Tosi, M., 2007, in "*From Stars to Galaxies*" (Venezia, October 16-20 2006). To appear in ASP Conf.Ser., A.Vallenari, R.Tantalo, L.Portinari, A.Moretti eds; astro-ph/0701138

Feedback During Early Stages of Reionization and the Shapes of Quasar HII Regions

Zoltán Haiman[1], Andrei Mesinger[1,2], Roban Kramer[1]

[1] Department of Astronomy, Columbia University, USA
[2] Department of Astronomy, Yale University, USA

Context: The first generation of stars likely formed at redshifts $z > 20$, at locations corresponding to rare peaks of the fluctuating primordial density field. In the absence of any feedback processes, these stars could form in abundance and they, and their accreting black hole (BH) remnants, could significantly reionize the intergalactic medium (IGM). However, the population of the first stars and BHs were likely self-regulating due to their global chemical, radiative, and thermodynamical impact on the IGM, and further star-formation and reionization was delayed as a result. In addition, the relative contribution of stars and black holes to reionization, as a function of redshift, remain poorly understood.

Aims: The goal of the recent research I will present is to clarify the sign and importance of radiative feedback at the highest redshift, and to identify some characteristic signatures of quasar (as opposed to stellar) HII regions that could be revealed in future 21cm and Lymanα observations.

Results: I will argue that star-formation was suppressed at high redshift in the lowest mass ($\sim 10^6 M_\odot$) minihalos by an early H_2–dissociating background and that this suppression was exacerbated by a prior photoionization heating of the IGM, and by the strong clustering of the earliest ionizing sources. The low electron scattering optical depth in the three-year WMAP data offers empirical support that the ionizing photon production in the earliest minihalos was indeed suppressed. I will also briefly discuss two aspects of quasar HII regions – the distortion of their apparent shapes due to finite light travel time, and the sharpness of their boundaries – and quantify the detectability of these features in future observations.

Flows, Filaments and Fragmentation: The Formation of Molecular Clouds in Colliding HI-Flows

Fabian Heitsch[1], Adrianne Slyz[2], Julien Devriendt[3], Lee Hartmann[1], Andreas Burkert[4]

[1] Dept. of Astronomy, U of Michigan, USA
[2] Dept. of Astrophysics, U Oxford, UK
[3] ENS Lyon, Observatoire de Lyon, France
[4] Universitäts-Sternwarte München, Germany

Context: Molecular clouds in the Galaxy show an abundance of internal structure, both in density and velocity (e.g. Stutzki & Güsten 1990; Falgarone 1990; Mizuno et al. 1995). The density contrasts are non-linear – independent of the importance of gravity (Williams et al. 1995) –, and the molecular clouds exhibit non-thermal line-widths (Falgarone & Philips 1990; Williams et al. 2000), generally interpreted as supersonic turbulence. Filaments seem to dominate the morphologies in (column) density and velocity (e.g. Bally et al. 1987; Mizuno et al. 1995; Hartmann 2000; Churchwell et al. 2004).

Growing evidence that star formation in molecular clouds sets in immediately after or even during cloud formation (Hartmann et al. 2001; Hartmann 2003 and references therein) indicates that this wealth of structure must mainly arise during the cloud formation process. This has led to a picture in which molecular clouds are envisaged as transient objects forming in large-scale converging flows of atomic hydrogen rather than as well-defined entities in a quasi-equilibrium stage (Ballesteros-Paredes et al. 1999; Hartmann et al. 2001; Pringle et al. 2001; Hartmann et al. 2003).

Aims: The rapid onset of star formation in molecular clouds entails two consequences:

(1) The formation mechanism must not only provide the cloud with the observed level of turbulence, but it must also imprint *non*-linear density perturbations as the seeds for *local* gravitational collapse to occur rapidly. Otherwise, global collapse of the cloud would occur on similar timescales as local collapse (Burkert & Hartmann 2004).

(2) Molecule formation, specifically H_2 and CO, needs to occur on the assembly timescale of the cold neutral cloud.

We will demonstrate with the help of numerical models the physical mechanisms controlling cloud formation in colliding flows, allowing the rapid fragmentation of the flows and the formation of localized high-density perturbations as well as the generation of turbulence.

Results: Cloud formation in converging flows allows the natural generation of observed substructure and turbulence with a minimum of assumptions. In detail:

1. The converging flows fragment due to a combination of strong dynamical and thermal instabilities. The dominant dynamical instabilities are the Non-linear Thin Shell Instability (NTSI, Vishniac 1994) and the Kelvin-Helmholtz-Instability. Together with the Thermal Instability (TI, Field 1965) – mainly due to the HFS-CII line at 158μ – they lead to the formation of small (0.1 pc) size fragments in a large-scale turbulent slab.

2. Line widths typical for the cold neutral medium of a few km s^{-1} are reproduced by the models. The cold gas is nominally supersonic.

3. However, the line widths within the isolated cold regions are at most sonic. Thus, the "supersonic" line widths are a consequence of cold regions moving with respect to each other within a warmer medium. The term "supersonic" does not necessarily describe the hydrodynamic state of the cold gas.

4. The cold core mass distribution follows approximately $dN/d(lnM) \propto M^{-0.7}$. The closeness to mass distributions observed for molecular clouds (e.g. Heithausen et al. 1998) suggests that the molecular core mass distribution might well be set already during the cloud formation process.

5. The strong fragmentation and the small filling factor of the cold (and dense) gas tends to promote and accelerate the formation of molecular hydrogen.

On the structure of the turbulent atomic interstellar gas

Hennebelle Patrick[1], Audit Edouard[2], Inutsuka Shu-ichiro[3]

[1] École normale supérieure et Observatoire de Paris, France,
[2] Service d'Astrophysique, CEA/DSM/DAPNIA/SAp, C. E. Saclay, F-91191 Gif-sur-Yvette Cedex, France,
[3] Department of Physics, Kyoto University, Japan

Context: The atomic interstellar gas is a 2-phase and turbulent medium. Modeling such flow is a challenging issue because of the large scale dynamics which is required. This is also of great relevance in the context of molecular clouds formation since those clouds form by condensation of interstellar atomic gas.

Aims: Here, we present very large numerical simulations (2D and 3D) allowing to describe accurately the various physical scales relevant for HI over 3 to 4 orders of magnitude in spatial scales. As an example, Fig. 1 shows the density field of a bidimensional numerical simulation with $10{,}000^2$ grid points. As can be seen, the structure of the resulting 2-phase flow is very complex. Various statistics inferred from the simulations will be presented, such as the mass spectrum of the CNM clouds or the column density distribution.

Results: As illustrated by Fig. 2, low column density CNM structures as recently observed by Braun & Kanekar (2004) are naturally formed in the simulations. Detailed comparisons with observations will then be made with special emphasis on the Millenium survey carried out by Heiles & Troland (2005). Synthetic HI spectra, both in emission and in absorption, have also been calculated and present similarity with observed spectra (see Fig. 2).

References:

Hennebelle P., Audit E., Miville-Deschênes M.-A., 2007, A&A, 465, 445,
Hennebelle P., Audit E., 2007, A&A, 465, 431,
Audit E., Hennebelle. P., 2005, A&A, 433, 1

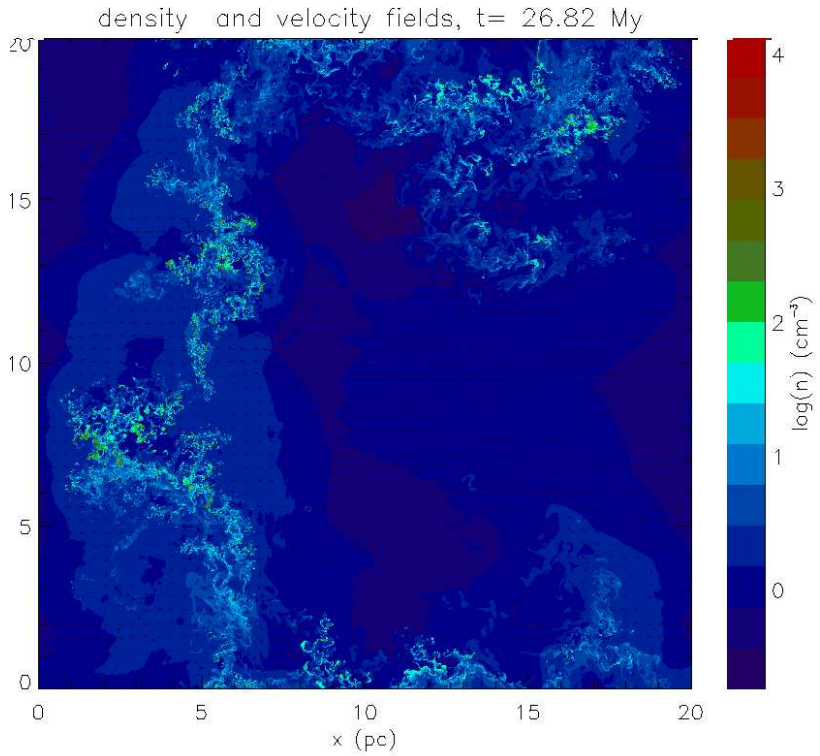

Figure 1: Density field of a bidimensional $10{,}000^2$ cells numerical simulation of a collision between the HI flows.

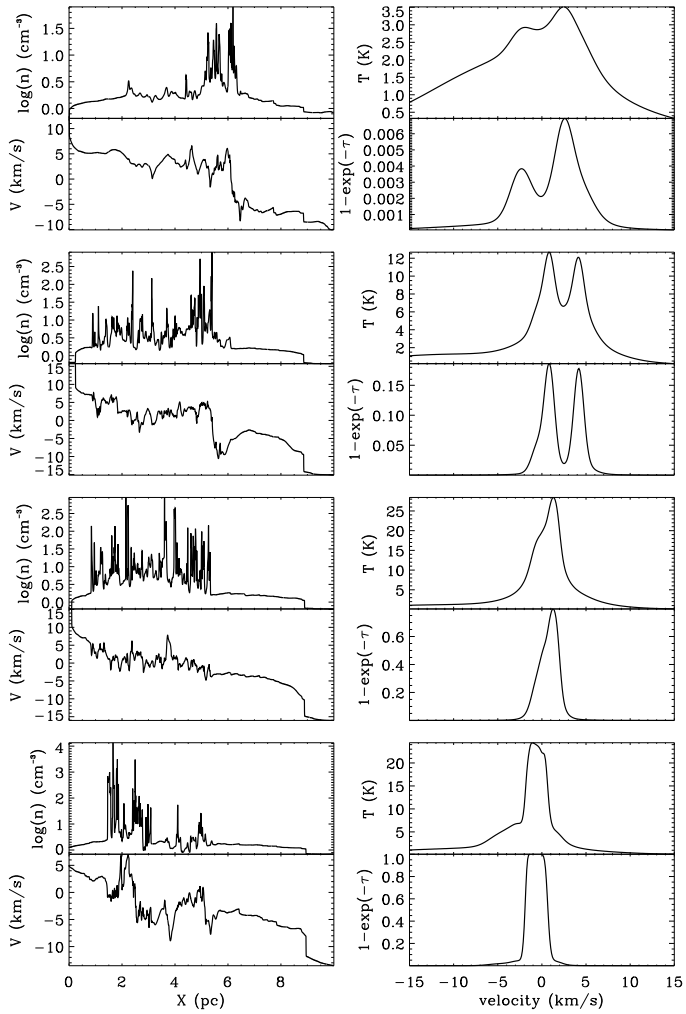

Figure 2: Density and velocity field along four lines of sight. Synthetic emission and absorption spectra calculated along these lines of sight.

Too small to form a galaxy? Gas condensation in dwarf galaxies

Matthias Hoeft[1], **Gustavo Yepes**[2], **Stefan Gottlöber**[3]

[1] Jacobs University Bremen, Germany
[2] Universidad Autonoma de Madrid, Spain
[3] Astrophysikalisches Institut Potsdam, Germany

Context: To form a galaxy a minimal halo mass is necessary. Comparing the luminosity function of galaxies to the halo mass function of the cosmological concordance model indicates that halos with a mass below about $10^{11}\ M_\odot$ have in average a very high mass-to-light ratio (v. d. Bosch, Yang, et al., 2007, MNRAS 376). Several origins are conceivable: For instance, the gas density in small halos could be too low to convert cold gas into stars, the cooling time of the halo gas could exceed the Hubble time, supernovae could efficiently remove the galactic gas, or the concordance model could overpredict the abundance of dwarf halos. One often invoked remedy, which causes long cooling times, is the photo-ionization by the cosmic UV-background. Energetic photons ionize the gas in the dwarf galaxies, therefore only a small fraction of hydrogen remains neutral. The corresponding photo-heating increases the gas pressure and a large fraction of the pre-galactic gas is removed. A crucial question is what is the lower mass limit set by photo-heating and under which conditions the observed mass scale of $10^{11}\ M_\odot$ is realized.

Aims: We wish to derive the effect of UV-heating by the means of high-resolution numerical simulations. On the basis of a large number of zoom-simulations, focussing on the formation of dwarf galaxies in different environments, we wish to derive the lower mass threshold for galaxy formation as induced by the UV-heating. A comparison with the observed mass threshold will indicate if additional processes, as gas removal by supernovae have to be efficient in dwarf galaxies. Moreover, a crucial part of our work is to investigate how exactly UV-heating hampers gas condensation. Different models are discussed in literature, cf. Gnedin (2000, ApJ 542) and Hoeft et al. (2007, MNRAS 375). We derive an analytic method to estimate the lower mass limit. By the help of that model we investigate the impact, e.g., of a harder UV-spectrum, as indicated by recent analyses of quasar spectra

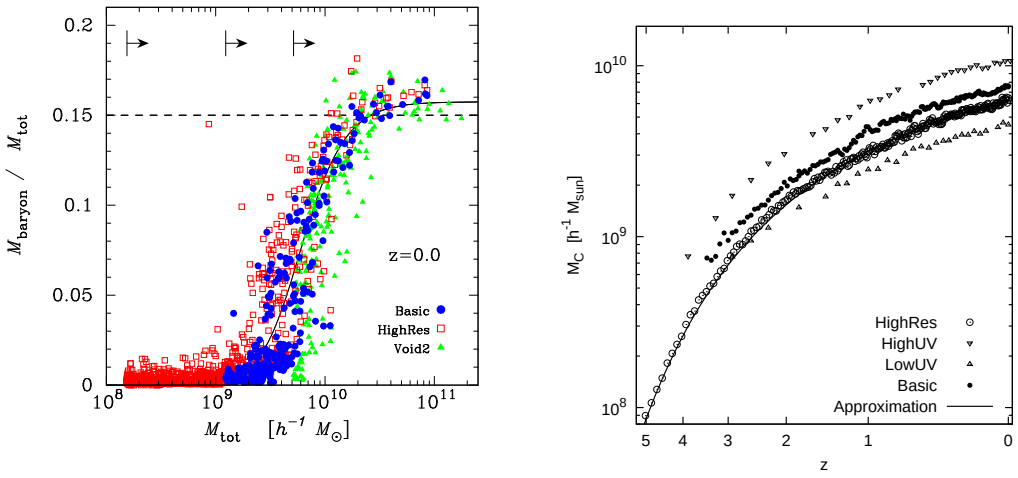

Figure 1: *Left panel:* Resolution study. The baryon fraction in halos with different masses at $z = 0$ for several numerical resultions. The mass scale at which halos become virtually free of baryons depends only negligibly on the resolution. *Right panel:* Time evolution of the characteristic mass.

(Agafonova et al. 2007, A&A 461). Moreover, this model allows us to investigate the galaxy formation mass threshold at at earlier times.

Results: We study the formation of dwarf galaxies in different cosmological environments using high-resolution smoothed-particle hydrodynamics (Gadget2) simulations. UV-background radiation is known to photo-evaporate baryons out of dwarf galaxies. We show to which extent this effect reduces the gas condensation and thereby lowers the star formation rates. For a Haardt & Madau UV-background model, with reionisation at redshift $z = 6$, our samples of simulated galaxies show that halos with masses below a characteristic mass of $M_c(z = 0) = 6.5 \times 10^9\, h^{-1}\, \mathrm{M}_\odot$ contain significantly less baryons than the Universe in average, see Fig. 1 left panel. A s,all fraction of galactic baryons is in a condensed cold phase or they is already locked up in stars and therefore resist evaporation. We find that in halos with mass $M \leq M_c$ photo-heating suppresses *further* cooling of gas. The redshift and UV-background dependent characteristic mass $M_c(z)$ can be understood from the equilibrium temperature between heating and cooling at a characteristic overdensity of $\delta \simeq 1000$. If a halo is massive enough to compress gas to this density despite the presence of the UV background, gas is free to 'enter' the condensed phase and cooling continues in the halo, otherwise

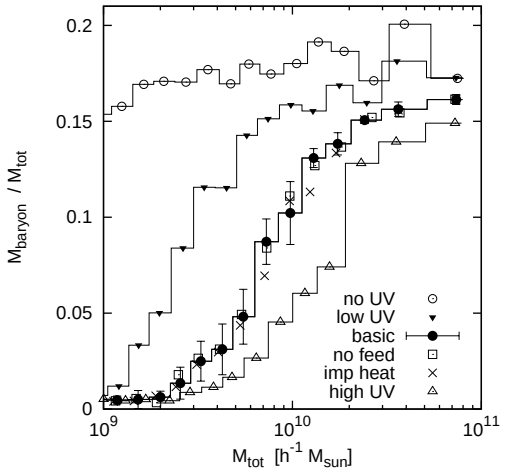

Figure 2: The impact of the UV-background flux density on the characteristic mass. Squares indicate no UV-heating, hundred times less and hundred times more than the Haardt & Madau model is shown, solid triangles open triangles and filled circles, respectively.

it stalls. We show that this behaviour is universal for different cosmological environments and depends only on the UV-background heating (cf. Fig. 2 right panel), which in turn hardly alters the characteristic mass, see Fig. 2. Hence, the value we found for the characteristic mass is a robust result. By analysing the mass accretion histories of dwarf galaxies –'dwarf' refers here to a total galactic mass below the characteristic mass– we show that they can build up a significant amount of condensed mass at early times before the epoch of reionisation. Later on, the amount of mass in this phase remains roughly constant, but the masses of the dark matter halos continue to increase. Consequently, photo-heating leads to a reduced baryon fraction in dwarf galaxies, endows them with a rather old stellar population, but still allows late star formation to some extent. While the number of galaxies at the faint end is significantly reduced due to photo-heating, additional physical feedback processes are required to explain the apparent paucity of dwarf galaxies.

Outer Gas Disks of Dwarf Irregular Galaxies

Deidre Hunter[1] and Bruce Elmegreen[2]

[1] Lowell Observatory, USA
[2] IBM T. J. Watson Research Center, USA

Context: Outer edges of galaxies present an extreme environment for star formation. Dwarf irregular (dIm) galaxies already challenge models of star formation because of their low gas densities even in the central regions. The outer parts of dIm galaxies, therefore, present a particularly difficult test of our understanding of the cloud/star formation process. Yet, we can trace stars even to a surface brightness level of μ_V = 29.5–30 mag/arcsec^2 while the gas drops to ever decreasing surface density levels.

Aims: We examine the outer gas disks of dwarf irregular galaxies through HI interferometric maps of 20 dIm, Blue Compact Dwarf, and Sm galaxies. We fit Sersic profiles to the azimuthally-averaged gas surface densities. The profile index reflects the degree of central concentration of the gas and how fast the density falls with radius.

Results: We explore the relationship between this and characteristics of the stellar component of the galaxy, including the star formation rate and distribution of the current star formation activity. We further discuss implications of the, often, lack of correspondence in rate of fall off of densities of gas, older stars, and newly formed stars.

Dynamics of Multi-Phase Interstellar Medium with and without Magnetic Field

Shu-ichiro Inutsuka[1], Hiroshi Koyama[2], Tsuyoshi Inoue[1], Patrick Hennebelle[3], and Masahiro Nagashima[4],

[1] Department of Physics, Kyoto University, Kyoto 606-8502, Japan
[2] Department of Astronomy, University of Maryland College Park, MD 20742-2421, USA
[3] Laboratoire de Radioastronomie Millimetrique, UMR 8112 du CNRS, Ecole Normale Superieure et Observatoire de Paris, 24 rue Lhomond, 75231 Paris Cedex 05, France
[4] Faculty of Education, Nagasaki University, Nagasaki 852-8521, Japan

Our understanding on the physical processes in the transition between warm neutral medium (WNM) and cold neutral medium (CNM) is dramatically increased in the last several years. In this talk we explain the basic property of thermal instability and the effect of magnetic field on it and analyze the propagation of a shock wave into WNM by taking into account radiative heating/cooling, thermal conduction, physical viscosity, and the magnetic field in one-, two-, and three-dimensional magnetohydrodynamical simulations. The results show that the thermal instability in the post-shock gas produces high-density cold cloudlets embedded in turbulent warm neutral medium. In the analysis of the complex dynamics of turbulent two-phase medium, we have found that the evaporating flow through the transition layer between cold and warm medium is unstable, which is analogous to the well-known Darrieus-Landau Instability of the flame front. We show our recent linear stability analysis of the transition layer, and discuss its role in the turbulence in two-phase medium. We also analyze the importance of ambipolar diffusion in producing moderately magnetized tiny cold cloudlets. The dynamical evolution driven by thermal instability in the post-shock layer is an important basic process for the transition from warm gases to cold gases, because the shock waves are frequently generated, e.g., by expansions of supernova remnants and HII regions in the Galaxy.

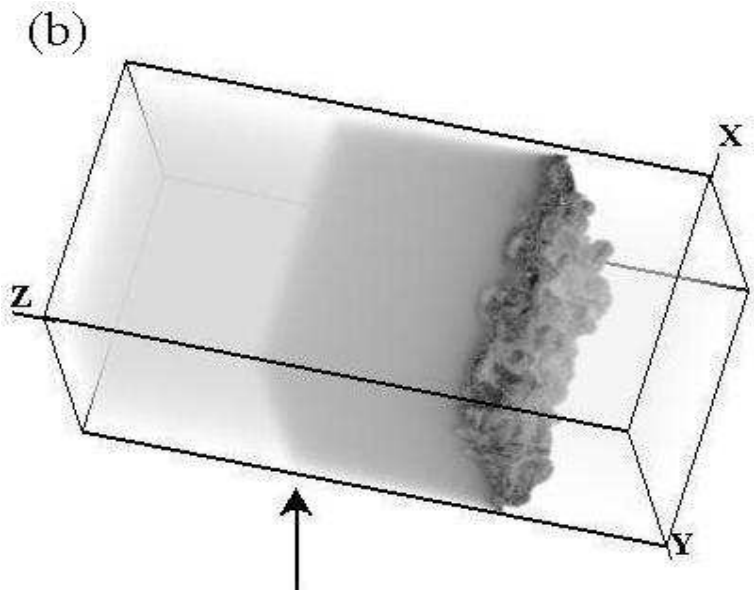

Figure 1: The volume rendering of high-density regions in the layer compressed by an interstellar shock wave propagating (to the left) into warm neutral medium. The arrow denotes the location of the shock front that remains stable. The post-shock cooling layer becomes thermally unstable and develops turbulent condensations.

Reference

Hiroshi Koyama & Shu-ichiro Inutsuka (2000) ApJ 532, 980, "Molecular Cloud Formation in Shock-Compressed Layers"

Hiroshi Koyama & Shu-ichiro Inutsuka (2002) ApJ 564, L97, "An Origin of Supersonic Motions in Interstellar Clouds"

Shu-ichiro Inutsuka & Hiroshi Koyama (2002) Ap&SS 281, 67, "Toward Understanding the Formation of Molecular Clouds"

Hiroshi Koyama & Shu-ichiro Inutsuka (2004) ApJ 602, L25, "The Field Condition: A New Constraint of Spatial Resolution in Simulations of Thermally Unstable Hydrodynamics"

Shu-ichiro Inutsuka & Hiroshi Koyama (2004) Revista Mexicana de Astronomia y Astrofisica Vol. 22, pp. 26, "The Formation of Molecular Clouds"

M. Nagashima, H. Koyama, & S. Inutsuka (2005) MNRAS 361, L25, "Evaporation and condensation of HI clouds in thermally bistable interstellar media: semi-analytic description of isobaric dynamics of curved interfaces"

Shu-ichiro Inutsuka, Hiroshi Koyama, & Tsuyoshi Inoue (2005) AIPCP 784, pp.318-328, "The Role of Thermal Instability in Interstellar Medium",

Tsuyoshi Inoue, Shu-ichiro Inutsuka, & Hiroshi Koyama (2006) ApJ 652, 1331, "Structure and Stability of Phase Transition Layers in Interstellar Medium"

Patrick Hennebelle, Shu-ichiro Inutsuka (2006) ApJ 647, 404, "Can WNM survive inside Molecular Clouds?"

Masahiro Nagashima, Shu-ichiro Inutsuka, & Hiroshi Koyama (2006) ApJ 652, L41, "How Long Can Tiny HI Clouds Survive?"

Hiroshi Koyama & Shu-ichiro Inutsuka (2006) submitted to ApJ (astro-ph/0605528), "Nonlinear Development of Thermal Instability without External Forcing"

Tsuyoshi Inoue, Shu-ichiro Inutsuka, & Hiroshi Koyama (2007) ApJ 658, L99, "The Role of Ambipolar Diffusion in the Formation Process of Moderately Magnetized Diffuse Clouds"

Masako Yamada, Hiroshi Koyama, Kazuyuki Omukai, & Shu-ichiro Inutsuka (2007) ApJ 657, 849, "Synthetic Observations of Carbon Lines of Turbulent Flows in Diffuse Multiphase Interstellar Medium"

HI 21cm absorption studies of damped Lyman-alpha systems

Nissim Kanekar

National Radio Astronomy Observatory, Socorro, USA

Context : HI 21cm absorption studies of galaxies lying along the line of sight towards radio-loud background QSOs provide an interesting probe of physical conditions in the neutral gas content of the absorbers, yielding information on their kinematics, mass, physical size and ISM conditions. In the case of the damped Lyman-α systems (DLAs), where the HI column density can be independently determined from the Lyman-α line, such observations allow a measurement of the spin temperature T_s, the column-density-weighted harmonic mean of the temperatures of different HI phases along the line of sight. One may thus study the redshift evolution of the distribution of gas between different temperature phases, as well as its relation to other observables such as the metallicity, star formation rate, etc. Earlier observations have found the distribution of spin temperatures to be different at high and low redshifts, with all known high z DLAs having high T_s values (≥ 1000 K) and a mix of low and high T_s systems at $z < 1$. This suggests an evolution of the temperature distribution with redshift, with small fractions of the cold phase present in high z DLAs. The low redshift results also indicated that T_s might serve as a tracer of the nature of an absorber, with low T_s values (≤ 300 K) seen in low z DLAs identified with bright disk galaxies and higher values (≥ 1000 K) obtained in dwarf or LSB galaxies.

Aims : Unfortunately, a combination of three factors (the paucity of DLAs towards bright radio quasars, the poor frequency coverage of radio telescopes and terrestrial radio interference (RFI) at the frequencies of interest) has meant that, until recently, only three DLAs have been detected in redshifted 21cm absorption at $z > 1.7$. In addition, almost no 21cm searches had been carried out in absorbers in the redshift range $0.7 \leq z \leq 1.7$ (the "redshift desert"), and with no detections. The advent of new instruments such as the Giant Metrewave Radio Telescope (GMRT) and the Green Bank Telescope (GBT) with excellent low frequency coverage has opened up a new

window for DLA studies in the 21cm line. I report here on deep 21cm observations of DLAs towards radio-loud quasars with the GMRT and the GBT and their implications for physical conditions in the absorbing gas. I will also discuss a survey for damped Lyman-α absorption towards QSOs detected in the 365 MHz Texas survey, to find high z candidates suitable for follow-up 21cm absorption studies, as well as a programme to obtain high resolution Very Long Baseline Array (VLBA) images of the background QSOs at frequencies close to that of the redshifted 21cm line. Finally, I will briefly summarize results of recent searches (by us and others) for 21cm absorption in a large sample of strong MgII absorbers in the redshift desert, resulting in the first detections of 21cm absorption here.

Results:

21cm absorption searches in DLAs : We have searched for 21cm absorption in 25 DLAs with $0.8 \leq z \leq 3.5$ over the last three years, with the GMRT, GBT and Westerbork Synthesis Radio Telescope. This has resulted in four new detections, three at $z > 2$, and eleven strong lower limits ($\geq$ 1000 K) on the spin temperature. There are now thirty-two absorbers with T_s measurements or lower limits, with eighteen of these at $z > 1.5$. Seventeen of the latter have high spin temperatures, $\geq$ 1000 K, while five of the fourteen systems at $z < 1.5$ have low values, $T_s \leq 300$ K, a clear difference between T_s distributions at high and low redshifts. Our VLBA observations also find that covering factor effects are unlikely to be significant for the high z DLAs of our sample.

Higher T_s values are to be expected in smaller galaxies (like dwarfs), whose low metallicities and pressures are not conducive to the formation of the CNM. Such systems hence have a substantially higher fraction of warm HI than normal spirals, and, therefore, a higher T_s on an average line of sight. On the other hand, spiral disks like the Milky Way have roughly equal fractions of warm and cold HI; lines of sight through such systems would, on average, yield significantly lower T_s values.

If the high T_s values seen in DLAs arise because these are small galaxies where the ISM is inefficiently cooled due to the lack of metals (and hence a lack of radiation pathways), an anti-correlation would be expected between spin temperature and metallicity. We have indeed detected the expected anti-correlation between metallicity and spin temperature (at $\sim 3.5\sigma$ significance, via a Kendall-τ test) in the 25 DLAs of our sample with estimates of both quantities. All known effects (e.g. using the HI column density determined

from the Lyman-α line in the 21cm equation, differences between the QSO size in the radio and optical wavebands, etc) would *increase* the scatter in the correlation. We hence conclude that DLA spin temperatures obtained from 21cm absorption studies are likely, on average, to provide a reliable estimate of the distribution of gas between warm and cold phases and, further, that the observed difference in the spin temperature distribution between high z and low z DLAs is genuine, with high z DLAs containing larger fractions of the warm phase of neutral hydrogen than typical in local spiral disks, primarily due to their lower metallicities.

21cm absorption searches in MgII absorbers :

We also find that the fraction of 21cm detections at low redshifts ($\sim 83\%$ at $z < 0.7$) is far higher than at $z > 1.7$ ($\sim 33\%$). However, the important redshift range $0.7 < z < 1.7$ is almost entirely unpopulated, as very few DLAs are known towards radio-loud quasars at these redshifts. Unfortunately, it is precisely in this redshift range that the star formation activity in the Universe is known to peak and one thus expects to see significant evolutionary effects here. For example, in the case of the 21cm line, one would expect to find the onset of stronger 21cm absorption and significantly lower spin temperatures here, as the increased star formation should result in an increased metallicity and thus, in significant gas cooling.

We are hence carrying out a search for 21cm absorption in a sample of strong metal-line absorbers in the redshift desert. All systems have rest MgII 2796 and FeII 2600 equivalent widths larger than 0.5 A with the ratio of these widths $W^{\rm MgII}/W^{\rm FeII} < 2$, expected to have a 50% chance of being DLAs. So far, 35 absorbers have been observed in the 21cm line with the GBT and GMRT, with four confirmed and three tentative detections, all at $z > 1$. Combined with similar work from other groups, there are now eleven new 21cm absorbers in the redshift desert, suggesting that the cold gas fraction does increase in this range. Work on this sample is presently in progress.

Environmental effects on the HI mass function, and the evolution of galaxies in groups.

Virginia Kilborn[1], Duncan Forbes[1], Sarah Brough[1], Baerbel Koribalski[2]

[1] Swinburne University of Technology, Australia
[2] Australia Telescope National Facility, Australia

Abstract: We have recently completed a deep, blind HI survey of 16 nearby galaxy groups, as part of the GEMS study. Complementing the HI data we have obtained deep ROSAT X-ray images, and complete optical data from the 6dFGS, allowing us to fully understand the processes occuring in these groups. We find that while there is a general trend for those groups with intra-group X-ray emission to contain less HI near their centres (similar as seen in rich clusters), there are exceptions to this trend, and the HI content of the groups is more heavily dependent on galaxy morphology. I will conclude with a discussion of how the group environment affects the evolution of constituent galaxies.

Introduction: It is becoming increasingly realised that the galaxy group environment plays an important influence on the evolution of galaxies. To study the evolution of galaxies in groups, we have conducted a multi - wavelength survey of groups, looking at X-ray, optical, and HI properties, called GEMS - the Galaxy Evolution Multiwavelength Study (see Forbes et al. 2006 for details). There are around 60 groups in GEMS, and we have obtained wide-field HI observations for 16 of the groups using the Parkes telescope mounted with the multibeam receiver. We observed a $\sim 5.5 \times 5.5$ degree region around each of the groups, to an HI mass sensitivity of $\sim 5 \times 10^8 M_\odot$. Further details of the observations can be found in Kilborn et al. (2006, 2005).

Results:

HI content: We find that the HI content of our GEMS groups is diverse, from detecting nearly every member in the group, to detecting one, or

even no members. Figure shows velocity integrated HI maps of two of our groups, NGC 1052 and NGC 1407. These groups look very different in HI emission - while almost every galaxy in the NGC 1052 group is detected in HI, only a few galaxies at the edge of NGC 1407 are detected. NGC 1407 has extended X-ray emission associated with the centre of the group, indicating a hot intra-group medium. The group has a high early-type fraction, and a bright central elliptical galaxy, indicating this is a dynamically mature group (Brough et al. 2006). In contrast, the NGC 1052 group shows no extended X-ray emission, although X-ray emission was detected with the central elliptical galaxy. The early-type fraction is low, and spatially the group is quite extended and irregular. Brough et al. (2006) conclude this group is dynamically immature and coming together for the first time. This scenario fits well with the observed HI emission from these two groups. In the dynamically mature NGC 1407 group, we detect little HI emission (similar to clusters), whereas in the dynamically immature NGC 1052 group we detect most of the galaxies in HI. This picture does not fit exactly for all the groups however - for example, the NGC 524 group displays all other indicators that this is a dynamically old group, such as high early type fraction, central elliptical galaxy, and we detected none of the galaxies within the group.

Correlation with X-ray emission: One of our main objectives with the GEMS HI survey was to determine the relationship, if any, between the HI content of groups, and the X-ray emission of the group. To do this, we determined the total HI content of each group within the r500 radius, and compared this with the X-ray emission of the groups. We found that there was a weak anti-correlation between total HI content of a group, and the X-ray luminosity of the group - this anti-correlation was slightly stronger when we looked at total HI content versus X-ray temperature. We found no relationship between the extent of the central group X-ray emission, and the total HI content of the group.

HI clouds: Of the over 200 HI sources we detected in the GEMS HI survey, we only detected one HI cloud that didn't have a visible optical counterpart when we looked on the DSS images (Kilborn et al. 2006). This source, GEMS_NGC3783_2, has an HI mass of $\sim 4 \times 10^8 M_\odot$, and is over 200kpc in project distance from the nearest bright galaxy. It is 450kpc in projected distance from the nearest bright HI-rich spiral galaxy. We conclude that this HI cloud is likely the result of a tidal interaction between the

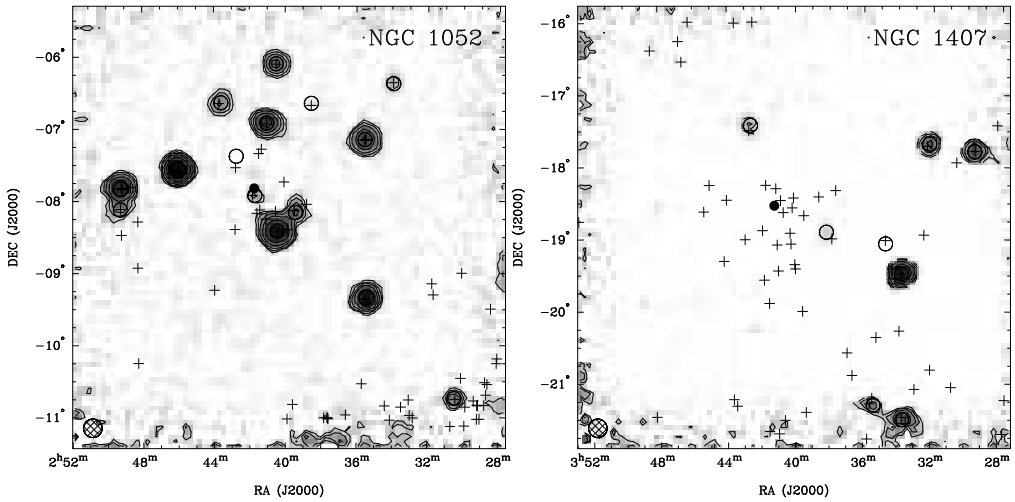

Figure 1: Velocity integrated HI maps of two GEMS groups, NGC 1052 (left) and NGC 1407 (right). The contours and greyscale show HI emission, the crosses are previously optically catalogued galaxies, and the circles are GEMS detections.

bright early-type galaxy NGC 3706, and the HI-rich spiral ESO 378-G 003, although we are puzzled as to why there is no other tidal debris found in the field.

References:

Brough, S., Forbes, D. A., Kilborn, V. A., Couch, W. 2006, MNRAS, 370, 1223

Forbes, D. A. et al. 2006, PASA, 23, 38

Kilborn, V. A., Koribalski, B. S., Forbes, D. A., Barnes, D. G., Musgrave, R. C. 2005, MNRAS, 356, 77

Kilborn, V. A., Forbes, D. A., Koribalski, B. S., Brough, S., Kern, K. 2006, MNRAS, 371, 739

A new tool to study warped galaxies

Uli Klein[1], Gyula Józsa[1], Franz Kenn[1], Tom Oosterloo[2]

[1] AIfA, Bonn, Germany
[2] ASTRON, Dwingeloo, The Netherlands

Context: Kinematic analyses based on spectroscopy are an important tool to constrain the dynamical structure and hence the distribution of matter in galaxies. The discovery and description of global features in the kinematics of galaxies, such as the flatness of rotation curves (Rubin & Ford 1970, ApJ, 159, 379; Bosma 1981, AJ, 86, 1825), directly influenced cosmology. Since then, the increase of computational power enabled theorists to provide testable predictions on the mass distribution on sub-galaxy scales for given cosmological models (e.g. Navarro et al. 1997; ApJ, 490,493; Moore et al. 1999; MNRAS, 310, 1147, Reed et al. 2005; MNRAS, 357, 82), such that kinematical studies can be utilised as immediate tests for cosmology. While in recent years the debate concentrated mainly on the spherical distribution of Dark Matter in relaxed systems (e.g. de Blok et al. 2003, MNRAS, 340, 657; Gentile et al. 2004, MNRAS, 351, 903), deviations from this, which are evident from lopsidedness or warping, now come into the focus of theoretical research in the cosmological context (Sharma & Steinmetz 2005, ApJ, 628, 21; Gao & White 2006, MNRAS, 373, 65). The aim to constrain the structure of anisotropies in the DM distribution imposes an observational challenge, requiring both observations with high sensitivity, as well as appropriate analysis tools.

Aims: A new tool to perform tilted-ring analyses has therefore been established that permits to derive the structure and kinematics of gaseous disks of galaxies. This publicly available software tool TiRiFiC[3] permits a direct fit of a "tilted-ring model" to spectroscopic data cubes. The algorithm generates model data cubes from the tilted-ring parametrisation of a rotating disk, which are automatically adjusted to reach an optimum fit via a chi-squared minimisation method to an observed data cube. Our method is not affected by the well-known problem of beam smearing that occurs when fitting to a velocity field. The software is able to parametrise HI disks of

[3] http://www.astro.uni-bonn.de/~gjozsa/tirific.htm

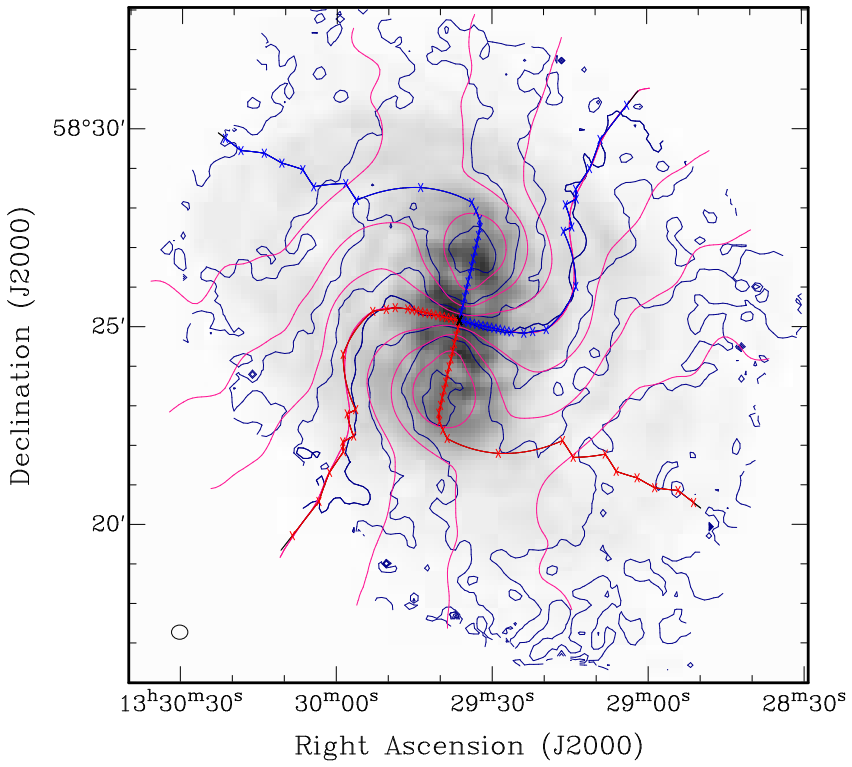

Figure 1: Column density of neutral hydrogen of NGC 5204, with the velocity field of the original data (blue iso-velocity contours) and of the model data (pink contours) superimposed. The over-plotted lines represent the kinematical major and minor axes. The red kinematical major axis lies in the receding part of the galaxy, the blue kinematical major axis in the approaching part.

galaxies that are intersected twice or more by the line-of-sight, i.e. if the disks are heavily warped or seen edge-on. Furthermore, our method delivers the surface-brightness profile of the examined galaxy, along with the orientational parameters and the rotation curve (see Józsa et al., 2007, A&A, in press, astro-ph/0703207).

Results: Here we present the exemplary analysis of the warped spiral galaxy NGC 5204, a small galaxy of Magellanic type. It is supposed to lie at the border of the M 101 group, at 4.6 Mpc distance. Fig. 1 shows the map of surface brightness (moment 0, or HI column density) in grey-scale, with the velocity field superimposed. In Fig. 2 the tilted-ring parametrisation of NGC 5204 is displayed.

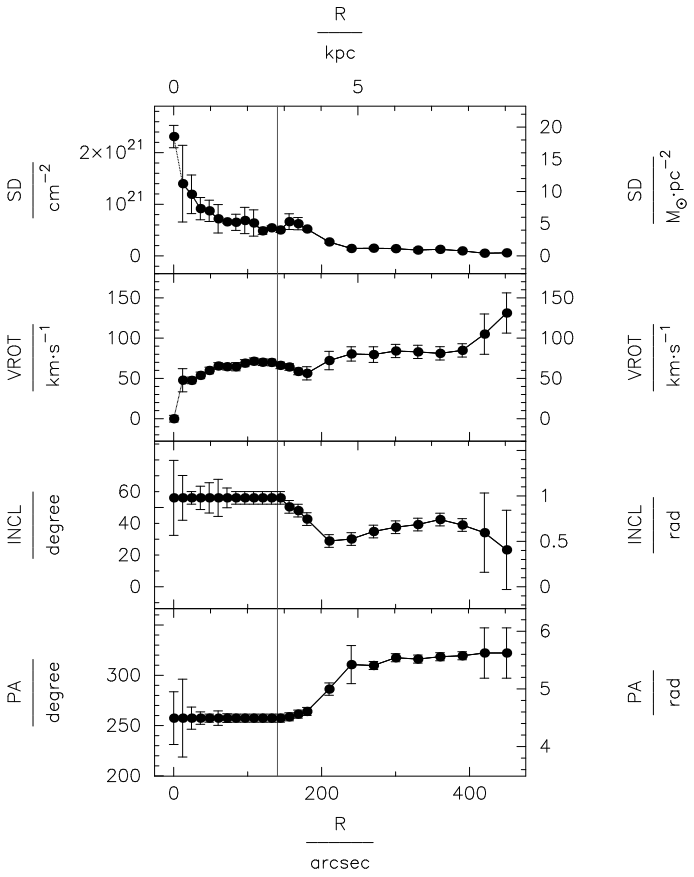

Figure 2: Fitted parameters for NGC 5204. The vertical line denotes the optical radius R_{25}.

Like the other galaxies of our sample, the warp of NGC 5204 exhibits the following features (see also Józsa, 2007, A&A, in press): i) At large radii the HI disk settles to a relatively coplanar disk that is inclined with respect to the inner disk, ii) At the radius where the warp starts, the measured rotation velocity changes. iii) At the same radius, the surface density of the warped HI layer drops, decreasing only very slowly beyond that galacto-centric distance.

The change in the rotation velocity indicates that the radius at which the warp starts marks the transition between two dynamical regimes, an inner one governed by the stellar disk and an outer one determined by the Dark-Matter halo.

The Local Volume HI Survey (LVHIS)

Bärbel Koribalski

CSIRO Australia Telescope National Facility

The 'Local Volume' — the sphere of radius ∼10 Mpc centered on the Local Group — includes at least 500 known galaxies. What makes this volume special is the fact that we can obtain (a) accurate velocities and independent distances for all its member galaxies, (b) the most detailed and sensitive multi-frequency observations, and (c), as a result, a complete census of the Local Volume (LV) galaxies and their properties. This allows us to create a dynamic 3D view of the Local Universe, leading to a thorough understanding of the local flow field, ie. the Hubble flow and its dispersion. Interferometric H I measurements in particular provide a greater understanding of the overall matter distribution (baryonic and non-baryonic) in the Local Volume and are crucial to accurately define the low-mass end of the H I mass function.

Reliable, independent distance estimates for LV galaxies are being gathered either from the luminosity of Cepheids, the tip of the red giant branch, or surface brightness fluctuations. These are listed in *'A Catalog of Neighboring Galaxies'* (Karachentsev et al. 2004, AJ 127, 2031) together with the optical and H I properties of 451 LV galaxies. To expand and deepen our knowledge of the nearby Universe several teams are currently targeting LV galaxies, among them the *"Local Volume HI Survey"* (LVHIS; Koribalski et al.), the *"Faint Irregular Galaxies GMRT Survey"* (FIGGS; Begum et al.), *"The HI Nearby Galaxy Survey"* (THINGS; Walter et al.), and the *"VLA-ANGST HI Survey"* (Ott et al.).

Using the Australia Telescope Compact Array (ATCA), the LVHIS team[4] is producing detailed H I distributions, mean H I velocity fields and 20-cm radio continuum maps for a complete sample of more than 70 southern galaxies selected from HIPASS (see, eg., Koribalski et al. 2004, AJ 124, 16). Each galaxy is typically observed for 3×12 hours total, using different array configurations, to achieve good *uv*-coverage (out to 1.5 km baselines), medium

[4]The LVHIS team members are: Bärbel Koribalski (PI), Lister Staveley-Smith, Erwin de Blok, Jürgen Ott, Helmut Jerjen, Igor Karachentsev, Angel Lopez-Sanchez, Emma Kirby, Nic Bonne and Janine van Eymeren.

resolution and high sensitivity. The low-resolution ATCA observations are complete and the results, in particular the H I moment maps of all observed galaxies, are displayed on the web at www.atnf.csiro.au/research/LVHIS. — Complementary projects include an H-band survey of all southern LV galaxies with the Anglo-Australian Telescope (AAT) and an Hα survey with the ANU 2.3-m telescope. — The LVHIS project goals are:

(1) Investigation of **local galaxy environments**: Using H I synthesis observations we trace the faint outer envelopes of the known LV galaxies (see Fig. 1) as well as detect their low-mass companions down to H I mass limits of $\sim 10^4 \times D^2$ $M_\odot$. We are also searching for neutral gas that is not taking part in the regular galaxy rotation, e.g. high velocity clouds and tidal streams. So far, only a few previously uncatalogued galaxies have been found while asymmetric gas envelopes are common. Several result have been shown in Koribalski (2006, ESO Workshop on "Groups of Galaxies in the Nearby Universe", Springer, p. 27).

(2) Determination and analysis of H I **rotation curves**: These will allow us to estimate the total mass and therefore the dark matter content of individual LV galaxies and trace virtually all of the galactic dark matter in the Local Volume. We will take into account the influence of non-circular motions on the shape of rotation curves and explore a variety of models that optimally fit the best-determined curves.

(3) Determination of the true **Tully-Fisher** (TF) relation (incl. the baryonic TF): This will be achieved using independent distances, well- determined H I rotational velocities and (c) a homogeneous set of optical & infrared magnitudes. The sensitive H I velocity fields obtained in the LVHIS project are currently being used by Nic Bonne (ANU, PhD student) to determine galaxy rotation curves, $v(r)$, inclination angles, $i(r)$, and position angles, $PA(r)$, while Emma Kirby (ANU, PhD student) is analysing the deep AAT H-band images so far obtained for 55 LV galaxies.

(4) Determination of the H I **mass function** for the Local Volume: by obtaining accurate H I masses for a complete sample of nearby galaxies with well established distances, we can significantly improve our knowledge of the faint end of the H I mass function.

(5) Estimate of accurate **star formation rates** (or upper limits) for the sample from the 20-cm radio continuum flux density to equally faint limits ($\sim 2 \times 10^{-5} D^2$ $M_\odot\,yr^{-1}$). These will be compared to SFR estimates obtained from SINGS (Kennicutt et al. 2003) and enable us to investigate on which scales the radio-infrared correlation breaks down. We will be able to estimate

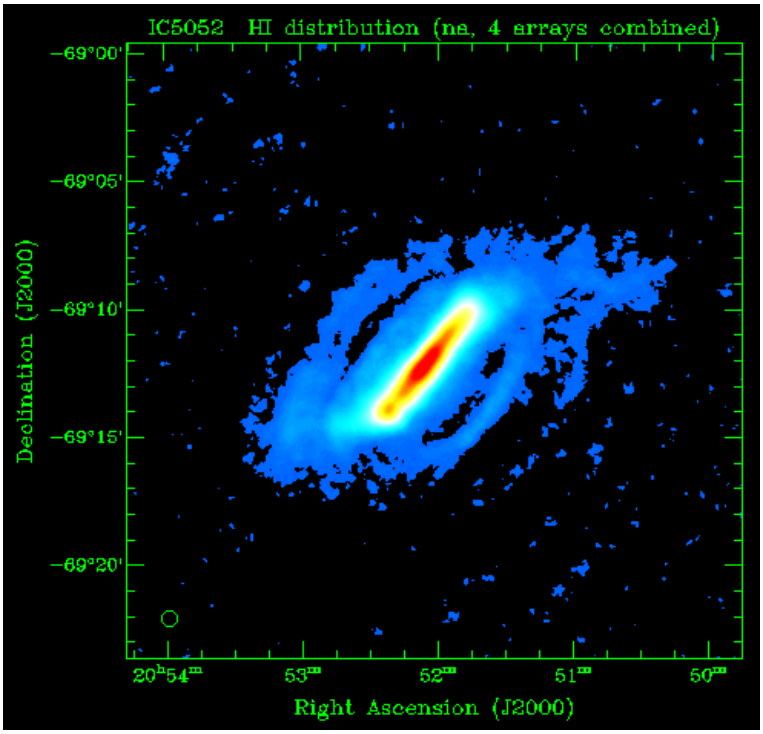

Figure 1: ATCA H I distribution of the nearby spiral galaxy IC 5052. While optical and infrared images of IC 5052 (type SBd) show a rather flat, edge-on galaxy, the observed H I envelope indicates an extended and highly warped gaseous disk.

the overall SFR density at $z = 0$ and compare with values measured at other wavelengths.

ATCA observations for the *"Local Volume HI Survey"* (LVHIS) will be completed in about a year, but further observations with the GMRT, WSRT and the eVLA are needed to complete the census of Local Volume galaxies. All-sky and deep H I surveys planned with the Australian SKA Pathfinder, a large interferometer to be located in Western Australia, will provide the next step in our understanding of the Universe.

Neutral Hydrogen Gas in Star Forming Galaxies at z=0.24

Philip Lah[1], Jayaram N. Chengalur[2], Frank H. Briggs[1,3], Matthew Colless[4], Roberto De Propris[5], Michael B. Pracy[1] & W. J. G. de Blok[1]

[1] Research School of Astronomy & Astrophysics, The Australian National University, Australia
[2] National Centre for Radio Astrophysics, India
[3] Australian Telescope National Facility, Australia
[4] Anglo-Australian Observatory, Australia
[5] Cerro Tololo Inter-American Observatory, Chile

Context: The cosmic star formation rate density is known to increase by an order of magnitude between the present time and z $\sim$ 1. However, the cosmic density of neutral gas is poorly constrained over this redshift range. Consequently, we are missing a key element in our understanding of galaxy evolution, that of the fuel supply for new stars.

In the local universe (z $\sim$ 0) the quantity of atomic hydrogen gas in galaxies has been measured with good precision using HI 21 cm emission surveys. However using radio observations of HI 21 cm emission to constrain the neutral gas density at cosmologically significant distances is difficult. This is because the flux from most individual galaxies at these redshifts falls below the detection limit of current radio telescopes in reasonable observing times.

Observations of damped Lyα absorption in QSO spectra have proven very effective at measuring the density of atomic hydrogen at high redshifts, z $>$ 1.5. However, it is difficult to constrain the neutral gas density from observations of damped Lyα absorbers at intermediate redshifts, since at these redshifts the Lyα line is not accessible by ground-based telescopes, and the average number of damped Lyα absorbers per unit redshift is low.

Aims: The aim of our project is to measure the amount of neutral gas in galaxies at moderate redshifts using the HI 21cm line by coadding the

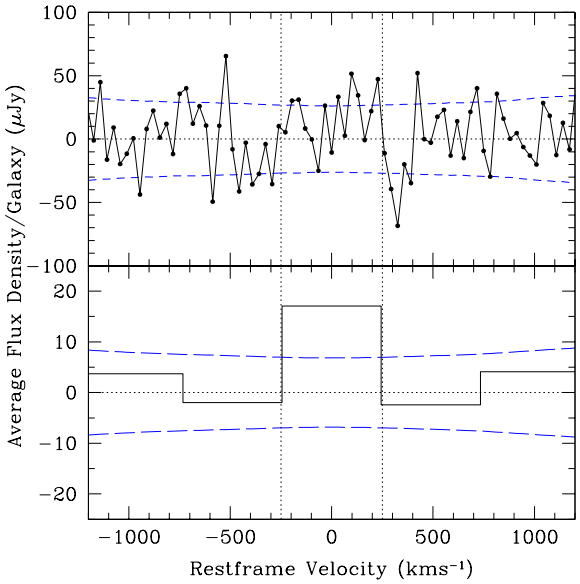

Figure 1: The average HI galaxy spectrum created from coadding the signal of all 121 galaxies with known optical redshifts. The top spectrum has no smoothing or binning and has a velocity step size of 32.6 $\mathrm{km\,s^{-1}}$. The bottom spectrum has been binned to ∼500 $\mathrm{km\,s^{-1}}$. For both spectra the 1σ error is shown as dashed lines above and below zero.

signal from multiple galaxies using their predetermined optical position and redshifts. By this method we are able to make useful measurements of the integrated 21cm flux from the HI mass in galaxies for comparison with the damped Lyα observations.

For this project we used the Giant Metrewave Radio Telescope (GMRT) to measure the atomic hydrogen gas content of star-forming galaxies at z = 0.24 (i.e. a look-backtime of ∼3 Gyr). Our sample of galaxies were selected from Hα-emitting field galaxies detected in a narrow-band imaging survey with the Subaru Telescope. The Anglo-Australian Telescope was used to obtain precise optical redshifts for these galaxies.

Results: In ∼40 hours of integration, we measure an average atomic hydrogen gas mass of $(2.26 \pm 0.90) \times 10^9$ $\mathrm{M_\odot}$ from the coadded signal of 121 galaxies as seen in Figure 1 (from Lah et al. 2007, MNRAS, 376, 1357). We translate this HI signal into a cosmic density of neutral gas at z = 0.24 of

$\Omega_{\rm gas} = (0.91 \pm 0.42) \times 10^{-3}$ as seen in Figure 2. This is the current highest redshift at which the neutral gas density has been constrained from 21 cm emission. Figure 2 also shows the z = 0 gas density from 21 cm surveys and previous results from damped Lyα systems at higher redshifts. Our value is consistent with that estimated from damped Lyα systems at the redshift of interest but has the advantage that it applies to a narrow range of redshifts z $\sim$ 0.24. Longer radio integration should allow for measurements of the gas density with significantly better precision.

Using our data, we also find that the correlations between the Hα luminosity and the radio continuum luminosity and between the star formation rate and the HI gas content in star-forming galaxies at z = 0.24 are consistent with the correlations found at z = 0. These two results suggest that the star formation mechanisms in field galaxies $\sim$3 Gyr ago were not substantially different from the present, even though the star formation rate is 3 times higher.

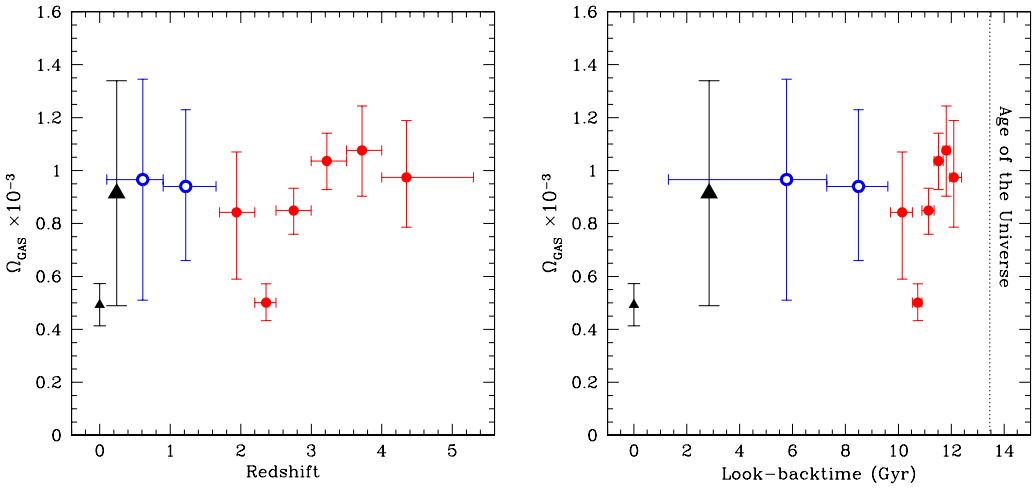

Figure 2: The neutral gas density of the universe as a function of redshift (on the left) and look back time (on the right). The small triangle at z = 0 is the HIPASS 21 cm emission measurement from Zwaan et al. 2005, MNRAS , 359, L30. The large triangle at z = 0.24 is our HI 21 cm emission measurement made using the GMRT. The open circles are damped Lyα measurements made using HST by Rao et al. 2006, ApJ, 636, 610. The filled circles are damped Lyα measurements from Prochaska et al. 2005, ApJ, 635, 123.

Recent Results from The HI Nearby Galaxy Survey

A. Leroy[1], F. Walter[1], W.J.G. de Blok[2], E. Brinks[3], F. Bigiel[1]

[1] Max Planck Institut für Astronomie, Germany
[2] Research School of Astronomy and Astrophysics, Mount Stromlo, Australia
[3] Center for Astrophysics Research, University of Hertfordshire, UK

Context: The HI Nearby Galaxy Survey (THINGS, Walter et al. 2007)[5] consists of maps of 34 nearby galaxies made with the Very Large Array. These data have angular resolution $\approx 7''$, velocity resolution ≈ 5 km s^{-1}, and sensitivity to column densities N(HI)$< 10^{20}$ cm^{-2}. Most targets are also part of the *Spitzer* Infrared Nearby Galaxies Survey (SINGS, Kennicutt et al. 2003, PASP, 115, 928) and the GALEX Nearby Galaxy Survey (NGS, Gil de Paz et al. 2006, astro.ph, 6440).

Aims: The science goals of THINGS are very wide ranging. First results include: high quality rotation curves for most THINGS galaxies with accompanying mass modelling (de Blok et al. 2007)[1]; a catalog of HI holes in the ISMs of nearby galaxies (Bagetakos et al. 2007)[1]; a detailed study of non-circular motions in two nearby irregulars (Oh et al. 2007)[1]; a study of the distribution of peak surface brightnesses across THINGS (Usero et al. 2007)[1]; and measurements of the outer edge in THINGS disk galaxies (Portas et al. 2007)[1]. I will highlight results of these projects.

I will present a more detailed description of work studying star formation (SF) laws in the THINGS, SINGS, and NGS overlap. This work addresses the following questions: 1) Are recipes from the literature capable of reproducing the observed star formation in THINGS (Leroy et al. 2007)[1]? 2) Does the "Kennicutt Law" (i.e. $\Sigma_{\rm SFR} \propto \Sigma_{\rm gas}^{1.4}$, Kennicutt 1998,ApJ,498,541) hold at 500 pc on a pixel-by-pixel basis within THINGS? (Bigiel et al., 2007)[1]. 3) How does the relationship between $\Sigma_{\rm SFR}$ and $\Sigma_{\rm HI}$ vary with spatial scale? (Bigiel et al., 2007)[1].

Results: We construct maps of the star formation surface density, $\Sigma_{\rm SFR}$, by combining GALEX FUV maps with *Spitzer* 24 μm maps. This estimate of $\Sigma_{\rm SFR}$ is sensitive to both obscured and unobscured star formation; it is derived from and compatible with the hybrid Hα/24 approach to deriving

[5]THINGS papers in preperation with submission planned for Summer 2007.

the SFR described by Calzetti et al. 2007 (in prep).

Can star formation recipes from the literature reproduce the observed $\Sigma_{\rm SFR}$ *maps?* Figure 1 shows the accuracy of 6 proposed SF recipes as a function of radius for THINGS spirals (Leroy et al. 2007)[1]. We test an unmodified Kennicutt Law (Kennicutt 1998, top left) and a Kennicutt Law combined with thresholds based on the Toomre-Q parameter (Kennicutt 1989,ApJ,344,685, Martin and Kennicutt 2001, ApJ,555,301, top middle), shear (Hunter, Elmegreen, and Baker 1998,ApJ,493,595, top right), and N(H) (Schaye 2004, bottom middle). We also test a recipe with a fixed SF efficiency per orbital timescale (Kennicutt 1998, bottom left) and the pressure-based prescription described by Blitz & Rosolowsky (2006,ApJ,650,933, bottom right).

Figure 1 shows that some mechanism for damping star formation is indeed required in the outer disks, though an unmodified Kennicutt Law performs quite well over the optical disk. All 5 mechanisms for damping yield good median accuracies even beyond the optical radius. Threshold-based recipes produce higher scatter than the efficiency-per-orbit or pressure formulation.

Does the star formation law hold on 500 pc scales in SINGS? Figure 1 shows a pixel-by-pixel plot of $\Sigma_{\rm SFR}$ as a function of $\Sigma_{\rm HI}$ across THINGS (Bigiel et al. 2007)[1]. We plot results for only disk galaxies and restrict ourselves to 0.3 $r_{25} < r < r_{25}$ in order to sample the HI-dominated regime only and remain within the star forming disk. There is a clear, significant relationship between Σ_{HI} and $\Sigma_{\rm SFR}$, though the scatter plot is not exactly what one would expect from the form of the Kennicutt Law, shown in the middle panel. The most visible difference is the presence of additional star formation at low HI columns in our data. This may reflect the importance of H_2 even in the HI-dominated region of the disk or a breakdown of our SF tracers.

How does the star formation law vary with spatial resolution? We convolve our maps to progressively lower spatial resolutions to study how the relationship between the two quantities vary with spatial scale (Bigiel et al. 2007)[1]. At each resolution, we derive the best fit power law slope and coefficient relating the two quantities. Somewhat surprisingly, we find very little dependence on scale, suggesting that the star formation law relating total gas content to star formation across an optical disk holds with relatively small variation down to $\sim$ 500 pc spatial scales.

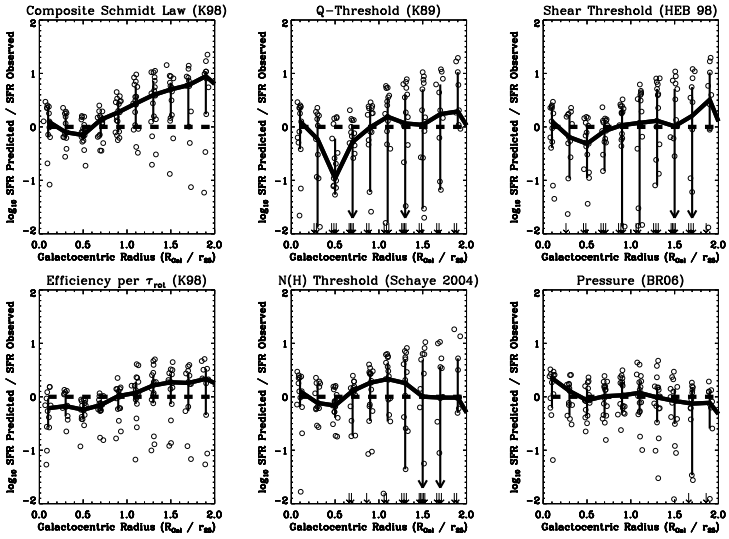

Figure 1: Black line: median accuracy, defined as log predicted / observed SFR, as a function of radius / r_{25} for 6 SFR recipes applied to $\sim$ 18 THINGS spiral galaxies. Circles and arrows show individual galaxies, vertical lines the 50% range. Damping to the Kennicutt Law is needed; all 5 other recipes yield resonable median accuracies. Threshold-based recipes have a tendency to yield subcritical disks and therefore show larger scatter than the "efficiency per orbit" or pressure recipes.

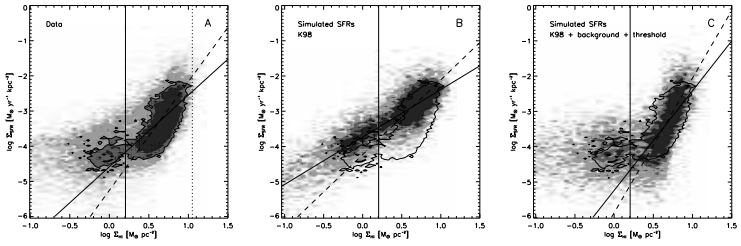

Figure 2: Star formation as a function of HI surface density in the HI-dominated region of THINGS spirals (Bigiel et al. 2007). The left hand plot, A, shows the data at 500 pc resolution, a clear relationship is evident. The middle plot, B, shows the expected distribution given a Kennicutt (1998) law applied at 500 pc resolution (the contour shows the data from plot A). The right hand plot, C, shows that the data are better reproduced with an additional SFR component that is largely independent of HI, perhaps the influence of H_2 in the outer disk or a breakdown in our SF tracers.

Observing the Epoch of Reionization with MWA

Colin Lonsdale, for the MWA Collaboration

MIT Haystack Observatory, USA

The MIRA Widefield Array (MWA) is a powerful new low-frequency radio array under development by a consortium of US, Australian and Indian institutions, to be built in the radio-quiet environment of outback western Australia. Major construction is scheduled to begin early in 2008, with commissioning around the end of 2008. The array is designed to produce high-fidelity information over a very wide and seamless field of view, many hundreds of square degrees, over the 80-300 MHz frequency range. As such, it will be possible to attempt a high precision measurement of the power spectrum of 21cm line fluctuations from the epochs of reheating and reionization between redshifts of 6 and 12. Pursuit of this scientific goal has driven many aspects of the system design, particularly with respect to controlling systematic errors, and providing the best possible basis for separating and removing contaminating foreground signals. The array comprises 512 antenna "tiles", each having 16 dual-polarization active dipoles. All 125,000 baselines are cross-correlated to yield unprecedented spatial frequency coverage and point spread function quality, as a starting point for an innovative and ambitious real-time high precision calibration system.

As a primary science driver for the array, EoR observations will take priority during prime night-time observing periods, and during the first year of full operations (currently projected to start in early 2009), of order 2000 hours of integration time will be shared between perhaps 3 target fields. If thermal noise limits can be reached, this will yield sensitivity to the EoR power spectrum with high SNR for redshifts between 7 and about 10, with decreasing SNR beyond that.

The array will be described, and the current state of progress reviewed, with emphasis on the targeted design features relevant to EoR studies. The techniques to be used in EoR data analysis will be presented, and some of the astrophysical insights that we might hope to gain with MWA data will be discussed. Future directions for the MWA program will be outlined.

The nature of ionizing sources at zsim6

Sangeeta Malhotra

Arizona State University, USA

It is clear that low luminosity galaxies dominate the ionizing photon budget at zsim6. What then is the nature of these galaxies including the opacity which affects the escape of ionizing photons, stellar IMF which would affect the number of ionizing photons and the clustering of these sources, which would affect the distribution of ionizing photons. I will discuss what we have learnt about these questions from spectroscopic surveys in the HUDF: GRAPES and PEARS.

Probing the End of Reionization via QSO H_{II} Regions.

Antonella Maselli[1], Simona Gallerani[2], Andrea Ferrara[2] & T.R. Choudhury[3]

[1] Max-Planck-Institut für Astrophysik, Karl-Schwarzschild-Strasse1, 85748 Garching, Germany
[2] [2] SISSA/International School for Advanced Studies, via Beirut 2-4, 34014 Trieste, Italy
[3] Institute of Astronomy, Madingley Road, Cambrige CB3 OHA, UK

Context: Whether reionization is completed at z=6 or it is just turning at the end of the overlap phase is still a matter of debate. Nevertheless getting new insights in this issue will provide a better understanding of the nature of luminous sources at various redshift, and ultimately in non-linear processes of structures formation. Different kind of observations and methods have been proposed and use to measure the mean neutral hydrogen fraction at this epoch, but the outcomes are still affected by non-negligible observational uncertainties and assumptions made on the model parameters.

Aims: High redshift quasars can be used as powerful probes of the ionization state of the universe, via the signatures left from their surrounding H_{II} region in their absorption spectra. The aim of this work is to investigate the possibility of constraining the ionization state of the Intergalactic Medium (IGM) at $z \approx 6$ by measuring the size of the H_{II} regions in high-z quasars spectra. The extent of H_{II} regions around high-z luminous quasars at $z \approx 6$ is infact strongly dependent on x_{HI} and it is actually observable in high-z quasar spectra as the non-zero flux stretch of the spectrum extending from the quasar location to the red side of the Gun-Peterson (GP) trough.

Results: Improving with respect to previous modeling, we have performed a combination of multi-phase SPH and 3D radiative transfer simulations to reliably predict the properties of typical high-z quasar regions, embedded in a partly neutral IGM (see Fig.1).

From the analysis of mock spectra along lines of sight through the simulated QSO environment we find that the H_{II} region size derived from quasar

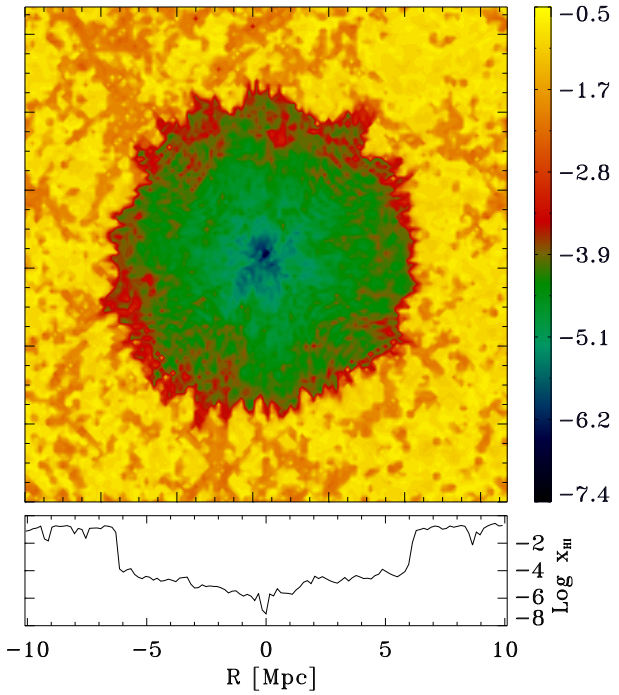

Figure 1: Map (upper panel) and cut (lower panel) of the simulated $x_{\rm HI}$ (logarithmic scale) across the quasar (located at the center of the box). The quasar H_{II} region is clearly identified.

spectra (R_f) is on average 30% smaller than the physical one (see Fig.2), an effect that we have called *apparent shrinking*. Additional maximum likelihood analysis shows that this offset induces an overestimate of the neutral hydrogen fraction, $x_{\rm HI}$, by a factor > 3. By applying the same statistical method to a sample of observed quasar spectra, our study favors a mostly ionized ($x_{\rm HI} < 0.06$) universe at $z = 6.1$.

For more details see Maselli et al. 2007 (*MNRAS*, 376, 34) and references therein.

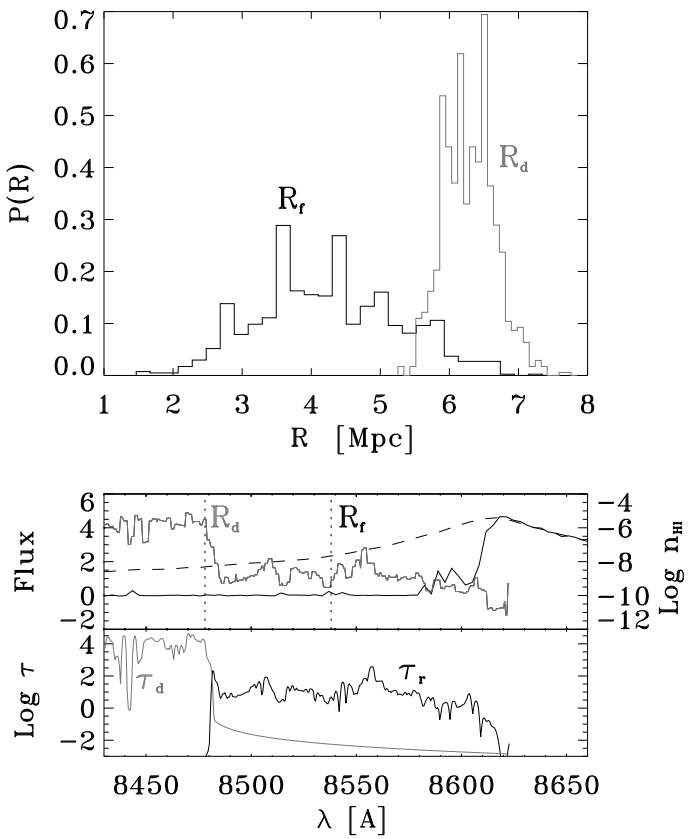

Figure 2: *Upper panel:* Probability distribution function for R_d and R_f (physical units) using 1000 LOS through the simulation box. The offset between the two distributions quantifies the apparent shrinking (see text). *Central panel:* Illustrative template (dashed line) and absorbed (solid dark) spectra, along with the $n_{\rm HI}$ density distribution (light gray) as a function of observed wavelength, for a representative LOS. *Bottom panel:* Contributions to the total GP optical depth, τ, from neutral hydrogen within (τ_r, dark) and outside (τ_d, light gray) the $\rm H_{II}$ Region for the same LOS shown in the middle panel.

Constraints from High-Redshift Absorption Spectra

Andrei Mesinger

Yale Center for Astronomy and Astrophysics, Yale University, New Haven, CT 06520

Context: The epoch of reionization, when the radiation from early generations of astrophysical objects ionized the intergalactic medium (IGM), offers a wealth of information about cosmological structure formation and physical processes in the early universe. Only recently have we begun to gather clues concerning this epoch. The Thomson scattering optical depth, $\tau_e = 0.09 \pm 0.03$, measured from the polarization anisotropies in the cosmic microwave background (CMB) by the *Wilkinson Microwave Anisotropy Probe* (*WMAP*), suggests that cosmic reionization began at redshift $z \gtrsim 10$. However, the current uncertainty of this value, and the fact that the optical depth measures only an integrated electron column density, means that many possible competing reionization scenarios can still be accommodated.

The main difficulty in furthering our theoretical understanding of this important epoch lies in the enormous dynamic range required to accurately model it. Ionized regions are expected to reach characteristic sizes of tens of comoving Mpc, which is over seven orders of magnitude in mass larger than the pertinent cooling mass, corresponding to gas with a temperature of $T \sim 10^4$ K. The required dynamic range is even larger if smaller "minihalos" below this cooling threshold are important during reionization. Because of the steep mass dependence of halo abundances, halos with masses close to the cooling mass could dominate the photon budget.

Aims: We seek to further our understanding of current high-redshift observations, specifically their impact on reionization. We separately model the spectra of each of the $z > 6.2$ quasars, seeking to *independently* constrain the hydrogen neutral fraction, the size of surrounding HII region, and the quasar's ionizing emissivity.

To further aid in the interpretation of current and upcoming high-redshift observations, we also introduce approximate but efficient methods for generating halo distributions at high redshifts as well as for generating the asso-

ciated ionization maps.

Results: We make use of hydrodynamical simulations of the intergalactic medium (IGM) to create model quasar absorption spectra. We compare these model spectra with the observed Keck spectra of three $z > 6.2$ quasars with full Gunn-Peterson troughs: SDSS J1148+5251 ($z = 6.42$), SDSS J1030+0524 ($z = 6.28$), and SDSS J1623+3112 ($z = 6.22$). We fit the probability density distributions (PDFs) of the observed Lyman α optical depths (τ_α) with those generated from the simulation, by adopting a template for the quasar's intrinsic spectral shape, and exploring a range of values for the size of the quasar's surrounding HII region, R_S, the volume-weighted mean neutral hydrogen fraction in the ambient IGM, $\bar{x}_{\rm HI}$, and the quasar's ionizing photon emissivity, $\dot{N}_Q$. In order to avoid averaging over possibly large sightline–to–sightline fluctuations in IGM properties, we analyze each observed quasar independently. We find the following results for J1148+5251, J1030+0524, and J1623+3112: The best–fit sizes R_S are 40, 41, and 29 (comoving) Mpc, respectively. For the later two quasars, the value is significantly larger than the radius corresponding to the wavelength at which the quasar's flux vanishes. These constraints are tight, with only $\sim 10\%$ uncertainties, comparable to those caused by redshift–determination errors. The best–fit values of $\dot{N}_Q$ are 2.1, 1.3, and 0.9×10^{57} s^{-1}, respectively, with a factor of ~ 2 uncertainty in each case. Finally, the best–fit values of $\bar{x}_{\rm HI}$ are 0.16, 1.0, and 1.0, respectively. The uncertainty in the case of J1148+5251 is large, and $\bar{x}_{\rm HI}$ is not well constrained. However, for both J1030+0524 and J1623+3112 we find a significant lower limit of $\bar{x}_{\rm HI} \gtrsim 0.033$. Our method is different from previous analyses of the GP absorption spectra of these quasars, and our results strengthen the evidence that the rapid end–stage of reionization is occurring near $z \sim 6$.

Detailed theoretical studies of the high-redshift universe, and especially reionization, are generally forced to rely on time-consuming N-body codes and/or approximate radiative transfer algorithms. We present a method to construct semi-numerical "simulations", which can efficiently generate realizations of halo distributions and ionization maps at high redshifts. Our procedure combines an excursion-set approach with first-order Lagrangian perturbation theory and operates directly on the linear density and velocity fields. As such, the achievable dynamic range with our algorithm surpasses the current practical limit of N-body codes by orders of magnitude. This is particularly significant in studies of reionization, where the dynamic range

is the principal limiting factor because ionized regions reach scales of tens of comoving Mpc. We test our halo-finding and ionization-mapping algorithms *separately* against N-body simulations with radiative transfer and obtain excellent agreement. We compute the size distributions of ionized and neutral regions in our maps. We find even larger ionized bubbles than do purely analytic models at the same volume-weighted mean hydrogen neutral fraction, $\bar{x}_{\rm HI}$, especially early in reionization. We also generate maps and power spectra of 21-cm brightness temperature fluctuations, which for the first time include corrections due to gas bulk velocities. We find that velocities widen the tails of the temperature distributions and increase small-scale power, though these effects quickly diminish as reionization progresses. We also include some preliminary results from a simulation run with the largest dynamic range to date: a 250 Mpc box that resolves halos with masses $M \geq 2.2 \times 10^8 M_\odot$. We show that accurately modeling the late stages of reionization, $\bar{x}_{\rm HI} \lesssim 0.5$, requires such large scales. The speed and dynamic range provided by our semi-numerical approach will be extremely useful in the modeling of early structure formation and reionization.

Star Formation in Extended HI Disk Galaxies

Gerhardt Meurer

Department of Physics and Astronomy, The Johns Hopkins University, USA.

Here I report on ACS imaging of two galaxies with extended HI disks: NGC2915 and DDO154. We observed these galaxies with the Wide Field Camera using the g (F475W), V (F606W), and I (F814W) filters with the field placed at the outermost isophote detectable from the ground. Both galaxies are near enough that they are easily resolved into stars with ACS. In NGC2915 we clearly see two stellar populations. The surface density of old stars has an exponential decline out to the edge of the frame matching that detected from the ground, while the younger blue stellar population has a more clumpy distribution which is similar to that seen in HI. In DDO154, stars are also seen well beyond the outermost isophote detected from the ground. Neither galaxy has a well defined edge to the stellar distribution. I compare the number of blue stars found in the outer disks of galaxies with H-alpha observations and make the case that outer disks are under represented in O stars for their observed number of later spectral types. This is used to argue that, effectively, the IMF is not constant, a result that is consistent with results from comparison of H-alpha and UV (Galex) radial profiles. I end the talk by examining the dynamics of outer galaxy disks and show evidence that the optical limits imply that the local dynamical time plays an important role in the star formation law.

The early galaxies: formation and radiation

Smadar Naoz[1], Rennan Barkana[1]

[1] School of Physics and Astronomy, The Raymond and Beverly Sackler Faculty of Exact Sciences, Tel Aviv University, Tel Aviv 69978, ISRAEL

Context: The formation of the first galaxies in the universe has been studied for many years. In particular, the first observable star is most likely to have formed 30 million years after the big bang (at redshift 65). The first galaxies released UV radiation which in return produced fluctuations in the 21-cm power spectrum. Additional gas is also expected to have collected in star-less minihalos which affected reionization through the recombination rate. Thus, considering the formation and properties of the first luminous objects both in the linear and non-linear regime is of high importance.

Aims: In the linear regime we investigate the relation between the baryon and the dark matter fluctuations. The suppression of baryon density fluctuations compared to the dark matter, due to baryonic pressure, occurs below a characteristic mass scale. Previous calculations predict that the suppression occurs up to a mass of $\sim 10^6$ $M_\odot$, which suggests that pressure has a central role in determining the properties of the first luminous objects at early times. The characteristic mass scale is also important for predicting the fraction of the cosmic gas that is in minihaloes in early times.

Expanding our investigation to the non-linear regime, we calculate in detail the spherical collapse of high redshift objects in a cold dark matter universe. We include the gravitational contributions of the baryons and radiation and the memory of their kinematic coupling before recombination.

The well-known solution for the collapse of a halo in an Einstein de Sitter (EdS) universe yields a critical overdensity, in the corresponding linearly extrapolated calculation, of $\delta_c = 1.686$, a value that does not depend on the halo mass or collapse redshift. With the ΛCDM cosmological parameters, the contribution of the photons to the expansion of the universe cannot be neglected when considering the formation of the first objects. Moreover, the baryons make a non-negligible contribution compared to the dark matter, and their different evolution must be included in the collapse process. We

perform a precise calculation of non-linear collapse including all of the appropriate physical ingredients. In particular, in order to predict when the first observable star was most likely to have formed, we need to account for the light travel-time from distant galaxies, for Poisson and density fluctuations on all scales, and for the effect of very early cosmic history on galaxy formation.

Results: We show that the expected characteristic mass scale is substantially lower than suggested by previous calculations (by a factor of $\sim 3-10$, depending on redshift), and thus the effect of baryonic pressure on the formation of galaxies up to reionization is only moderate. This reduction in the characteristic mass scale is a result of including the fact that the baryons have smoother initial conditions than the dark matter. This smoothing is due to the aftereffects of the coupling with the radiation before recombination. This yields lower pressure gradients than previous estimations in the period from cosmic recombination to $z \sim 200$, after which the gas cooled down adiabatically and the pressure dropped. At $z \sim 10$ the suppression of the baryon fluctuations is still sensitive to the history of pressure in this high-redshift era. We calculate the fraction of the cosmic gas that is in minihaloes and find that it is substantially higher than would be expected with the previously estimated characteristic mass.

We use our precise calculation to predict a more accurate halo mass function as a function of redshift, and in particular, we also predict when the first star that astronomers can observe (i.e., in our past light cone) formed in the Universe.

Regarding another important effect of high-redshift galaxies, recent work has shown that fluctuations in the Ly-alpha radiation emitted by these galaxies produced fluctuations in the 21-cm power spectrum. We investigate previously neglected physical effects on the radiation, which should make it easier for future observations to detect the signal from these early galaxies.

The Strongest MgII Absorbers

Daniel Nestor

Institute of Astronomy, Cambridge, UK

Recent large absorption-line surveys have allowed for the study of absorbers across a wide range of line-strengths. I will describe ongoing progress in our understanding of the nature and origin of MgII absorbing gas, as well as the galaxies with which they are associated, though the study of the strongest MgII systems at intermediate redshift. This progress has come through a combination of techniques including image and spectra stacking, the effects of absorbers on background QSOs, and traditional imaging with follow-up spectroscopy of host galaxies. In particular, I will discuss our work on ultra-strong MgII absorbers: their hosts and environments; their relation to outflows of enriched gas into the IGM through interactions and/or superwinds; their relationship to high-z Lyman-break galaxies, local dwarfs, and DLAs; their true incidence (after correcting for dust-induced biases); and their overall importance to our understanding of star formation and the enrichment of HI gas.

Molecular fractions in Damped Lyman-α systems

Pasquier Noterdaeme[1], Patrick Petitjean[2,3], Cedric Ledoux[1] & Raghunathan Srianan[4]

[1] European Southern Observatory, Alonso de Córdova 3107, Casilla 19001, Vitacura, Santiago, Chile
[2] Institut d'Astrophysique de Paris, CNRS - Université Pierre et Marie Curie, 98bis Boulevard Arago, 75014, Paris, France
[3] LERMA, Observatoire de Paris, 61 Avenue de l'Observatoire, 75014, Paris, France
[4] IUCAA, Post Bag 4, Ganesh Khind, Pune 411 007, India

We present the Ultraviolet and Visible Echelle Spectrograph survey for molecular hydrogen in high redshift Damped Lyman-α systems (DLAs). We built a sample of 67 DLAs/strong sub-DLAs, with $N(\mathrm{H\,I}) \geq 10^{20}$ cm^{-2} and $z_{\rm abs} > 1.8$. We detect H_2 in 13 of these systems and measure upper-limits on $N(H_2)$ for the remaining ones. We show there is no evolution of the fraction of H_2-bearing DLAs with cosmic time in the redshift range $1.8 < z_{\rm abs} < 4.2$. There is no dependence of the column-density of molecular hydrogen on the column density of neutral hydrogen. On the contrary, there is a clear dependence of $N(H_2)$ with the column density of iron in dust. H_2-bearing DLAs are rare and each system provides new clues on the understanding of the interstellar medium at high-redshift.
We study the excitation mechanisms in a newly detected H_2-bearing DLA and show an increasing velocity dispersion (Doppler parameter) with the energy of the rotational level. Together with the excitation diagram, this shows that turbulence or C-shocks may be an important excitation source for H_2 in DLAs.

Data-mining 21cm data sets

Peng Oh

UC Santa Barbara, USA

I discuss novel means of extracting information about the reionization epoch from forthcoming 21cm data sets. Most work to date has focussed on the power spectrum. While there is a good deal of information in the power spectrum, the 21cm field during reionization is a highly non-Gaussian field, and optimal techniques to extract the reionization signal should focus on statistics specifically tuned to the presence of large holes in the 21cm signal. The growth and percolation of HII regions as a function of redshift is a key (perhaps the key) observable in studies of reionization, and provides our best constraint on structure and star formation at high redshift. I discuss the following:

—statistical detection of ionized bubbles. I show how mixture modelling of the 21cm PDF can be used to stastically detect the presence of HII regions and extract the HII filling factor as a function of redshift.

—direct detection of ionized bubbles. The largest bubbles can be detected in imaging data. I discuss an optimal algorithm for detecting edges against a noisy stochastic background.

–Foreground subtraction—I discuss the thorny issue of foregrounds, and some issues in foreground subtraction.

HI Survival in a Group Environment

Amitesh Omar[1,2]

[1]Sterrewacht, Leiden University, 2333CA, Leiden, The Netherlands
[2]ARIES, Manora Peak, Nainital 263129, India

Context: Several clusters have been surveyed in the HI 21-cm line in order to understand the effects of cluster environment on the galaxies. More than one gas removal process can be identified working in a cluster environment. The results also point towards a significant removal of gas before the cluster evolves from merger of small groups. It is not clear though that how much of gas removal takes place during merger phases (i.e., in a group environment).

Aims: I will be presenting results from an HI imaging survey of a large nearby ($\sim$20 Mpc) group Eridanus using the Giant Meterwave Radio Telescope (GMRT). This group appears to be a conglomeration of several small groups in a merging phase. This paper presents an analysis of gas removal processes working in a large group likely to form a cluster.

Results: Large HI deficiency has been seen in many late-type galaxies in this group. An analysis of the data suggests that the observed HI deficiency is mostly due to tidal interactions. Follow-up observations reveal HI streamers and puzzling HI morphologies in the group. Some of the HI morphologies are strikingly similar to that expected from ram-pressure as seen in cluster environments. A possible effect of the warm-hot Inter-Galactic Medium (IGM) on shaping the HI disks in galaxies will be discussed. The HI study of this nearby group can be analogues to studying HI in groups/clusters during their hierarchical formation at high redshifts.

Radiative feedback from the first stars and formation of the second-generation stars

Kazu Omukai

National Astronomical Observatory of Japan, Japan

The first-generation stars are considered to be very massive (>a few $100M_\odot$). They emit a tremendous amount of UV photons, and photoionize/dissociate the surrounding gas, thereby prohibiting the subsequent star formation. According to recent studies, radiative feedback onto nearby halos is not as significant as originally postulated, but still very effective within the same halo. By this mechanism, the star formation efficiency of the first stars is kept very low. After the death of the first stars, provided outside the pair-instability mass range (150-250$M_\odot$), they become black holes without metal ejection. In the surrounding fossil HII regions, although with the primeval composition, lower-mass stars (a few tens $M_\odot$) can be formed owing to the initial high degree of ionization.

The faint end of the HI mass function

Tom Oosterloo, Katarina Kovac, Marc Verheijen, & Thijs van der Hulst

ASTRON, The Netherlands

I report on a HI survey was carried out using the Westerbork Synthesis Radio Telescope (WSRT) in the direction of the Canes Venatici (CVn) groups of galaxies covering about 90 deg^2, with a sensitivity of 0.8 mJy/beam over 33 km/s. The bestfitting Schechter function has a slope of -1.17 down to masses of 3 106 solar masses. Combined with optical data we study various Tully-Fisher relations. The main conclusion is that the TF relation established by the WSRT CVn galaxies follows the TF relation established by brighter and faster rotating galaxies. Fainter and slower rotating WSRT CVn galaxies do not indicate any break in these TF relations. When compared to previous estimates of the BTF relation in the literature, our data provide no indication that galaxies with small profile widths (e.g. below 90 km/s) lie systematically below the BTF established by larger systems.

Reionization Search at GMRT

Ue-Li Pen

CITA, Canada

We report on the status of the reionization search at GMRT. Based on current simulations, a 100h GMRT field is forecast to yield a 20 sigma detection of the reionization power spectrum. A major observing campaign is under way which includes a new software correlator, and new analysis pipeline.

HI Gas and Metals through Cosmic Times

Céline Péroux

Observatoire Astronomique de Marseille-Provence, Marseille, France

A complementary method to the emission selection of high-redshift galaxies consists in the observation of absorbers along the line of sight toward a background quasar. This selection technique has a constant sensitivity at all redshifts up to $z = 6$ (i.e. no redshift desert) and allow to select all types of galaxies regardless of their luminosity or star formation rate. The highest column density absorbers, the Damped Lyman-α (DLAs) systems, in particular, can be used to determine the cosmic evolution of HI gas in the Universe, $\Omega_{\rm HI}$, and the global metallicity in the gas phase. Since stars are known to form from HI gas, $\Omega_{\rm HI}$ provides an indirect tracer of the history of star formation. Recent results from several parallel VLT programmes aiming at determining the cosmological evolution of the metallicity in the absorbing gas are presented.

An All Sky Survey of Hydrogen Emission

Jeff Peterson

Carnegie Mellon University, USA

Context: The proposed Hubble Sphere Hydrogen Survey will use a telescope with collecting area 400,000 square meters, over ten time the size of any that exists today. Built of fixed cylinders, the telescope will observe along the meridian and accumulate 21 cm signals over a several years.

Aims: The goal is to build up a sensitive three dimensional image of the structure of neutral hydrogen.

Results: A prototype telescope is under consrtuction in Pittsburgh.

A Survey for Molecular Hydrogen in Damped Lyman-α Systems

Patrick Petitjean[1], Pasquier Noterdaeme[2], Cédric Ledoux[2] & Ragunathan Srianand[3]

[1] Institut d'Astrophysique de Paris, 98bis Boulevard Arago, 75014 - France; petitjean@iap.fr
[2] European Southern Observatory, Alonso de Córdova 3107, Casilla 19001, Vitacura, Santiago, Chile; cledoux@eso.org, pnoterda@eso.org
[3] IUCAA, Postbag 4, Ganeshkhind, Pune 411007, India; anand@iucaa.ernet.in

Context: Deriving the physical conditions of the Inter-Stellar Medium in the remote Universe is of prime importance for our understanding of how the first stars form and evolve to build up galaxies. Molecular hydrogen is the most abundant molecule in the Universe and the primary coolant of the gas in the early stages of star formation but it is also very difficult to detect directly. Usually, emission lines from the tracer molecule CO are used but only very bright objects can be detected at high redshift. At the moment, the only way to detect molecular hydrogen directly at high redshift is to search for the absorption signature of the molecular UV lines in Damped Lyman-α systems.

Aims: We are conducting a survey of molecular hydrogen in DLA systems at $z_{\rm abs} > 1.8$, using the Ultra-Violet and Visible Echelle Spectrograph at the European Southern Observatory's Very Large Telescope down to a detection limit of typically $N(H_2) \sim 2 \times 10^{14}$ cm^{-2}. As the H_2 absorption transitions have rest-wavelengths in the UV, the observations are challenging because the lines are blended with the numerous absorptions from the intergalactic medium and data with both high spectral resolution and high signal-to-noise ratio are needed. In all of the systems, we measure metallicities relative to Solar, [X/Y] = log N(X)/N(H)$-$log(X/H)$_\odot$ (with either X=Zn, or S, or Si), and depletion factors of Iron, [X/Fe], supposedly onto dust grains.

Results: We have constructed a sample of 67 systems with log N(H I) (cm^{-2}) > 20 where it is possible to detect H_2 or at least to derive an upper limit on the column density. 14 have firm detections of associated H_2 absorption lines. The highest detection redshift is $z_{\rm abs} = 4.224$. There is a clear correlation between metallicity and the presence of H_2, 50% or the systems with metallicity larger than -1.3 solar have associated H_2 absorption. The mean kinetic temperature of the gas corresponding to DLA subcomponents in which H_2 absorption is detected, derived from the ortho-to-para ratio, 153±78 K, is higher than that measured in the ISM (77±17 K) and the Magellanic clouds (82±21 K). The pressure, measured using C I fine-structure excitation, is higher than what is measured along the ISM sightlines, corresponding to $T = 100-300$ K and $n_{\rm H} = 10-200$ cm^{-3}. From the column densities of the high-J rotational levels, we derive that the typical radiation field in the H_2 bearing components is of the order of or slightly higher than the mean UV field in the Galactic ISM.

Radio Signatures of Reionization

Nada Petrovic

University of California Santa Barbara, USA

We study two different radio signatures of early star formation. First, we investigate hydrogen radio recombination lines from star forming regions, both as a foreground for 21cm observations and as a window into galaxy formation. Secondly, we consider carbon and oxygen fine-structure lines in both star-forming regions and the intergalactic medium. We give particular emphasis to the 63 micron line from OI, since OI is in charge exchange equilibrium with HI. Such lines can potentially be detected from the epoch of reionization with the next generation of CMB experiments. Their fluctuations, and in particular cross-correlation with the 21cm signal, could teach us a great deal about the topology of reionization and metal pollution.

The bispectrum of redshifted 21-cm fluctuations from the dark ages

Annalisa Pillepich[1], Cristiano Porciani[1], Sabino Matarrese[2]

[1] Institute for Astronomy, ETH Zurich, 8093 Zurich, Switzerland
[2] Dipartimento di Fisica "G. Galilei", Università di Padova; and INFN Sezione di Padova, I-35131 Padova, Italy

Context: During the dark ages (the time between recombination and the formation of the first stars), the cosmic microwave background (CMB) is coupled to atoms of neutral hydrogen through spin-flip 21-cm transitions. Due to the resonant nature of the interaction, neutral hydrogen at redshift z imprints a signature at a wavelength of $21.12\,(1+z)$ cm in the CMB. The brightness temperature of the CMB at radio wavelengths thus probes the three-dimensional neutral hydrogen distribution at $30 < z < 100$. This accurately traces dark-matter inhomogeneities down to the Jeans length (~ 10 comoving pc corresponding to angular separations of $\sim 10^{-2}$ arcsec). On smaller scales, the finite pressure of the gas keeps the baryons uniformly distributed. Brightness-temperature fluctuations in the redshifted 21-cm background from the cosmic dark ages can thus be used to determine the statistical properties of density fluctuations in the early Universe.

In Pillepich et al. 2007, ApJ, 662, 1 in press (astro-ph/0611126), we focused on the three-point statistics. We first derived the most general expansion of brightness-temperature fluctuations up to second order in terms of all the possible sources of spatial anisotropies. We then computed the angular bispectrum of brightness-temperature fluctuations generated prior to the epoch of hydrogen reionization.

Aims: Measuring the bispectrum of fluctuations in the 21-cm background will ultimately allow to quantify the degree of non-Gaussianity (NG) of the density field at high-redshift. Such a non-Gaussianity has two possible origins: non-linearity due to the usual Newtonian gravitational instability and non-Gaussianity which is intrinsic in the mechanism generating the primordial seeds, i.e. arising during or immediately after inflation. The

latter contributions to non-Gaussianity are usually expressed through a *non-linearity parameter* $f_{\rm NL}$ which measures the strength of quadratic terms in the *primordial* gravitational potential (e.g. Salopek & Bond 1990, Phys. Rev. D, 42, 3936). The most stringent limits on $f_{\rm NL}$ are based on the analysis of CMB anisotropies from three-year WMAP data (Spergel et al. 2006, astro-ph/0603449) and give $-54 < f_{\rm NL} < 114$ (2σ confidence level). The high-resolution observations of CMB anisotropies by the *Planck* satellite should reduce the 2σ detection threshold to $|f_{\rm NL}| \sim 10$.

Searches for primordial NG based on the large-scale structure of the Universe where the relevant observables probe the density field (e.g. three-point statistics of the galaxy distribution) are plagued with two problems. First, the density field is related to the gravitational potential through the Poisson equation so that its Fourier modes weigh the non-gaussian contributions with extra k^{-2} terms and only the largest scales may keep memory of primordial NG. Moreover, the ratio of Newtonian non-linear terms to intrinsical non-gaussian terms roughly scales like $(1+z)^{-1}$, so that non-gaussian signatures in the local Universe are easily masked by the effects of gravitational instability. In this sense, the 21-cm background at large redhifts appears as an extremely promising dataset to search for primordial NG able to provide constraints on $f_{\rm NL}$ which can be complementary and possibly competitive with those based on CMB anisotropies.

Results: Using second order perturbation theory, we have computed analytically and evaluated numerically the angular bispectrum of redshifted 21-cm fluctuations down to a few arcsecond angular scales ($\ell \simeq 10^5$). Figure 1 shows that the angular bispectrum of brightness-temperature fluctuations is dominated by the contribution due to non-linear gravity (with the possible exception of the largest angular scales). The residual dependence on the amount of primordial NG is small but still measurable.
Our signal-to-noise analysis for an ideal experiment (full sky, limited only by cosmic variance, with perfect foreground subtraction) indicates that studies of the 21 cm bispectrum can provide a unique test of the gravitational instability scenario for structure formation, as low-frequency radio experiments with arcmin angular resolution can easily detect the NG produced by the evolution of non-linear gravity with signal-to-noise ratio of order 100 (see Figure 2). On the other hand, detecting the signature of primordial NG is much more challenging but still possible. An ideal experiment limited only by cosmic variance and with an angular resolution of few arcsec has the po-

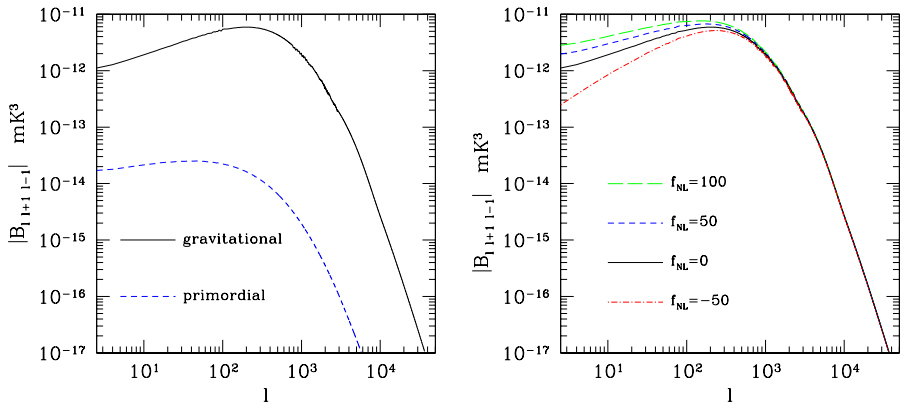

Figure 1: The bispectrum of 21-cm anisotropies B_{ℓ_1,ℓ_2,ℓ_3} measured by an ideal experiment with 0.1 MHz bandwidth centered around $z = 50$. We consider here quasi-equilateral ($\ell_2 = \ell_1 + 1, \ell_2 = \ell_1 - 1$) configurations. In the left panels, the contributions of non-linear gravity (solid) and of primordial non-Gaussianity (with $f_{\rm NL} = 1$; dashed) are compared. The right panels show the total bispectrum for different values of the non-linearity parameter.

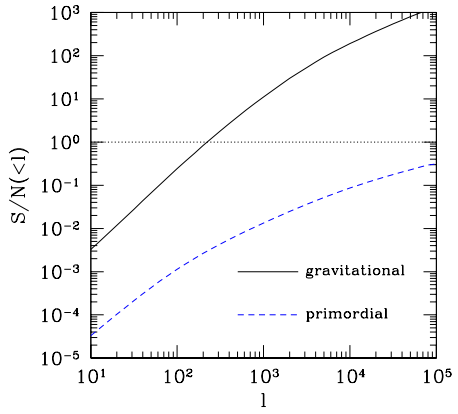

Figure 2: Cumulative signal-to-noise ratio for the measurement of the bispectrum of 21-cm anisotropies using modes up to a maximum value of ℓ. Solid lines refer to non-Gaussianity generated by gravity while dashed lines indicate the primordial signal with $f_{\rm NL} = 1$. These quantities have been computed using the signal-to-noise ratio per mode of the quasi-equilateral configuration (left).

tential to detect primordial NG with a non-linearity parameter $f_{\rm NL} \sim 1$. The combined use of tomographic techniques and optimal estimators can then be used to test the origin of the perturbations that seeded structure formation in the Universe.

HI Filaments in the Virgo Cluster

Attila Popping[1,2], Robert Braun[2]

[1] Kapteyn Astronomical Institute, P.O. Box 800, 9700 AV Groningen, The Netherlands
[2] CSIRO-ATNF, P.O. Box 76, Epping, NSW 2121, Australia

Context: In the last few years the realization has emerged that the universal baryons are almost equally distributed by mass in three components: (1) galactic concentrations, (2) a warm-hot intergalactic medium (WHIM) and (3) a diffuse intergalactic medium. These three components are predicted by hydrodynamical simulations and are probed by QSO absorption lines. To observe the WHIM in neutral hydrogen, observations are needed which are deeper than log(NHI)=18. The WHIM should appear as a Cosmic Web, underlying the galaxies with higher column densities. Until now it has been really hard to detect HI gas with such low column densities or give good predictions of the HI distribution, based on numerical simulations.

Aims: To get a good overview of the distribution and kinematics of the Cosmic Web, a deep survey of 1500 square degrees of sky was undertaken, containing the galaxy filament extending between the Local Group and the Virgo Cluster. Furthermore we looked at SPH-simulations to determine neutral fractions of the gas and try to reproduce the statistics as given by QSO absorption lines.

Results: In the total power data we reach column densities of $\sim$log(NHI) = 17.5, where the WHIM starts to become visible. In the data some extended structures can be seen, connecting the large galaxies. We present HI distribution functions of numerical simulations, after determining the neutral fraction of the hydrogen gas and correcting for self shielding.

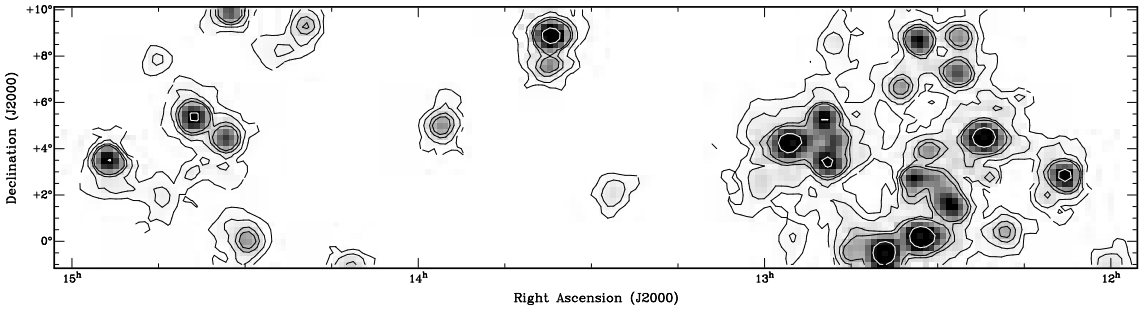

Figure 1: Integrated HI emission of the central part of the Virgo Cluster. Contour levels are at 5×10^{17}, 2×10^{18}, 6×10^{18}, 1×10^{19} and 5×10^{19} cm^{-2}. Extended structures with very low column densities can be seen around the galaxies as predicted.

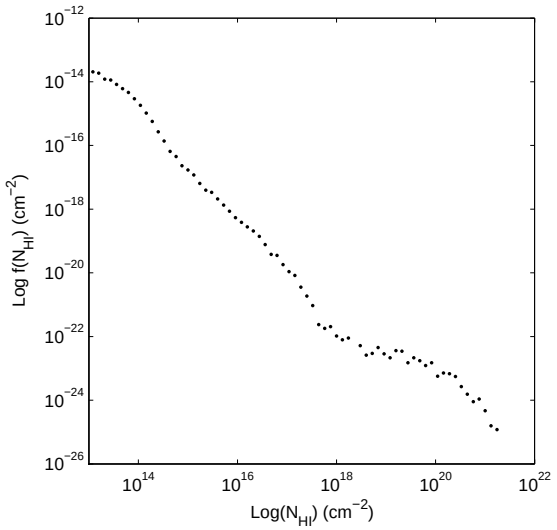

Figure 2: A preliminary distribution function of HI column densities determined from the SPH simulation shown in Fig.3. Most current HI observations have density limits of log(N$_{HI}$)=19-20. Below these densities the gas is not self shielding anymore to the inter-galactic ionization radiation. This transition can be seen as a plateau in the distribution function. Below log(N$_{HI}$)=17 the gas is optically thin and the neutral fraction is determined by the balance between ionization and recombination.

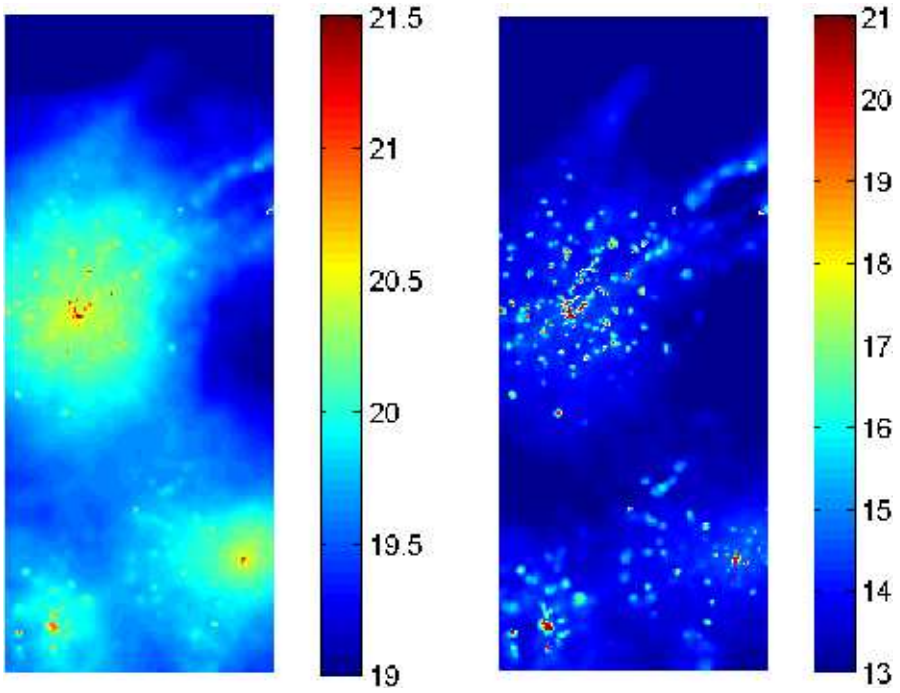

Figure 3: Left panel: Integrated total H column density in an SPH simulation (kindly provided by R. Davé). The size of the box is 900 × 2200 kpc, with a 5 kpc resolution. Right panel: Integrated HI column density for the same box. At every point in the simulation the neutral fraction is calculated from the balance between recombination and ionization. For high volume densities, the neutral fraction is corrected for self shielding.

The HI Frequency Distribution of the High z Universe

Jason X. Prochaska

UCO/Lick Observatory, USA

I will review measurements of the HI frequency distribution $f(N)$ measured at high redshift $z > 2$ as determined from analysis of quasar absorption line systems (QALs). These results are determined primarily through Voigt profile fits of the Lyα ($\lambda = 1215.67$Å) transition. At lower HI column densities ($N_{\rm HI} < 10^{14}{\rm cm}^{-2}$), the Ly$\alpha$ transition is optically thin and $N_{\rm HI}$ is easily determined; these lines, which dominate $f(N)$, comprise the bulk of the 'Lyα forest'. At the largest HI column densities ($N_{\rm HI} > 10^{20}{\rm cm}^{-2}$), the Lorentzian damping wings of the Lyα profile can be resolved with moderate resolution (FWHM $\approx$ 2Å) spectrometers. These damped Lyα (DLA) systems trace galaxies in the young universe. The majority of QALs comprising the middle range of HI column densities ($N_{\rm HI} = 10^{15} - 10^{20}{\rm cm}^{-2}$) are optically thick to ionizing radiation and are referred to as the Lyman limit systems (LLS; $\log N_{\rm HI} \geq 17.1$).

I will provide a brief introduction into the techniques of QAL analysis and then describe recent results on $f(N)$ derived from a sample of ≈ 1000 DLA systems discovered in the Sloan Digital Sky Survey. I will compare these measurements with 21cm HI studies at $z = 0$ and DLA surveys at $z \sim 1$ to investigate redshift evolution in the HI content of star-forming galaxies. I will then extend the discussion of $f(N)$ into the LLS regime with emphasis on the super LLS ($N_{\rm HI} > 10^{19}{\rm cm}^{-2}$). One observes a flattening of $f(N)$ at these column densities which suggests a phase transition from predominantly neutral gas (DLAs) to predominantly ionized gas (LLS). I will review the measurements of $f(N)$ from the Lyα forest and comment on departures from the canonical $f(N) \propto N^{-1.5}$ power-law.

Altogether, these observations describe $f(N)$ across 10 decades in $N_{\rm HI}$, but there remains a gap in our knowledge for $N_{\rm HI} \approx 10^{15} - 10^{19}{\rm cm}^{-2}$. I will describe current efforts to fill this gap.

Finally, I will conclude by compare these results with cosmological simulations of the young universe. I will use those results to explore answers to

several key questions about the distribution of gas in our universe: Where are the baryons at high z? Where is the majority of neutral gas and how is it distributed within galaxies? Where are the majority of metals in the young universe?

The Galactic 'Feed Me' Cry: Hydrogen in the Halo

Mary Putman

University of Michigan, USA

Galaxies represent mass reservoirs where neutral hydrogen was dense enough to form stars and survive reionization. These early galaxies continued to accrete gas to form the distribution of stars and gas we observe today. The methods of gas accretion for a galaxy like the Milky Way may include the stripping of fuel from satellite galaxies and the condensing of clouds within a remnant hot halo. I will discuss the ongoing quest to understand the relationship between the multiple gas phases in the Galactic halo and their relative baryonic mass contributions. The gaseous tracers of galaxy formation and evolution in the halo include concentrations of primarily neutral hydrogen and an extended diffuse halo medium (to at least the distance of the Magellanic Clouds). Gas accretion will be discussed in the context of simulations of galaxy formation, the interaction of halo clouds with the diffuse medium, and the current population of Milky Way satellites.

Observations of HI near Lyman Break Galaxies

Olivera Rakic[1], Joop Schaye[1], Charles C. Steidel[2], Anthony Aguirre[3]

[1] Leiden Observatory, Leiden University, P.O. Box 9513, 2300 RA Leiden, The Netherlands,
[2] California Institute of Technology, MS10524, Pasadena, CA 91125,
[3] Department of Physics, UCSC, Santa Cruz CA 95064

Context: The best way to constrain characteristic energy scale of galactic winds is to observe galaxies and the intergalactic medium simultaneously and to see how much have winds disturbed and/or enriched the surroundings of the galaxies. By seeing how far are galactic winds able to propagate, it would be possible to estimate their typical energy. We study the intergalactic medium around Lyman Break Galaxies (LBGs) by analyzing high resolution spectra of 5 QSOs at $z > 3$, with ~ 200 LBGs with spectroscopic redshifts in the fields around them, and 10 QSOs at $z < 3$ with ~ 800 spectroscopic LBG redshifts, using pixel optical depth correlation techniques. Most of the galaxies are within 6 Mpc/h comoving from the lines of sight to the QSOs.

Aims: We measured the distribution of HI absorption as a function of separation from Lyman break galaxies.

Results: Our lower redshift sample shows enhanced HI absorption up to ~ 4 Mpc/h around observed galaxies. Signal for higher redshift sample is not as clear, which can possibly be explained by the galaxy sample incompleteness and/or an intrinsic evolution of the Lyman-α forest from $z \sim 3$ to $z \sim 2$. The latter may cause the contrast between galaxy environments densities and the average density of the Universe to be smaller at higher redshifts, and therefore harder to detect.

The effect of star formation and feedback on neutral gas kinematics in z=3 galaxies.

Alexei Razoumov[1], Michael Norman[2], Jason Prochaska[3], Jesper Sommer-Larsen[4], Arthur M. Wolfe[2]

[1] Institute for Computational Astrophysics, Saint Mary's University, Canada,
[2] Department of Physics, and Center for Astrophysics and Space Sciences, University of California, San Diego, USA,
[3] Department of Astronomy and Astrophysics, and UCO/Lick Observatory, University of California, Santa Cruz, USA,
[4] Dark Cosmology Centre, Niels Bohr Institute, University of Copenhagen, Denmark

We use state-of-the-art numerical galaxy formation models to study gas kinematics in z=3 damped Ly-alpha systems. We show that none of the current models can reproduce the high-end tail of the observed velocity width distribution of low-ionization species tracking neutral hydrogen. Although there is general understanding that large velocities should be linked to feedback from star formation in the central cores of high-redshift galaxies, the precise mechanism is hidden in the details of complex interactions in the clumpy interstellar medium on scales which we are hoping to probe with our simulations.

Testing Reionization with Lyman Alpha Galaxies

James Rhoads

Arizona State University, USA

Lyman alpha galaxies offer tests of the ionization fraction of intergalactic gas with several advantages. First, they are sensitive to neutral fractions around 50%, corresponding to the central phase of reionization. Second, they are local, allowing one to probe scales down to 10 comoving Mpc. And third, they can be applied using technology that is on sky already in 2007. I will begin by discussing the basic physics of Lyman alpha reionization tests. I will then discuss their application to date, which shows that the neutral fraction at z=6.5 is below 50%. Finally, I will outline future prospects for the field.

The First Galaxies and the Quest for their Fossils

Massimo Ricotti

Dept. of Astronomy, University of Maryland, College Park, MD, 20742 USA

Context: Key questions on the nature of the smallest galaxies in the universe remain to be answered. Feedback processes are crucial in determining the properties of the first small-mass galaxies and whether they can form or not. In previous works we have argued that the negative feedback from the dissociation of H_2 is not the dominant mechanism that regulates the formation of the first galaxies and that H_2 re-formation and photo-heating produced by ionizing radiation play the dominant role in shaping their properties. Although star formation in the first galaxies is self-limited and they do not contribute much to reionization, we found that a numerous population of faint primordial dwarfs may have formed in the early Universe and should have left observable signatures of their passage.

Aims: The most interesting possibility to test our models and simulations on the formation of the first galaxies comes from observations of dwarf galaxies in our Local Volume. Our aim is to predict the properties and the number of the surviving fossil of the first galaxies in our cosmic neighborhood at $z = 0$. Most primordial dwarfs will be destroyed by merging into larger galaxies but a fraction will survive and have observational properties that we can calculate.

Results: The analysis of the primordial dwarfs in our simulations support a primordial origin for most dwarf spheroidal galaxies observed in the Local Group. In addition we have predicted the existence of a numerous fainter and lower surface brightness population of dwarfs that recently have been discovered mining the SLOAN data archive. Remarkably, the number of known dwarfs in the Local Group has nearly doubled in the last two years giving us confidence that we are on the right track. Finally, I will present preliminary results on the predicted spatial distribution of the fossils of the first galaxies in the Local Group and Local Volume and comment on what can be learned by comparing these simulations to observations.

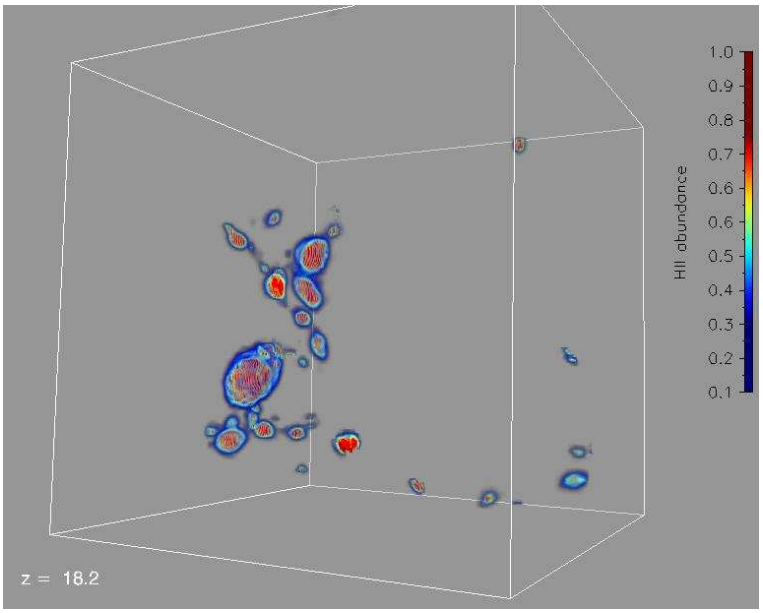

Figure 1: Ionized bubbles produced by the radiation from the first galaxies. The 3D rendering shows highly ionized gas (in red) and partially ionized gas (in blue) at redshift $z \approx 13$.

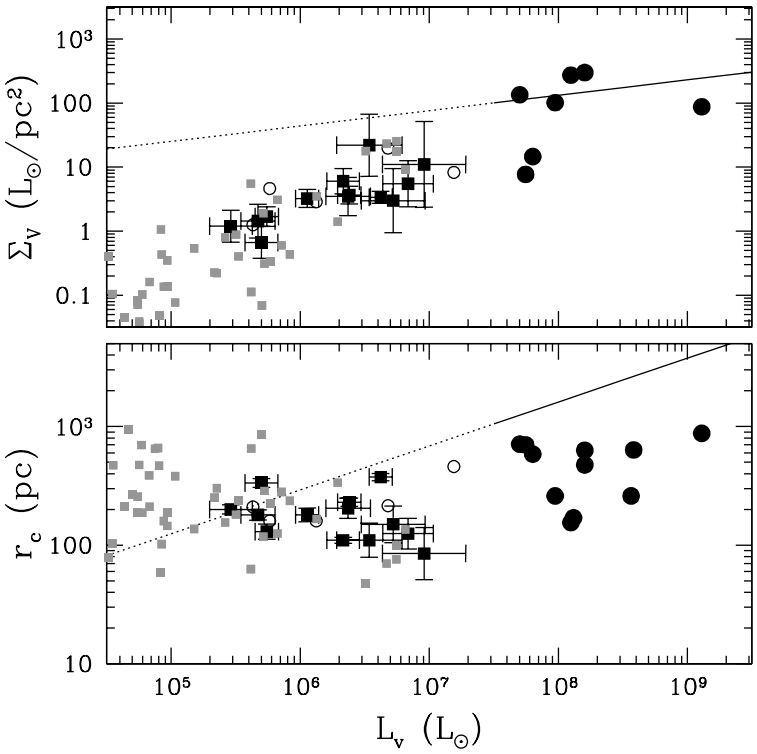

Figure 2: Surface brightness (top panel) and core radius (bottom panel) as a function of the V-band luminosity for the simulated (gray squares) and observed dwarfs (black squares and circles). For comparisons, the scaling relationships (solid lines) for the more luminous Sc-Im galaxies ($10^8 L_\odot < L_B < 10^{11} L_\odot$) derived by Kormendy & Freeman (2004) are shown.

Observational Perspectives on Molecular Cloud Formation

Erik Rosolowsky

NSF Astronomy & Astrophysics Postdoctoral Fellow
Harvard-Smithsonian Center for Astrophysics, USA

Context: The problem of molecular cloud formation in a galactic context remains open despite decades of research into cloud origins. Simple models have been forwarded to explain a subset of the observed features of the molecular cloud population in our galaxies. However, all models are either flawed or lack sufficient detail to accurately predict features of molecular clouds. This process represents one of the least poorly understood processes in mass transfer between stars and the ISM and among the different phases of the ISM.

Aims: In my presentation, I will outline the basic problem of molecular cloud formation and discuss several observational results that a successful theory of molecular cloud formation should explain. Since many of the new results are from extragalactic observations, they are necessarily restricted to the study of GMCs.

Results: Recent extragalactic observations that have bearing on the problem of molecular cloud formation have produced new results that can be broadly divided into three categories.

1. *Neutral Gas Morphologies and the Locations of GMCs* – GMCs are located exclusively on high-column density structures of atomic gas in every instance where the observation has been made (see Fig. 1 and [2]). However, the reverse is not true: many atomic structures exist with no evidence for significant molecular mass. Broadly, this implies atomic gas is the progenitor material for GMCs, as has been argued in the past. More importantly, it emphasizes the importance of studying the structure of the *atomic* ISM as this structure governs the spatial distribution and the formation mechanism of GMCs. Note that galaxies without significant spiral structure (e.g. the LMC) can be quite prolific at forming molecular clouds which are similar to those found in the Milky Way. Hence, spiral structure is only important for cloud formation inasmuch as it dictates the structure of the atomic ISM from which GMCs form.

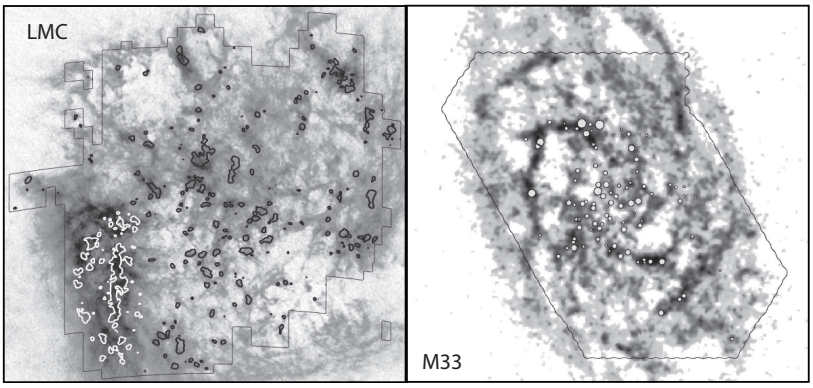

Figure 1: Integrated intensity of 21-cm emission with locations of GMCs indicated for the LMC and M33 (from Blitz et al. 2007). This figure illustrates the correlation of GMCs with high-column density atomic structures.

Secondly, in cases where a disk geometry is well established, the neutral ISM has a larger fraction in the molecular state in the center of the galaxy rather than at the edge. Many conditions of the galactic environment vary monotonically with radius and come combination of these must regulate the effectiveness GMC formation. Again, a successful theory should identify these features and predict the correct variation of molecular gas fraction as a function of environment.

2. *Variations of Larson's Laws and Mass Distributions in an Extragalactic Context* – Larson [5] first identified power law scalings between the macroscopic features of molecular gas. Since then, these scalings have become well-characterized in the solar neighborhood and can be succinctly expressed as a power law size-line width relationship ($\sigma_v = \sigma_0 R^{\beta}$) and that the virial parameter of clouds is near unity ($\alpha = 5R\sigma_v^2/GM \sim 1$). While these relationships hold in the solar neighborhood for constant values of σ_0 and β, one or both of these values are different in external galaxies and the center of the Milky Way [2,7,9,12]. The change is in the sense that, for a given scale, GMCs have larger line widths in molecule rich regions and smaller line widths in dwarf galaxies. Similar galaxies (e.g. the Milky Way and M31) have similar constants in their relationships [8]. These variations imply a coupling between GMC properties produced and the larger galactic environment that should be explained.

In addition to differences in Larson's Laws, the mass distribution of GMCs

also varies among galaxies. The canonical power law $dN/dM \propto M^{-1.6}$ is only applicable for the inner Milky Way. In the outer Galaxy [4] and M33 [3] show good evidence for significant departures from the inner Galaxy value and there is evidence for the absence of high mass GMCs in some locations (though the truncation mass may vary across the galaxy) [10].

3. *Angular Momentum Defects and Magnetic Fields* – In our Galaxy [1] and others [8,11], the specific angular momentum of molecular clouds is significantly lower than the material out of which they must have formed for most collapse geometries. A successful theory should explain whether this angular momentum is (a) shed through braking (b) contained in cloud-to-cloud motions (c) never imparted to GMCs because of collapse geometry or (d) none of the above. Interestingly, recent results argue that the mean magnetic field in Milky Way GMCs is well-aligned with the galactic plane [6] and direct investigations of magnetic fields will be necessary to clarify the importance of magnetic fields at controlling the angular momentum distribution in GMCs.

A concluding caveat: the above results arise largely from the Local Group of galaxies which have, nearly everywhere, their interstellar media dominated by the atomic phase of gas. It is fortunate that the condensed, star-forming structures simultaneously undergo a phase change so that they contrast with the background ISM. This is not true in all galaxies, in particular starbursts and (U)LIRGs where the global ISM is molecular and it is likely that not all of that material is found in the star forming structures.

References

[1] Blitz, L. 1993, in Protostars and Planets III, 125–161
[2] Blitz, L., Fukui, Y., Kawamura, A., Leroy, A., Mizuno, N., & Rosolowsky, E. 2007, in Protostars and Planets V, ed. B. Reipurth, D. Jewitt, & K. Keil, 81–96
[3] Engargiola, G., Plambeck, R. L., Rosolowsky, E., & Blitz, L. 2003, ApJS, 149, 343
[4] Heyer, M. H., Carpenter, J. M., & Snell, R. L. 2001, ApJ, 551, 852
[5] Larson, R. B. 1981, MNRAS, 194, 809
[6] Li, H., Griffin, G. S., Krejny, M., Novak, G., Loewenstein, R. F., Newcomb, M. G., Calisse, P. G., & Chuss, D. T. 2006, ApJ, 648, 340
[7] Oka, T., Hasegawa, T., Sato, F., Tsuboi, M., Miyazaki, A., & Sugimoto, M. 2001, ApJ, 562, 348
[8] Rosolowsky, E. 2007, ApJ, 654, 240
[9] Rosolowsky, E. & Blitz, L. 2005, ApJ, 623, 826
[10] Rosolowsky, E., Keto, E., Matsushita, S., & Willner, S. 2007, ArXiv Astrophysics e-prints
[11] Rosolowsky, E. W., Plambeck, R., Engargiola, G., & Blitz, L. 2003, ApJ, 599, 258
[12] Rubio, M., Lequeux, J., & Boulanger, F. 1993, A&A, 271, 9

Constraints on reionization from intergalactic metals at $z \sim 6$

Emma Ryan-Weber[1], **Max Pettini**[1], **Piero Madau**[2]

[1] IoA, Cambridge, UK
[2] University of California, Santa Cruz, USA

Context: As the epoch of reionization is approached, intergalactic Lyman-α absorption line features become increasingly difficult to observe. On the other hand, metal lines continue to probe the IGM unhindered at $z \sim 6$ and provide a direct observation of the products of the earliest episodes of star formation.

Aims: We have obtained near-Infrared spectra (ISAAC/VLT and NIRSPEC/ Keck) of ten high redshift QSOs to search for triply ionized Carbon (C IV) in the Intergalactic Medium between redshifts 5.12 and 6.23.

Results: We have successfully detected intervening C IV absorption line systems along different lines-of-sight. Preliminary results suggest that metals are widespread in the high redshift IGM and that the mass density of intergalactic C IV ions at $z \sim 6$ is maintained at the same level as seen at intermediate redshifts; there is no decrease in mass density of C IV as one would expect from the decrease in cosmic star formation rate density at $z > 6$. The results suggest that a significant fraction of metals we detect at $z \sim 6$ must have been generated in galaxies at $z > 8$; the same galaxies that are likely to be responsible for the reionization of the Universe.

The dwarf LSB galaxy population in different environments.

Sabina Sabatini[1], Jonathan Davies[2], Sarah Roberts[2], Roberto Scaramella[1]

[1] INAF - Osservatorio Astronomico di Roma, Italy
[2] Cardiff University, UK

Context: The nature of the dwarf galaxy population as a function of location in the cluster and within different environments is investigated. We have previously described the results of a search for low surface brightness objects in data drawn from an East-West strip of the Virgo cluster and have compared this to a large area strip outside of the cluster.

Aims: In this poster we compare the Virgo Cluster East-West data (sampling sub-cluster A and outward) to new data along a North-South strip that samples a different region of the cluster (N,M clouds) and with data obtained for the Ursa Major cluster and fields around the spiral galaxy M101. The sample of dwarf galaxies in different environments is obtained from uniform data sets that reach central surface brightness values of 26 B/sq arcsec, and an apparent B magnitude of 21 (MB=-10 for a Virgo cluster distance of 16 Mpc). An important question is how well do these observations fit in with our current picture of galaxy formation and evolution?

Results: The aim of this search is to investigate how the environment affects galaxy evolution. We discuss and interpret our results on the properties and distribution of dwarf low surface brightness galaxies in the context of various physical processes that are thought to act on galaxies as they form and evolve (tidal interactions, morphological transformations, SN winds, pressure confinement, photoionization).

Early work on H_2 in the ISM

Ed Salpeter

Cornell University, USA

Before Bob Gould and I calculated forming H_2 on grain surfaces in 1963, Tommy Gold had already suggested that H_2 may be important near the Galactic Plane. However, even Tommy, usually so exuberant, greatly underestimated the amount of H_2. A generation earlier the similarly exuberant Arthur Eddington completely neglected dust grains, neutral atoms and molecules. I will warn against us making similar neglects and underestimates in the future.

Cosmic stellar relics in the Galactic halo

Stefania Salvadori[1], **Raffaella Schneider**[2], **Andrea Ferrara**[1]

[1] SISSA/International School for Advanced Studies, Italy
[2] INAF/Osservatorio Astrofisico di Arcetri, Italy

Context: We study the stellar population history and chemical evolution of the Milky Way in a hierarchical ΛCDM model for structure formation. Using a Monte Carlo method based on the semi-analytical extended Press & Schechter formalism, we develop a new code GAMETE (GAlaxy MErger Tree & Evolution) to reconstruct the merger tree of the Galaxy and follow the evolution of gas and stars along the hierarchical tree.

Aims: Our approach allows us to compare the observational properties of the Milky Way with model results, exploring different properties of primordial stars, such as their Initial Mass Function (IMF) and the critical metallicity for low-mass star formation, Z_{cr}.

Results: In particular, by matching our predictions to the metallicity distribution function of metal-poor stars in the Galactic halo we find that: (i) a strong supernova feedback is required to reproduce the observed properties of the Milky Way; (ii) stars with [Fe/H]< -2.5 form in halos accreting Galactic Medium (GM) enriched by earlier supernova explosions; (iii) the fiducial model ($Z_{cr} = 10^{-4} Z_{\odot}$, $m_{PopIII} = 200 M_{\odot}$) provides an overall good fit to the MDF, but cannot account for the two HMP stars with [Fe/H]< -5; the latter can be accommodated if $Z_{cr} \leq 10^{-6} Z_{\odot}$ but such model overpopulates the "metallicity desert", i.e. the range $-5.3 <$ [Fe/H] < -4 in which no stars have been detected; (iv) the current non-detection of metal-free stars robustly constrains either $Z_{cr} > 0$ or the masses of the first stars $m_{PopIII} > 0.9 M_{\odot}$; (v) the statistical impact of truly second generation stars, i.e. stars forming out of gas polluted *only* by metal-free stars, is negligible in current samples; (vi) independently of Z_{cr}, 60% of metals in the Galactic Medium are ejected through winds by halos with masses $M < 6 \times 10^9 M_{\odot}$, thus showing that low-mass halos are the dominant population contributing to cosmic metal enrichment.

Cold gas accretion in galaxies

Renzo Sancisi[1,2], Tom Oosterloo[3], Thijs van der Hulst[2]

[1] INAF-Osservatorio di Bologna, Italy
[2] Kapteyn Astronomical Institute, the Netherlands
[3] ASTRON Dwingeloo, the Netherlands

Context: There is increasing evidence that accretion events play an important role in the formation of disks and the evolution of galaxies. This comes mainly from studies of the distribution and kinematics of stars in the Milky Way halo and in M31 and from HI observations of galaxies.

Aims: HI surveys of galaxies are a sensitive test of the existence of accretion and merger processes. As compared to stellar studies they have the advantage of providing at the same time information on gas densities and especially kinematics also for galaxies beyond the local group.

Results: We describe various examples which illustrate the phenomenon of gas infall in galaxies. With these observations we demonstrate that the HI is a formidable tool for this kind of work and that accretion of small and large amounts of gas is indeed taking place. Such accretion may also be, to some extent, at the origin of the gaseous halos which are being found around spirals.

Does nearly all of the intergalactic HI reside in metal-free gas?

Joop Schaye[1], Robert F. Carswell[2] & Tae-Sun Kim[3]

[1] Leiden Observatory, The Netherlands
[2] Institute of Astronomy, Cambridge, UK
[3] Astrophysikalisches Institut Potsdam, Germany

Measurements of the abundances of heavy elements in the intergalactic medium from quasar absorption lines implicitly smooth over large (10 - 100 kpc) scales. On smaller scales the metal distribution is essentially unknown. I will present new observational evidence, as well as theoretical arguments, indicating that the metals are poorly mixed on small scales. The implication is that nearly all of the intergalactic medium, and thus the universe, may be of primordial composition.

More information:
Schaye et al., 2007, MNRAS, submitted (astro-ph/0701761)

Star formation thresholds and the HI-H_2 transition

Joop Schaye

Leiden Observatory, The Netherlands

An intriguing fact about cosmic gas clouds is that the distribution of H I column densities cuts off around 1021.5 cm^{-2}, which corresponds to a gas surface density of about 4 $M_\odot/pc^2$. Observations of damped Ly-alpha (DLA) absorption systems further indicate that this cutoff decreases with increasing metallicity. It is generally assumed that this trend is due to a dust-induced selection bias: DLA systems with high N(HI) and high metallicity contain so much dust that the background quasi-stellar object becomes too dim to be included in optically selected surveys. I proposed instead that conversion to molecular hydrogen determines the maximum H I column density and showed that this works quantitatively. This explanation is supported by 21cm observations of nearby galaxies, which show a similar cutoff in their H I distribution that clearly cannot be explained by an extinction bias. The same holds for UV absorption measurements within the Galaxy.

The conversion to molecular hydrogen coincides with a sharp decrease in the temperature and thus a sharp decrease of the Jeans mass. Consequently, the gas will likely fragment into molecular clouds with small cross sections and star formation will presumably follow. Conversely, at lower H I column densities the UV (background) radiation keeps the gas sufficiently warm to be stable against fragmentation into molecular clouds, preventing star formation. I will show that models based on the hypothesis that the onset of thermal instability triggers gravitational instability and sets local star formation thresholds in the outer parts of galaxies can explain many observations of nearby galaxies.

More information:
Schaye, 2004, ApJ, 609, 667
Schaye, 2001, ApJ, 562, L95

Variance in the HI Mass Function

Stephen E. Schneider[1], AGES Collaboration[2]

[1] University of Massachusetts, USA
[2] www2.naic.edu/˜ ages/

Context: Several surveys of neutral hydrogen using the 21 cm line are currently underway, or have been completed in the last several years. Thanks to multi-beam receiver systems, "blind" surveys have become more efficient, and large catalogs of HI-selected samples of extragalactic sources are being generated.

One of the goals of these surveys is to establish the shape of the HI mass function. In studies published to date, there are disagreements about the shape of the mass function—particularly the faint-end slope. These disagreements can reach an order of magnitude for the number of sources with HI masses of from 10^7 to 10^8 solar masses. Given the limitations of past surveys, it is unclear whether these differences should be attributed to small-number statistics, differing analysis procedures, and/or physical variations caused by galaxies' environments.

Aims: This talk reviews the issues facing HI observers, discussing the limitations of existing surveys and the prospects for resolving the sources of variance.

The earliest surveys were severely limited by small-number statistics, so substantial fluctuations were to be expected at the faint end, where very few sources were detected. Recent surveys cover much larger areas and detect a correspondingly larger number of sources. There are hints of environmental influences, leading to variations in the HI mass function, but there is not even agreement on the sense of these differences.

It should be noted, however, that most of the current surveys have sensitivities no better than the early surveys. This low sensitivity drives the surveys to attempt to extract sources deep into the noise, and this can lead to biases in the interpretation of the detections of the weakest sources. The methods used to correct for detection sensitivity can potentially explain much

of the variance between surveys.

Results: The detection of low-mass HI sources in a blind survey remains a challenging problem. Worse, although the number statistics have been significantly improved, the ability to detect low mass HI sources remains limited to the very nearby environment.

This is illustrated in the figure below, where the masses and distances of sources detected in a typical shallow survey are simulated (dots in gray). Sources with less than about 10^8 solar masses of HI are only detected closer than the Virgo cluster.

For comparison, a deeper survey—spending an equal amount of time in total, but integrating 25 times longer—is also shown in the figure (black X's). At any given mass, fewer sources are detected, but their average distance is significantly larger, providing the possibility of sampling low-mass HI sources beyond the Local Supercluster.

The Arecibo Galaxy Environment Survey (AGES) is currently being undertaken with the Arecibo L-band Feed Array (ALFA). Its primary goal is to study the immediate environment of several nearby galaxies and groups, but its moderately long integrations provide an opportunity to search for galaxies at larger redshifts and to sample the HI mass function. Similarly, with the completion of additional receivers, there are possibilities for "piggybacking" on longer-integration searches for pulsars being made with ALFA.

The first field observed with AGES suggests variations of the mass function along that one line of sight, however, this is very tentative given the small number statistics. As these surveys are completed, it is likely that the low-mass population and its variance in the local universe will be much better characterized.

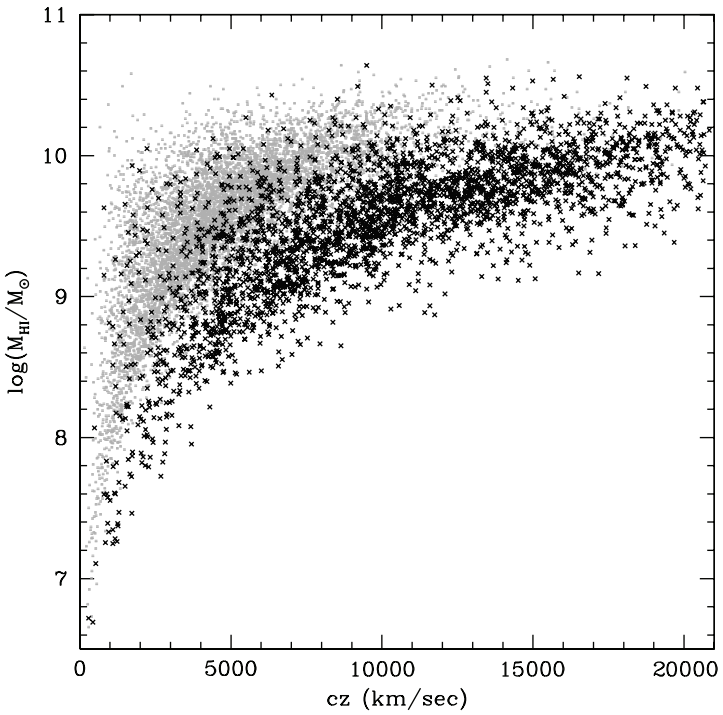

Figure 1: Comparison, based on simulations, of HI sources detected in a rapid, but shallow HI survey (gray dots) and a survey covering 25 times less area, but 25 times longer integrations at each point. The shallow survey detects many more sources, but it does not detect sources with low masses beyond the Local Supercluster.

21-cm signal fluctuations from inhomogeneous Lymann-alpha background during EoR:numerical simulations

Benoit Semelin, Françoise Combes, Hye Baek Sung

LERMA, Observatoire de Paris, France

Context: In the next decade, osbservations of the 21-cm emission from neutral hydrogen during the Epoch of Reionization will become available through such instruments as LOFAR and SKA. A great deal of efforts is currently being put into the predictiom of the signal statistical properties to optimize the design of the future instruments. Numerical simulations are picking up the chalenge with full 3D radiative transfer codes able to account for the complex geometry of the reionization process. As a member of SKA Design Study, our team has developed the code LICORICE which couples dymanic and radiative transfer, both in the continuum and in the ly-alpha line. We are investigating the impact of new sources of fluctuations in the 21-cm brightness temperature maps. Indeed, the brightness temperature depends on the difference between the hydrogen spin temperature and the CMB radiation blackbody temperature. Two processes are able to decouple the spin temperature from the CMB temperature: collisions (efficient in dense regions only) and the Wouthuysen-Field effect (pumping by Lyman-alpha photons). In this work, we focus on the later effect.

Aims: At this time, numerical simulations use a simplified version of the Wouthuysen-Field effect: they consider that the scattering rate of Lyman-alpha photons per atom, P_α, is uniform in the simulation box, depending only on the time. However, several authors have recently shown that fluctuations in P_α exist and can modify the 21-cm emission power spectrum (Barkana & Loeb 2005, Pritchard & Furlanetto 2006). They took into account fluctuations due to the distribution of the sources and due to a simple $1/r^2$ scaling for the flux. In this work, we study how the full 3D radiative transfer in the Lyman-alpha line implemented in LICORICE modifies the picture given by the previous authors.

Results: After runing the code through a series of validation tests, we have computed the P_α profile around a central source with a continuous flat spectrum in a uniform medium with critical baryon density at z=10. We find that the profile deviates from the $1/r^2$ scaling at small scales ($<$ 10 comoving Mpc) due to wing scatterings. Then, we investigate the effect of fluctuations in the gas density. We study several configurations (source inside an isothermal density profile, source inside a filament), and we find, in each case, strong fluctuations in the P_α map, induced by the density field. We conclude that a full treatment of the Lyman-alpha transfer as a post treatment of a cosmological simulation of the EoR, is probably relevent for the prediction of the 21-cm emission.

Observable Signatures of Cosmic Reionization and the End of the Dark Ages

Paul Shapiro

Department of Astronomy, The University of Texas at Austin, USA

When the universe was reionized, small-scale cosmic structure exerted a strong feedback effect which left its imprint on all scales from the smallest to the largest, and on the radiation backgrounds at a broad range of wavelengths. When the first stars formed inside minihalos of mass $\sim 10^5$ to 10^6 solar masses at redshifts $z > 20$, their ionizing radiation heated and expelled the gas inside their host minihalos and escaped to create intergalactic H II regions and begin cosmic reionization. As these H II regions grew, the ionization fronts which led their expansion encountered other minihalos, which blocked their path and trapped them, causing this minihalo gas, too, to be expelled in a photoevaporative wind. Further star formation inside minihalos was affected not only by these ionization fronts, but also by the rising dissociating background from more distant sources. Eventually, hierarchical clustering led to the formation of dwarf galaxies in excess of 10^8 solar masses, in which atomic cooling was effective enough to trigger more star formation, and their intergalactic H II regions grew and merged to become 10's of comoving Mpc's in size. Inside these photoheated H II regions, intergalactic gas pressure inhibited gravitational collapse on small mass scales, so the minimum mass of newly-formed galaxy sources rose to more than a billion solar masses. The process of reionization continued until the intergalactic H II regions finally overlapped everywhere, to fill space with highly ionized gas.

We have studied this process by a variety of techniques, on a hierarchy of mass- and length-scales. The latter span the range from the interiors of minihalos, to the giant H II regions produced by the clustered formation of galaxies in space and in time, to the large-scale structure of the patchy distribution of neutral and ionized gas in the universe during the epoch of reionization. These results lead to predictions of a fluctuating background of redshifted 21-cm line radiation, temperature and polarization anisotropy of the CMB, gaps in the Gunn-Peterson absorption spectra of high-z quasars, and distortion of the luminosity function and spatial clustering of Lyman alpha emission-line galaxies during this epoch, among other things. I will summarize the latest theoretical developments in this talk.

Constraints on the Escape Fraction at z∼1

Brian Siana

Spitzer Science Center, USA

We examine deep HST far-ultraviolet (1600 Angstroms) imaging of the HDF-North and the UDF to search for Lyman Continuum radiation escaping from 20 star-forming galaxies at z∼1.3. We see no detections, with limits to the relative escape fraction of $f_{esc,rel} < 0.16$-1.0 and a stacked limit of $f_{esc,rel} < 0.11$. This means there is at least a factor of 10 attenuation of the Lyman Continuum in addition to the attenuation measured in the UV-continuum (at 1500 Angstroms). We see no evidence of the large relative escape fractions near unity observed in some Lyman Break Galaxies at z $\sim$ 3, though our sample is less luminous than the typical L* LBGs. We will also present results from a much deeper campaign of LBG analogues at z∼1 in the larger GOODS fields.

Are There Dark Galaxies in the Local Group?

Joshua Simon[1], Marla Geha[2], Tim Robishaw[3], & Leo Blitz[3]

[1] Caltech, USA
[2] Herzberg Institute of Astrophysics, Canada
[3] UC Berkeley, USA

Context: The Cold Dark Matter (CDM) cosmological model predicts that massive galaxies such as the Milky Way should be surrounded by large numbers of dark matter-dominated satellite halos. The relatively modest populations of observed dwarf galaxies orbiting the Milky Way and M31, however, seem to conflict with this prediction (Kauffmann, White, & Guiderdoni 1993; Klypin et al. 1999; Moore et al. 1999). This apparent disagreement between the expected and observed numbers of dwarf galaxies has become widely known as the "substructure" or "missing dwarfs" problem.

If the CDM paradigm of structure formation is correct, then the Milky Way must have ≥ 100 low-mass satellites. Searching for observational evidence for the existence of these objects therefore represents a critical test of the CDM model, as well as an opportunity to improve our understanding of galaxy formation (and non-formation) at the bottom of the mass function.

Aims: We will discuss ongoing work that takes two parallel approaches to studying the missing satellite problem. First, we investigate the impact of the unexpected Sloan Digital Sky Survey (SDSS) discovery of a huge population of new, ultra-faint Local Group dwarf galaxies on our understanding of the substructure problem. Since 2005, at least 20 of these galaxies have been identified, nearly doubling the previous census of Local Group dwarfs. Almost all of these objects have surface brightnesses and luminosities that are significantly lower than those of any previously-known galaxies. We present new stellar kinematics measurements for 8 of the ultra-faint dwarfs, determine their masses and mass-to-light ratios, and use these measurements to reassess whether we are still missing any dwarfs.

Second, we consider the possibility that high-velocity clouds (HVCs) could be the gaseous counterparts of large numbers of low-mass dark matter

halos in the Local Group (Blitz et al. 1999; Braun & Burton 1999). The key obstacle to realistically evaluating this hypothesis has been our lack of knowledge about the distances and masses of HVCs, both on an individual basis and as a population. We present wide-field, high-resolution Arecibo H I maps of a sample of ~ 10 HVCs. The majority of the clouds have highly complex and disordered kinematics, but several objects show the apparent signature of rotation. If these HVCs are indeed rotating then they must be dark matter-dominated, and are plausible candidates for some of the missing satellites.

Results: We have obtained Keck/DEIMOS spectroscopy of $18 - 214$ stars in the dwarf galaxies Canes Venatici I, Canes Venatici II, Coma Berenices, Hercules, Leo IV, Leo T, Ursa Major I, and Ursa Major II. We measure stellar velocity dispersions for each galaxy and compute total masses that range from 1.2×10^6 $M_\odot$ up to 2.8×10^7 $M_\odot$. The ultra-faint dwarfs have V-band mass-to-light ratios of $140 - 1000$, making them the darkest known galaxies.

After correcting for the partial sky coverage of the SDSS, the projected number of Milky Way satellites over the entire sky is 59, more than a factor of 5 increase over the previously-known dwarfs. We display the effect of the new dwarfs on the cumulative number of Milky Way dwarf galaxies as a function of circular velocity in Figure 1. Although these objects reduce the under-abundance of dwarf galaxies to a factor of ~ 4 compared to the most recent simulations by Diemand et al. (2007), the missing satellite problem remains. If we postulate that dwarf galaxies are only able to form in the dark matter halos that acquire substantial mass before the epoch of reionization, the observed and predicted circular velocity functions can be brought into reasonable agreement as long as the Local Group was reionized before $z = 8$ (right panel of Figure 1).

To investigate a possible connection between HVCs and the missing satellites, we used Arecibo to create ~ 1 deg^2 H I maps of a sample of ~ 10 HVCs. Robishaw, Simon, & Blitz (2002) already demonstrated that one of these objects has a velocity gradient indicative of rotation, and is likely to be strongly dark matter-dominated. On the whole, the clouds display complex kinematics, with typical internal velocity gradients of ~ 10 km s^{-1} on small angular scales. We show that if these HVCs are gravitationally bound, they must be made largely of dark matter; if not, their lifetimes are rather short. We identify several more HVCs with major-axis velocity gradients that may be interpreted as rotation, and suggest that these objects are consistent with

being dark galaxies — low-mass dark matter halos that contain some gas but never formed stars.

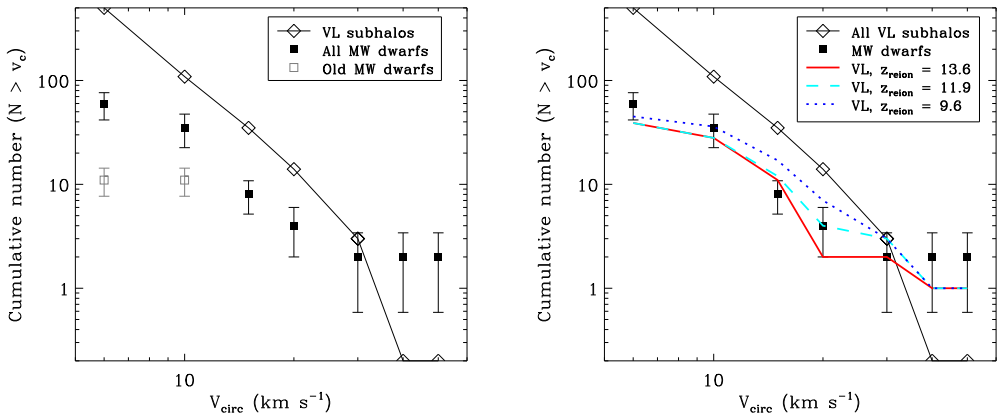

Figure 1: (*Left*) Cumulative number of Milky Way (MW) satellite galaxies as a function of halo circular velocity. The filled black squares include our new circular velocity estimates as well as all of the previously-known MW dwarfs. The open gray squares show the numbers without the new ultra-faint dwarfs. The solid line plus diamonds represents the subhalo abundance in the Via Lactea N-body simulation (Diemand et al. 2007). (*Right*) As in the left panel, but allowing for suppression of dwarf galaxy formation after reionization. The solid, dashed, and dotted curves show the circular velocity distribution for the 59 most massive Via Lactea subhalos if reionization occurred at $z = 13.6, 11.9$, and 9.6, respectively.

References:

Blitz, L., et al. 1999, ApJ, 514, 818
Braun, R., & Burton, W. B. 1999, A&A, 341, 437
Diemand, J., Kuhlen, M. & Madau, P. 2007, ApJ, 657, 262
Kauffmann, G., White, S. D. M., & Guiderdoni, B. 1993, MNRAS, 264, 201
Klypin, A., et al. 1999, ApJ, 522, 82
Moore, B., et al. 1999, ApJ, 524, L19
Robishaw, T., Simon, J. D., & Blitz, L. 2002, ApJ, 580, L129

The challenge of high redshifts: SKA pathfinders

Lister Staveley-Smith

School of Physics, University of Western Australia, Crawley, WA 6008, Australia.

Measurements of HI in emission via the 21cm line are extremely difficult at redshifts much above 0.1 with current radio telescopes. Future instrument such as the SKA are designed to map galaxies out to $z \sim 3$ but will not be available for at least another decade. In the meantime, several SKA 'Pathfinder' telescopes are under construction or are being planned. These will allow a unique investigation of the gas content of the intermediate-redshift Universe. For example; the evolution of the cosmic gas density will be measurable to redshifts of 0.8; the evolution of the mass function will be measurable to 0.5, and the evolution of the clustering properties of gas-rich galaxies will measurable to around 0.3. This adds up to a considerable advance on what is currently available and helps bridge the massive gap in lookback time between 21cm and ground-based QSO DLA measurements.

Whilst recent upgrades to existing facilities such as the WSRT, Arecibo and the eVLA will be useful for limited measurements at intermediate redshifts, the most significant advances will come from next-generation instruments with their vastly increased fields of view. These include the ATA, Apertif, MeerKAT and MIRANdA, which are all projected to have survey speeds (defined as $(A/T)^2\Omega$) greatly in excess of current instruments and, as shown in Fig. 1, are easily able to make surveys of several 100k galaxies. Such surveys will not only allow advances as outlined above, but will allow new synergies with surveys at other wavelengths.

Looking further ahead, the SKA will have the sensitivity to reach much higher redshifts and will provide much-needed input into the understanding of galaxy formation and gas evolution at high redshift. However, in doing so, there will be a number of challenges to be met, such as being able to achieve a sufficiently high dynamic range. These challenges will best be faced via a phased development beginning with a 10% SKA 'Phase 1' concept.

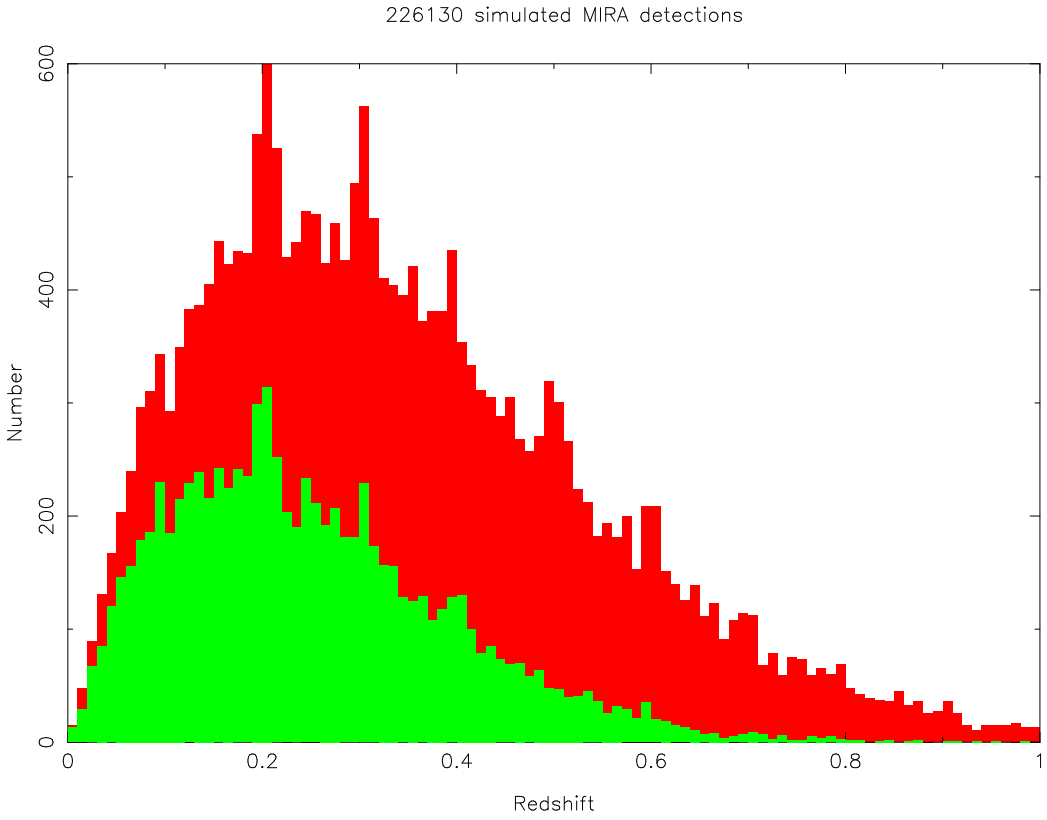

Figure 1: A simulated 1-year deep HI survey with the MIRANdA SKA pathfinder showing the significant numbers of galaxies beyond the current redshift limit of 0.1–0.2 for detection, via the 21cm line, of HI in emission. MIRANdA, and similar SKA pathfinders, are able to probe large volumes due to their wide fields-of-view. The lower histogram is a simulation based on a 30×12-m dish array; the upper histogram is based on an upgrade to 45 dishes with cooled receivers. See the MIRANdA science case for details: *http://www.atnf.csiro.au/projects/mira*.

Radiative feedback of POPIII stars

Hajime Susa[1] **& Masayuki Umemura**[2]

[1] Konan University, Kobe, Japan
[2] Center for Computational Science, University of Tsukuba, Japan

Context: The self-regulation of star formation in the first low mass halos is quite important, since it controls the Population III (POPIII) star formation activity in the early universe, which is the key for the reionization and the metal pollution of the universe. These problems have been studied intensively in the last decade, hence we already have some knowledge on these issues. However, studies which properly address the radiation transfer effects are still at the beginning, in spite of their great importance.

Radiation from the first generation stars play quite important roles on the formation of stars/galaxies through two main physical processes. Since first stars are expected to be very massive ($M > 100 M_{\odot}$), the amount of ultraviolet photons are quite large. Once these stars are formed, 1) emitted Lyman-Werner band photons photodissociate the hydrogen molecules in the neighborhood by Solomon process. Afterwards or simultaneously 2) ionizing photons propagate into surrounding media, and photoionize/heat up the gas. Since hydrogen molecules are the only coolant in low mass first generation objects, and the photoheated gas is too hot to be kept in such small dark halos, these radiative feedbacks are basically expected to have negative effects on the structure formation.

Aims: In this talk, we will present the results of 3D-RHD simulations of primordial star formation in the presence of ultraviolet radiation from neighboring other stars. We pay special attentin on the radiation transfer effects. We summarize the number of numerical results for various parameters, although some parts of the simulations are already reported elsewhere. The numerical simulations are performed on the FIRST cluster in University of Tsukuba.

Results: Figure 1 represents the summary of numerical runs without ionizing photons. The horizontal axis denotes the density of the collapsing prestellar core, when the neighboring star is ignited. The vertical axis shows

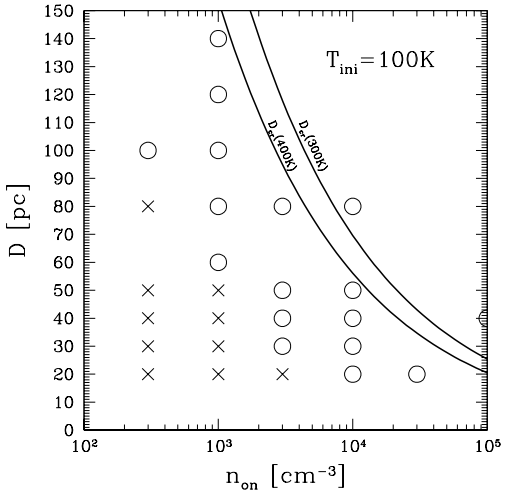

Figure 1: The conditions $t_{\rm dis} = t_{\rm ff}(D = D_{\rm cr})$ are plotted by solid lines on $n_{\rm on} - D$ plane for $T = 300, 400$K. Symbols represent the numerical runs without ionizing photons. Open circles denote the runs in which the clouds collapse successfully, whereas vertices represent the failed collapse.

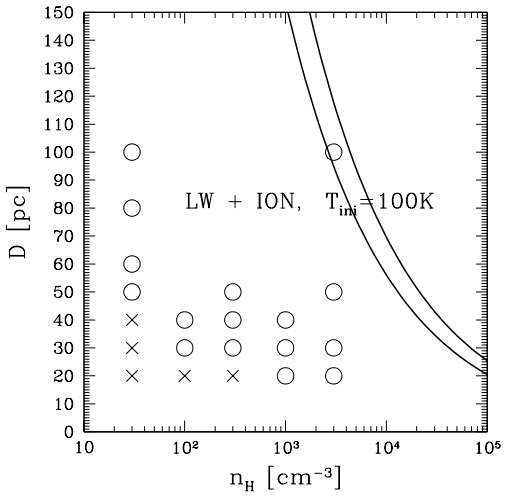

Figure 2: Same as Figure 1, except that the runs include the ionizing photons.

the distance between the source star and the collapsing prestellar core. The solid lines represent the loci along which $t_{\rm diss} = t_{\rm ff}$ is satisfied, where $t_{\rm diss}$ and $t_{\rm ff}$ denote the H_2 dissociation time scale and free-fall time scale, respectively.

If the condition $t_{\rm diss} < t_{\rm ff}$ is satisfied in the collapsing core, H_2 is destroyed before the core collapse proceeds. Since H_2 is the main coolant of primordial gas, the opposite condition $t_{\rm diss} > t_{\rm ff}$ could be regarded as the collapse criteria. In fact, this is true for quasi-statically contracting core, however, the gas can cool more easily in the dynamically collapsing cloud. Even if $t_{\rm diss} < t_{\rm ff}$ is satisfied at a certain snapshot, the contraction is not stopped immediately. The core collapses adiabatically after the H_2 dissociation, and the resultant high pressure of the compressed gas halts the collapse. We have to be careful it is possible to reform H_2 during the adiabatic contraction phase. In fact, the results of numerical simulations (open circles: collapse, whereas vertices: do not collapse) show that the primordial gas can cool even if $t_{\rm diss} < t_{\rm ff}$ is satisfied.

Figure 2 represents the results with ionizing photons. The presence of ionizing radiation seems to damage the prestellar core, since it heats up the gas up to 10^4K. However, results from numerical simulations show that ionizing radiation do not prevent the core from collapsing: rather, it alleviates the negative effects of Lyman-Werner radiation. Primary reason for this result is the self-shielding effects of ionizing radiation. The dense cores such as found in Figure 2 are easily shielded against external radiation. Secondly, the H_2 shell formed behind the ionization front shields the core from the incident LW radiation. Thirdly, the ionization-induced shock front mildly heats up the gas, which promotes the H_2 formation in the core. In summary, the primordial prestellar core $n_{\rm H} > 10^3{\rm cm}^{-3}$ is hardly prevented from collapsing, even if another source star is located very close to the core ($D < 100$pc).

References

Susa, H. 2007, ApJ, 659, 908
Susa, H., & Umemura, M. 2006, ApJL, 645, L93
Susa, H. 2006, PASJ, 58, 445

A new perspective on the fate of extended HI in spiral galaxies

David A. Thilker and GALEX Team

The Johns Hopkins University, USA

Context: The outer disks ($R > D_{25}$ radius) of spiral galaxies harbor a significant fraction of the HI mass in the universe at the present epoch. A clear observational picture for the evolution of this medium is crucial to models of HI survival or, alternatively, its transformation. Traditionally, the outer disk has been regarded as overwhelmingly stable against star formation (SF) due to threshold mechanisms (Martin & Kennicutt, 2001, ApJ, 555, 301), with rare exception (Ferguson et al., 1998, ApJ, 506, L19). However, GALEX ultraviolet imaging shows that recent SF in the low column density, outer disk environment is surprisingly pervasive (Thilker et al., 2005, ApJ, 619, L79 and Gil de Paz et al., 2005, ApJ, 627, L29) We label objects with spatially extended SF as extended UV-disk (XUV-disk) galaxies. Implications associated with this discovery are reviewed in regard to potential effects on (and demands from) the HI reservoir.

Aims: We searched for XUV-disk galaxies in the local universe ($D < 40$ Mpc) using observations of 189 S0-Sm galaxies from the GALEX Atlas (Gil de Paz et al., 2007a, ApJS in press), in comparison to archival vis-nIR imaging. We sought to quantify the incidence of the XUV-disk phenomenon, infer the causal factor(s), and place these systems into a cosmological context regarding the continuing formation of disk galaxies and evolution of HI in the Universe.

Results: XUV-disk galaxies fall into two major classes (Thilker et al., 2007, submitted to ApJS). Type 1 objects ($\sim$20% incidence) have structured, UV-bright/optically-faint emission features in the outer disk, beyond the anticipated SF threshold (Fig. 1). Type 2 XUV-disks ($\sim$10% incidence) show an exceptionally large, UV-bright/optically-low-surface-brightness (LSB) zone having blue $UV - K_s$ outside the effective extent of the inner, older stellar population, but not often reaching extreme galactocentric distance (Fig. 2).

Type 1 XUV-disks are associated with spirals of all types, whereas Type 2 XUV-disks appear to be predominantly found in late-type spirals. Type 2 objects are forming stars quickly enough ($sSFR = SFR/M_* > 10^{-9}$ yr^{-1}) to

double their [presently low] stellar mass in the next Gyr, assuming a constant SF rate. XUV-disks of both types, but esp. Type 1, are generally gas-rich (by about a factor two in M_{HI}/L_B from the sample median at fixed L_K).

Type 1 XUV-disks often have lower global star formation efficiency (SFE, measured as SFR/M_{HI}) than the L_K-dependent median for the sample, whereas Type 2 objects are typical of the sample at low L_K. In Type 1 XUV-disks the average SFE in the outer disk is particularly low (driving the global value down), but still reaches typical levels for an ordinary disk on localized scales. Gas consumption timescales ($1/SFE$) are several Gyr for most XUV-disks, though the issue is complicated (Gil de Paz et al., 2007b, ApJ in press) due to gas recycling and possible HI production via H_2 photodissociation.

A multicomponent model of SF in disk galaxies was presented by Elmegreen & Hunter (2006, ApJ, 636, 712) including not only Toomre instability but also secondary pathways to cloud collapse, such as spiral shocks, turbulence, and localized triggering – all of which can persist into the outer disk. Their model predicts the outer SF detected by GALEX in Type 1 XUV-disks. Claims of a SF threshold near the D_{25} radius appear to have marked a transition in the typical mode of cloud collapse leading to star formation. Indeed, HI mapping reveals a shift from CNM+WNM to mainly WNM past the optical radius (Braun, 1997, ApJ, 484, 637). The associated Σ_{SFR} [SFE] drop was accentuated by the use of Hα as a SFR tracer, which can miss SF occurring at low rates such that stochastic effects are important (Boissier et al., 2007, ApJS in press).

XUV-disks constitute a segment of the galaxy population either experiencing significant, continued gas accretion from the intergalactic medium (IGM), or fueled by a recent galaxy interaction/merger. Our data suggest that perturbation may stimulate XUV-disk SF, at least for Type 1 objects. Type 2 XUV-disk galaxies are more isolated. Cold accretion from the IGM with a high specific rate seems a probable mechanism for Type 2.

If XUV-disk activity is episodic, a majority (> observed incidence) of present-day spirals could be influenced by low-level outer disk SF. We speculate XUV-disk SF was a significant contributor to the dominant phase of disk building (Trujillo & Pohlen, 2005, ApJ, 630, L17) at earlier epochs, given that XUV-disks are the most actively evolving galaxies now growing via inside-out disk formation.

In summary, XUV-disk SF is one way that outer disk HI residing at the IGM interface is slowly consumed into stars and enriched.

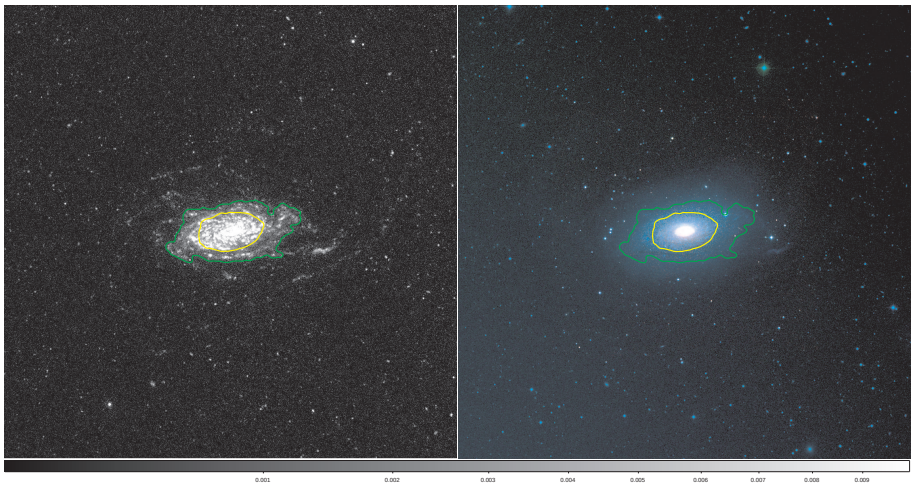

Figure 1: NGC 5055 (M 63), a Type 1 XUV-disk galaxy. We show GALEX FUV (*left*) and 2MASS-K_s, DSS2-red, DSS2-blue (*right* as R,G,B) imaging. Image size is $3 \times D_{25}$. The green contour marks the Σ_{SFR} where SF threshold mechanisms may begin to become important. The yellow contour encloses 80% of the K_s-band luminosity. NGC 5055 has prominent spiral-like XUV-SF features throughout a warped outer HI disk.

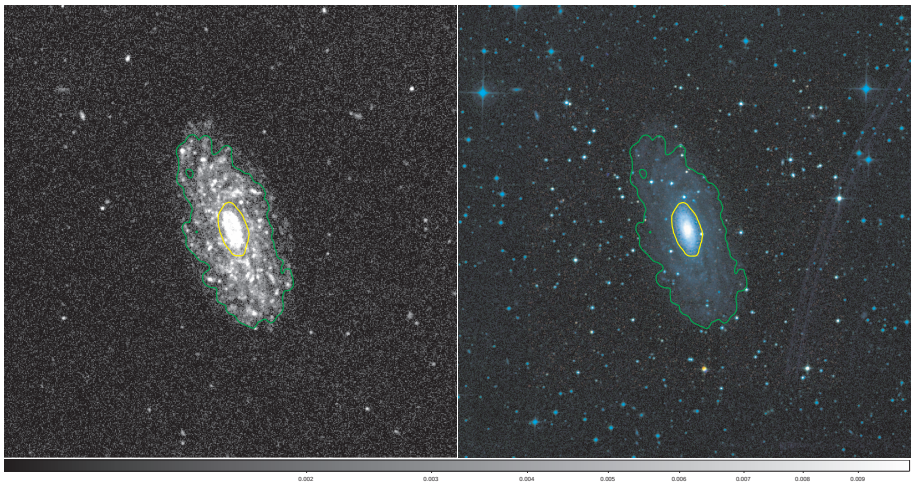

Figure 2: NGC 2090, a Type 2 XUV-disk galaxy. Images and contours are as in Fig. 1. The SF, optically-LSB zone (between contours) of this galaxy is many times larger than the effective size of the old stellar population (yellow contour), and has $FUV - K_s$ consistent with a burst having $t < 500$ Myr.

H I Survival in the Nearby Universe

Todd M. Tripp

Dept. of Astronomy, University of Massachusetts-Amherst, USA

During the last few years, our ability to study H I survival (and, more generally, the role of intergalactic gas in galaxy evolution) in the nearby Universe has greatly improved due to the combination of large-area galaxy redshift surveys (e.g., SDSS, 2dF), powerful multislit optical spectrographs, and high-resolution ultraviolet spectrographs (e.g., STIS and FUSE). UV spectroscopy of low$-z$ QSO absorption lines enables measurements of the distribution, physical conditions, and metal enrichment of baryons in the intergalactic medium, and combined with deep galaxy redshift surveys, the connections between the absorbers and galaxies/environment can be probed. This talk will review recent observations of low$-z$ absorbers and their environments. The first part of the talk will present examples of environments where intergalactic H I *does* survive, including X-ray bright galaxy groups as well as lower-density field regions, and the second part of the talk will discuss environments where H I *does not* survive due to processes such as ram-pressure and/or tidal stripping. The talk will also comment on measurements of the baryonic content, physical conditions, and metal enrichment of the low$-z$ IGM.

The figures present examples of absorption systems that will be discussed. Figure 1 shows a cluster of low-N(H I) Lyα absorption lines associated with a large-scale filament/sheet in a region near several Abell clusters (Aracil et al. 2006, MNRAS, 367, 139). This Lyα cluster arises in an intrafilament region and has high metallicity, but the nearest galaxy is > 135 kpc away. Here is the gas is highly ionized and may be ablating away. Figures 2-3 display a damped Lyα absorber/LSB galaxy that has a large H I envelope that survives despite being located in a region of high galaxy density (Rosenberg et al. 2006, AJ, 132, 478). Finally, Figure 4 shows the possible final fate of intergalactic gas: highly ionized O VI absorbers that are metal enriched, contain very little H I, and are (in some cases) far from luminous galaxies (Tripp et al. 2006, ApJ, 643, L77). With the deployment of COS next year, similar studies will become possible with substantially larger samples.

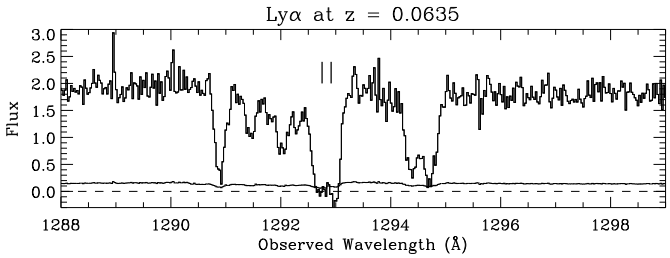

Figure 1: Lyα absorption cluster spread over $\approx$1000 km s^{-1} at $z_{\rm abs} = 0.0635$. These lines are located in a large-scale galaxy filament, and the central components (marked with two tick marks) are significantly metal enriched (see Aracil, Tripp et al. 2006, MNRAS, 367, 139).

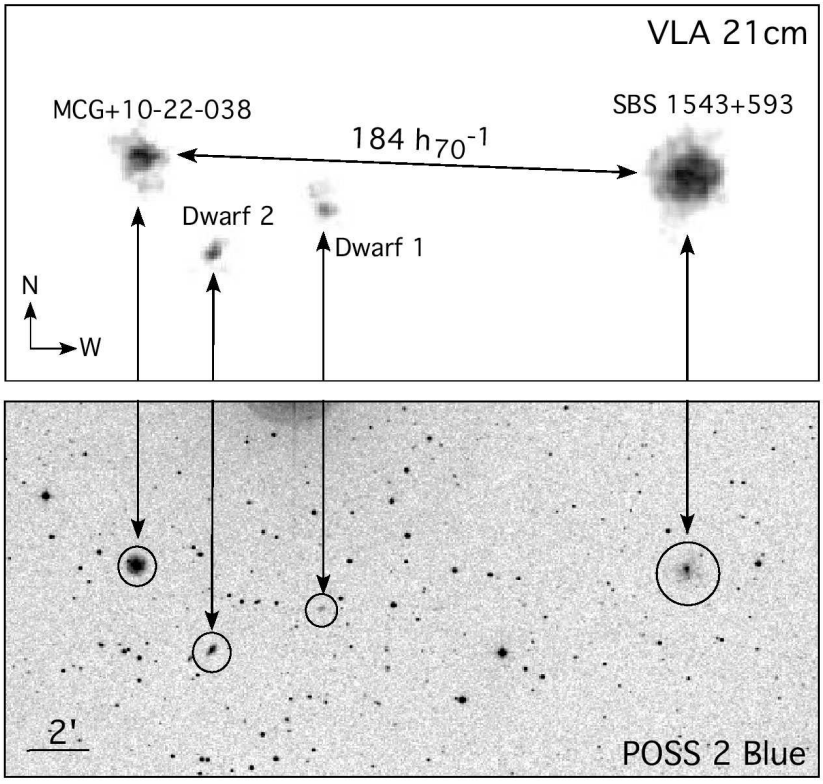

Figure 2: The low$-z$ damped Lyα absorber SBS1543+593 (galaxy at far right) imaged in the optical (lower panel, from POSS2 blue image) and in 21 cm emission (upper panel, from the VLA; see Rosenberg, Bowen, Tripp, & Brinks 2006, AJ, 132, 478).

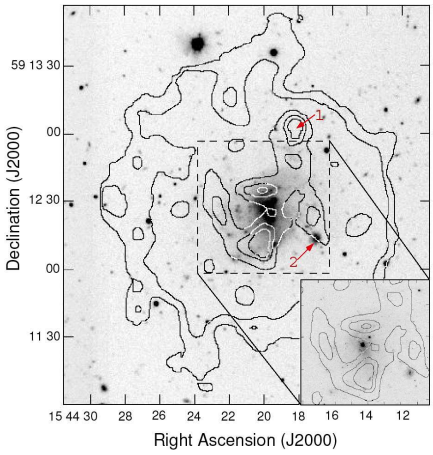

Figure 3: 21 cm emission map (lowest contour = 2×10^{20} cm^{-2}) overplotted on a grayscale image of the DLA SBS1543+593 (see Rosenberg et al. 2006).

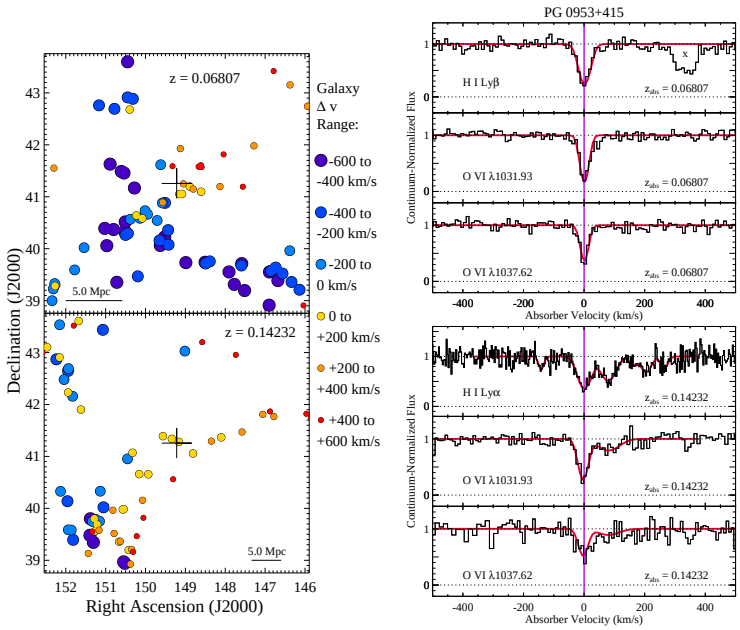

Figure 4: Right: SDSS map of galaxies near O VI absorbers at $z = 0.06807$ (top) and 0.14232 (bottom); symbol sizes indicate $\Delta v = z_{\rm galaxy} - z_{\rm abs}$ (see legend). Left: O VI and H I absorption lines associated with these large-scale structures (see Tripp, Aracil, Bowen, & Jenkins 2006, ApJ, 643, L77).

Probing the Universe with QSO Damped Lyman-Alpha Absorbers

David Turnshek

Department of Physics and Astronomy, University of Pittsburgh, USA

Results from surveys for QSO damped Lyman-alpha (DLA) absorbers are summarized. We discuss correlations between the measured properties of DLAs and how well DLAs sample the cosmic properties of the Universe: neutral-gas budget, molecular-gas budget, star formation history, and metal abundances.

Constraining dark matter through 21cm observations

Marcos Valdes

SISSA/International School for Advanced Studies, Italy

Beyond reionization epoch cosmic hydrogen is neutral and can be directly observed through its 21 cm signal. An analysis of the features of HI 21 cm maps from the so called Dark Ages could allow to put constrains on the existence and nature of decaying and annihilating Dark Matter (DM). In fact, if DM actually decays or annihilates, the injection of high energy photons into the IGM would heat and ionize the neutral gas, leaving an imprint on the 21 cm background signal which could be directly observed. We calculate the effects on HI 21 cm line signal produced by two among the most popular low mass DM candidates, i.e. LDM (we select a 10 MeV mass) and sterile neutrinos (25 keV). In the case of sterile neutrinos only the decay process is allowed; LDM particles instead can both decay and annihilate. We neglect heavier DM candidates (with mass larger than 100 MeV) because previous studies have already shown that, even assuming that all the energy released following annihilations is immediately absorbed by the IGM, they represent a negligible heating/ionization source for the gas. A detailed physical calculation of the fraction of the energy from DM decays/annihilations which is absorbed by the IGM accounts for effects on the ionized fraction and gas temperature which are considerably smaller than found by previous studies. Nevertheless we conclude that combined observations of the 21 cm background and of its gradient should be able to put constrains at least on LDM candidates. In fact, LDM decays (an- nihilations) induce differential brightness temperature variations with respect to the non decaying/annihilating DM case up to 8 (22) mK at about 50 (15) MHz. In principle this signal could be detected both by current single dish radio telescopes and future facilities as LOFAR; however, this assumes that ionospheric, interference and foreground issues can be properly taken care of.

Gas in the outer part of galaxies.

Jacqueline van Gorkom

Columbia University, USA

Where do galaxies end? In neutral hydrogen we can not even predict how far the gaseous disk extends by looking at an optical image. An easier question might be to ask what we expect for the gaseous disk in different stages of galaxy evolution. In current models of galaxy formation galaxies grow by merging. In the merger of two gas rich galaxies a new gaseous disk may form. As the galaxies grow the gaseous disk becomes less important and eventually mergers occur between gas poor, spheroid dominated, systems in which no further star formation occurs. These are called dry mergers.

In my talk I will look how this scenario compares with observations. Are red mergers dry, not necessarily. When do wet mergers form a new disk, why don't they all? The next question is what is the fate of the gaseous disk. I will show observations of gaseous disks in a wide range of environments that are undergoing trauma, some may be disappearing, others may still be growing. An additional and equally interesting question will be asked: where do clusters of galaxies end? The impact of the clusters extends much further than previously thought and it is seen to affect the fate of gaseous disks in more than one way.

The birth of HI in the dark age of World War II

Hugo van Woerden

Kapteyn Astronomical Institute, University of Groningen, The Netherlands

The history of HI goes back to 15 April 1944, when H.C. van de Hulst predicted the existence of the hyperfine transition in the ground state of neutral atomic hydrogen, at 21 cm wavelength. The existence of a spectral line at radio wavelengths, where interstellar extinction would be negligible, raised Oort's hope to unravel the structure of the Milky Way galaxy. Lack of equipment and experience delayed observations of the 21-cm line till 1951, when Ewen and Purcell at Harvard made the first detection, soon followed by Muller and Oort at Kootwijk. By 1957, the spiral structure of the Galaxy had been mapped, distribution and motions of HI measured in several galaxies, and physical properties of HI clouds determined.

My paper traces the development of HI research from the key question asked in January 1944 to its prominent role in interstellar, Galactic and extragalactic astronomy in the fifties and sixties (and thereafter).

Ultra-deep Westerbork HI observations of galaxy clusters at z=0.2

Marc Verheijen

University of Groningen / Kapteyn Astronomical Institute, The Netherlands

We report first results from ongoing ultra-deep HI observations of two galaxy clusters at z=0.2 and the large scale structure in which they are embedded. Of particular interest is the gas content of the blue galaxy population in the massive, lensing Butcher-Oemler cluster Abell 963 in relation to that of the galaxy population in the surrounding field. A total of 39 galaxies have been detected so far, with an interesting upper limit for a statistical non-detection of the blue B-O galaxies. The highest redshift HI emission detected to date originates from a system at z=0.224.

The Lyman-α Forest as a probe of Cosmplogy and Fundamental Physics

Matteo Viel[1,2]

[1] INAF-Osservatorio Astronomico di Trieste, via G.B. Tiepolo 11, I-34131 Trieste, Italy
[2] INFN/National Institute for Nuclear Physics, via Valerio 2, I-34127 Trieste, Italy

Context: The Lyman-α forest is a reliable tracer of the underlying dark matter distribution at redshifts ($z = 2 - 5.5$) and scales (1-80 comoving Mpc/h) not probed by other observables. Ten years ago, in 1997, Bi & Davidsen showed that when the simple physics of photo-ionized Lyman-α clouds is incorporated into a ΛCDM cosmological model of structure formation, many observable properties of the forest can be reproduced. Since then, significant progress has been made with accurate high resolution hydro-dynamical numerical simulations and thanks to the new data sets available (SDSS and high resolution spectra).

Aims: In my talk, I will underline the cosmological significance of the Lyman-α forest as a probe of the statistical properties of the dark matter density field. I will show how constraints on the dark matter power spectrum (amplitude, shape and curvature) can be obtained and how this measurement offers unique perspectives for fundamental physics such as neutrino masses and nature, inflation and the small scale properties of the dark matter component.

Results: I will summarize the results in terms of cosmological parameters with a particular emphasis to the sinergies with other observables such as the cosmic microwave background and weak lensing surveys. Furthermore, with the help of high redshift high resolution data I will try to answer the following question: "How cold is cold dark matter ?"

N(HI) versus Metallicity at $z \simeq 3$: Comparison of SPH cosmological simulations with observations of absorption systems

Giovanni Vladilo

Osservatorio Astronomico di Trieste, INAF, Trieste, Italy

Context: Damped Lyman α (DLA) systems are the densest concentrations of neutral gas observed as quasar absorption systems and represent one of the best probes of structure formation in the early Universe. The statistical distribution of DLA systems in HI column density and metallicity conveys information on galaxy formation, star formation, and galactic/IGM interactions at early cosmic epochs. Cosmological simulations with detailed microphysics and galaxy formation have started to yield predictions of the HI-Z distribution in DLA systems (Cen et al. 2003, ApJ, 598, 741), attaining a sub-galactic resolution appropriate for comparison with the observations (Nagamine, Springel & Hernquist 2004, MNRAS, 348, 421).

Aims: A method is presented for converting the DLA HI-metallicity distribution predicted by cosmological simulations into a simulated magnitude-limited survey of quasar absorbers. The effect of dust extinction is taken into account by using a relation between extinction and metal column density calibrated at high redshift (Vladilo et al. 2006, A&A, 454, 151). Also detection limits of metal lines, typical of real surveys, are taken into account.

Results: The detailed comparison with the observations evidentiates the risk of selection effects and gives indications for improving the physical ingredients of the simulations. The method is applied to test the results of new SPH hydrodynamical simulations with an improved description of the chemical enrichment.

Hot and cold gas around nearby galaxies

B.P. Wakker[1], B.D. Savage[1], K.R. Sembach[2], A.J. Fox[3], D.G. York[4], R. Wilhelm[5], J.C. Barentine [6], T.C. Beers[7], P. Richter[8]

[1] University of Wisconsin-Madison, [2] Space Telescope Science Institute, [3] Institut Astrophysique de Paris, [4] University of Chicago, [5] Texas Tech University [6] University of Texas [7] Michigan State University [8] Universität Postdam

Summary: Galaxies are surrounded by large gaseous halos. For the Milky Way observational evidence for this gas comes in several forms, including the high-velocity clouds seen in 21-cm HI emission and OVI absorption. We describe our recent determinations of distances to HVCs, the kinematical evidence that suggests that the Milky Way is surrounded by a population of clouds out to about 200 kpc, and our FUSE/HST survey of HI and OVI absorption around many nearby galaxies.

High-velocity clouds: High-velocity clouds (HVCs) are defined as clouds with velocities that are incompatible with differential galactic rotation, which in practice means $|v_{\rm LSR}|$>50 km s^{-1}. HVCs have a multiplicity of origins, and we can now link individual objects with particular origins (Wakker 2001, ApJS, 136, 463). Clouds with $|v_{\rm LSR}|$=50 to 100 km s^{-1} have near-solar metallicity and are located up to a few kpc above the Galactic plane; they sample the circulation of gas between Disk and Halo. Clouds in the Magellanic Stream have SMC-like metallicity and are explained as gas tidally extracted from the outer parts of the SMC 2 Gyr ago; other tidal streams may exist, but have not yet been identified as such. Several HVCs are found to have low metallicity, in particular the large northern clouds complex C (0.16 solar, summarized by Fox et al. 2004, ApJ, 602, 738) and complex A (∼0.1–0.3 solar). Complex C also has a subsolar N/O ratio, and high deuterium abundance (Sembach et al. 2004, ApJS, 150, 387). Distances to HVCs with $|v_{\rm LSR}|$>100 km s^{-1} have remained elusive, with only two upper limits known before last year: D=8–10 kpc for complex A (van Woerden et al. 1999, Nature 400, 138), D<8.8 kpc for cloud WW35 (Thom et al. 2006, ApJ, 638, L97).

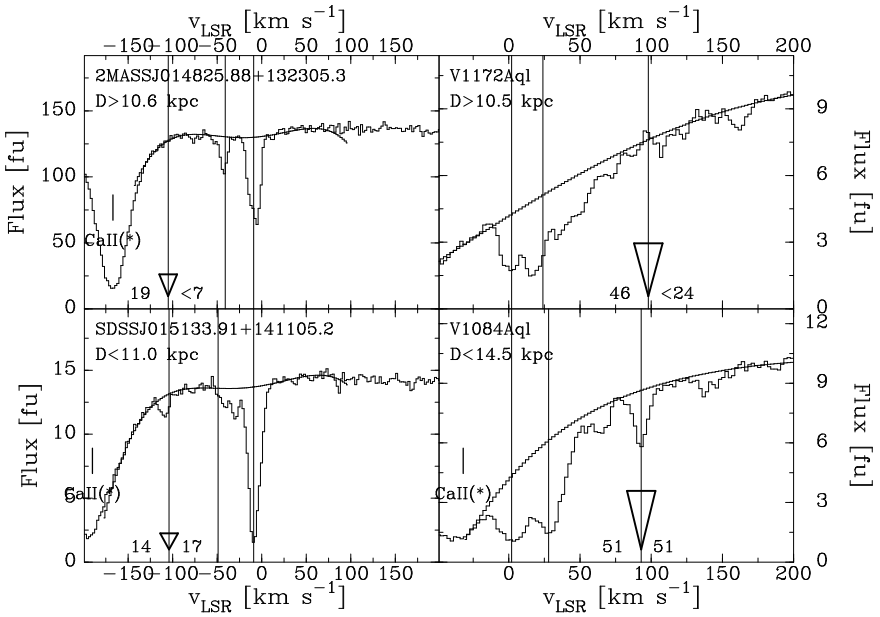

Figure 1: CaII K spectra for stars bracketing the distance to the Cohen Stream (in the Anti-Center complex; left), and complex GCP (HVC40−15+100; right). Vertical lines show the velocities of the HI emission, triangles give the expected strength of the HVC absorption lines.

We have used the photometric data in the SDSS and 2MASS surveys to identify 4000 candidate Blue Horizontal Branch and RR Lyrae stars at distances up to 100 kpc in 60 HVC fields. Using spectra provided by the SDSS, as well as additional observations at Apache Point Observatory, we have properly classified and measured distances for about 400 of these stars. Using VLT data for 24 stars we then determined distances to several HVCs (Fig. 1). The distances to complex A and the Anti-Center complex imply that they represent about 0.05 and 0.10 $M_\odot\,\mathrm{yr}^{-1}$ of accreting material. Complex C (expected distance 10–20 kpc) corresponds to 0.1–0.2 $(D/10\,\mathrm{kpc})^{-1}\ M_\odot\,\mathrm{yr}^{-1}$. Thus, these complexes contribute about 0.2–0.5 $M_\odot\,\mathrm{yr}^{-1}$ to the theoretically expected value of 1 $M_\odot\,\mathrm{yr}^{-1}$ of accreting material.

HVC kinematics: Most HVCs are less than a few degrees in diameter, so a direct distance determination using stellar probes is difficult. However, their velocity and sky distributions are best explained if there is a population of clouds whose velocities have a rotational component, an average random

velocity of $\sim$50 km s^{-1} and an average infall velocity of $\sim$50 km s^{-1}. The spatial scale of this population can only be set if it is assumed that M 31 has a similar population of clouds, in which case the scale is $\sim$200 kpc. If it were larger we would see many more HVCs in the region of the sky surrounding M 31.

HI and OVI around nearby galaxies: Using FUSE (the Far-Ultraviolet Spectroscopic Explorer) and STIS (the Space Telescope Imaging Spectrograph) we detected OVI, NV, CIV and CIII associated with almost all HVCs (Wakker et al., Savage et al., Sembach et al. 2003, ApJS, 146; Fox et al. 2006, ApJS, 165, 229). Detailed studies of the ionic ratios and the kinematics relative to HI (Fox et al. 2004, ApJ, 602, 738; 2005, 630, 332) show that these ions most likely originate in 10^5 K conductive interfaces between the cold high-velocity HI and a 10^6 K corona that extends at least as far out as the Magellanic Stream (50 kpc).

Using the RC3 and NED, we found all galaxies with v<3000 km s^{-1} and impact parameter <1 Mpc to each of 70 extragalactic targets observed with FUSE/HST. We then searched the FUSE/HST spectrum at the velocity of each galaxy and noted both detections and non-detections of HI and OVI. The main result is summarized in Fig. 2. HI absorption is found in 84 of 202 cases, OVI in 13 of 175 cases. For both ions the detection fraction decreases with impact parameter (as does the typical column density). Using the column densities of the OVI detections we estimate that the mass of the OVI producing gas is about 10^{10} $M_\odot$, assuming that: (a) OVI is 10% of total oxygen, (b) the gas has a metallicity of 0.1 solar, and (c) the fraction of area covered is proportional to the detection rate. For an infall velocity of 50 km s^{-1} this would supply new gas to galaxies at a rate of 5 $M_\odot$ yr^{-1}.

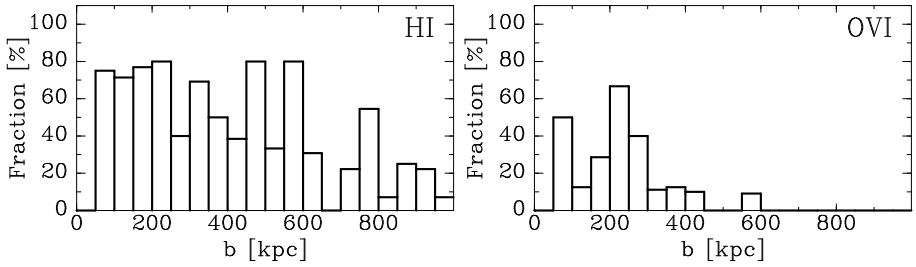

Figure 2: Plot showing the fraction of galaxies for which HI (left) or OVI (right) absorption is detected, as function of impact parameter.

Bimodality in DLAs

Arthur M. Wolfe

Department of Physics, and Center for Astrophysics and Space Sciences;
University of California, San Diego; 9500 Gilman Dr.
La Jolla; CA 92093-0424

Damped Lyα absorption systems (DLAs) comprise a population of objects that serve as neutral gas reservoirs for star formation at high redshifts, and as a result are crucial for understanding galaxy evolution and formation (e.g. Nagamine et al. 2004). On the other hand, the identity of high-z DLAs remains largely unknown. Although absorption-line data provide accurate measures of the H I column-density distribution function $f_{\rm HI}(N,X)$ and its moments, metallicity, dust content, cooling rates, etc., they do not reveal properties essential for identification such as mass, size, and morphology. For this purpose one must detect DLAs in emission. But since only a few high-z DLAs have been detected in emission (Møller et al. 2002; 2004), the current evidence is contradictory. Thus, while the strength of the cross-correlation function between DLAs and Lyman Break Galaxies (LBGs; Cooke et al. 2006) and the large median absorption-line velocity width suggest that DLAs reside in dark-matter halos with median mass $M_{\rm DM}^{\rm med}{\sim}10^{12}{\rm M}_\odot$ (Nagamine et al. 2007; Razoumov et al. 2006), the large area covering factor of DLAs is more naturally explained within the context of ΛCDM models by the numerous halos predicted with $M_{\rm DM}^{\rm med}{\leq}10^{10}{\rm M}_\odot$ (Haehnelt et al. 1998).

My purpose here is to present new evidence that sheds light on the nature of high-z DLAs. Specifically, I shall describe evidence for two distinct populations. The crucial parameter is the [C II] 158 μm cooling rate per H atom, ℓ_c, which divides the DLA sample in such a way that objects with $\ell_c > \ell_c^{\rm crit}$ differ fundamentally from those with $\ell_c < \ell_c^{\rm crit}$, where $\ell_c^{\rm crit} \equiv 10^{-27}$ ergs s^{-1} H^{-1}. The significance of $\ell_c^{\rm crit}$ follows from earlier work (Wolfe, Prochaska, & Gawiser 2003 [WPG03]; Wolfe, Gawiser, & Prochaska 2003 [WGP03]) in which we found that grain photoelectric heating by FUV radiation is the most plausible heat source to balance cooling in DLAs with $\ell_c > \ell_c^{\rm crit}$. Wolfe et al. (2004; WHGPL) then argued that 158 μm cooling in DLAs with $\ell_c < \ell_c^{\rm crit}$ arises in warm neutral medium (WNM) gas heated by soft X-ray and FUV background radiation. However, they could not exclude the possibility that such gas is also heated by radiation generated within the DLA. On the other hand, background heating is insufficient to balance cooling in DLAs with $\ell_c > \ell_c^{\rm crit}$. These DLAs are plausibly heated by locally generated

FUV radiation. Furthermore, 158 μm cooling in these DLAs arises in cold neutral medium (CNM) gas.

These results have implications for the mode of star formation in DLAs. WGP03 showed that the local FUV intensities needed to achieve thermal balance in DLAs with $\ell_c > \ell_c^{\rm crit}$ imply comoving star formation rate (SFR) densities, $\dot{\rho_*}$, comparable to $\dot{\rho_*}$ deduced for Lyman Break Galaxies (LBGs; Steidel et al. 2003); i.e. $\dot{\rho_*} \approx 10^{-1.5}$ to $10^{-0.8}$ $M_\odot$ yr^{-1} Mpc^{-3}. This suggests one of two possibilities: either DLAs with $\ell_c > \ell_c^{\rm crit}$ are physically associated with LBGs (Møller et al. 2002) or the similar values of $\dot{\rho_*}$ indicate a numerical coincidence. If these DLAs are *not* associated with LBGs, then *in situ* star formation throughout the neutral gas would be the predominant mode. Since the area covering factor for DLAs in the redshift interval z=]2.5,3.5] is given by C_A=0.33, in this case a significant fraction of the sky would be lit up by low surface brightness emission from spatially extended objects.

However, a recent search for such objects in the Hubble Ultra Deep Field (UDF) by Wolfe & Chen (2006: hereafter WC06) showed that such objects are rare. WC06 found that the comoving SFR density due to *in situ* star formation in DLAs is given by $\dot{\rho_*} < 10^{-2.7}$ $M_\odot$ yr^{-1} Mpc^{-3}, which corresponds to an FUV mean intensity of $J_\nu < 10^{-20}$ ergs cm^{-2} s^{-1} Hz^{-1} sr^{-1} per DLA. The implication is that FUV radiation generated by *in situ* star formation in DLAs cannot exceed the FUV background since at z= 3 the background mean intensity, $J_\nu^{\rm bkd}$ =(2−3)×10^{-20} ergs cm^{-2} s^{-1} Hz^{-1} sr^{-1} (Haardt & Madau 2003).

This result implies that *in situ* star formation is not the dominant star-formation mode in DLAs. Moreover the upper limits on J_ν show that heating due to *in situ* star formation is insufficient to balance cooling in DLAs with $\ell_c > \ell_c^{\rm crit}$ (WC06). By contrast, FUV radiation emitted by LBGs generates grain photoelectric heating that *is* sufficient to balance such cooling. For this reason WC06 suggested that these DLAs are extended neutral-gas layers heated by centrally located, compact LBGs. On the other hand since background heating can balance cooling in DLAs with $\ell_c < \ell_c^{\rm crit}$, and since the local $J_\nu < J_\nu^{\rm bkd}$, it is reasonable to conclude that DLAs with $\ell_c < \ell_c^{\rm crit}$ are heated by FUV background radiation alone.

In order to determine whether the 158 μm cooling rates divide DLAs into distinct populations we (Wolfe, Prochaska, & Jorgenson [in preparation 2007]) carried out several tests. We examined the ℓ_c distribution and I shall discuss the results of tests to assess whether the distribution is bimodal. We then divided our DLA sample into two sub-samples: objects with $\ell_c > \ell_c^{\rm crit}$ and those with $\ell_c < \ell_c^{\rm crit}$. For each sub-sample we assembled distributions of physical quantities such as absorption-line velocity width, metallicity, dust-to-gas ratio, and N(HI). We then tested whether both subsamples of a given pair can be drawn from the same parent population. Using conservative Kolmogorov-Smirnov tests we found the

probability that subsamples of velocity width, metallicity, and dust-to-gas ratio can be drawn from the same parent population is less than 10^{-4}. By contrast, subsamples of N(HI) are compatible with the null hypothesis.

Finally I shall discuss implications of these results. In particular, I describe evidence that ℓ_c is an indicator of dark-matter mass: DLAs with $\ell_c < \ell_c^{\rm crit}$ are in dark-matter halos with low masses, while object with $\ell_c > \ell_c^{\rm crit}$ are in halos with high masses. We speculate that the physical mechanism responsible for bimodality is the mode of accretion onto dark matter halos. DLAs with $\ell_c < \ell_c^{\rm crit}$ accumulate gas from the IGM in a cold accretion mode in which the gas never rises to the virial temperature of the halo, while DLAs with $\ell_c > \ell_c^{\rm crit}$ accumulate gas in a hot accretion mode (e.g. Dekel & Birnboim 2006). In this case the critical mass dividing the two masses is the 'shock mass' $M \approx 10^{11.6-12}$ M$_\odot$ (see Dekel & Birnboim 2006). Evidence for the presence of hot ($T \approx 10^6$ K) gas in DLAs stems from the recent detection of O VI absorption in a significant fraction of DLAs (Fox et al. 2007). If correct, these conclusions indicate that a significant fraction of DLAs are in massive halos, which is consistent with the Q5 numerical simulation of Nagamine et al. (2004;2007). I end by describing various tests of this hypothesis.

References:

Cooke, J., Wolfe, A. AM., Gawiser, E., & Prochaska, J. X., 2006, ApJ, 652, 994

Dekel, A., & Birnboim, Y. 2006, MNRAS, 368, 2

Fox, A. J., Petitjean, P., Ledoux, C., & Srianand, R. 2007, A&A, 465, 171

Haehnelt, M. G., Steinmetz, M. & Rauch, M. 1998, ApJ, 495, 647

Møller, P., Warren, S. J., Fall, S. M., Fynbo, J. U., & Jakobsen, P. 2002, ApJ, 574, 51

Møller, P., Fynbo, J. J. &, Fall, S. M., 2004, å, 422, L33

Nagamine, K., Springel, V., & Springel, F. 2004a, MNRAS, 350, 421

Nagamine, K., Wolfe, A. M., Hernquist, L., &Springel, V., & Springel, F. 2007, ApJ, 660, 945

Razoumov, A. O., Norman, M. L., Prochaska, J. X., & Wolfe, A. M., 2006, ApJ, 645, 55

Steidel, C. C., Adelberger, K. L., Shapley, A. E., Pettini, M., Dickinson, M., & Giavalisco, M. 2003, ApJ, 592, 728

Wolfe, A. M., & Chen, H.-W. 2006, ApJ, 652, 981

Wolfe, A. M., Gawiser, E., & Prochaska, J. X. 2003a, ApJ, 593, 235 (WGP03)

Wolfe, A. M., Prochaska, J. X., & Gawiser, E. 2003b, ApJ, 593, 215 (WPG03)

Wolfe, A. M., Howk, J. C., Gawiser, E., Prochaska, J. X., & Lopez, S. 2004, ApJ, 615, 625

Wolfe, A. M., Gawiser, E., & Prochaska, J. X. 2005, ARA&A, 43, 861

The Hardening of the UV Background near Quasars

G. Worseck[1], C. Fechner[2], L. Wisotzki[1], A. Dall'Aglio[1]

[1] Astrophysikalisches Institut Potsdam, An der Sternwarte 16, 14482 Potsdam, Germany
[2] Hamburger Sternwarte, Universität Hamburg, Gojenbergsweg 112, 21029 Hamburg, Germany

Context: In the vicinity of quasars the intergalactic medium is statistically more highly ionized due to the local enhancement of the UV flux that results in a statistically higher HI transmission ('void', Fig. 1). While this so-called proximity effect is known to exist on lines of sight towards quasars (e.g. Bajtlik et al. 1988, ApJ, 327, 570), a transverse proximity effect created by foreground quasars nearby the line of sight has not been clearly detected in the HI forest (e.g. Schirber et al. 2004, ApJ, 610, 105).

Intergalactic HeII absorption can be studied only towards the few quasars at $z > 2$ that are transparent in the far UV. Jakobsen et al. (2003, A&A, 397, 891) found a foreground quasar coinciding with a HeII void in the HeII Gunn-Peterson trough towards Q 0302−003 (Heap et al. 2000, ApJ, 534, 69), thereby presenting the first clear case of a transverse proximity effect. Moreover, due to the different ionization thresholds of HI and HeII a comparison of the absorption features yields an estimate of the fluctuating spectral shape of the intergalactic UV radiation field that is usually quantified by the column density ratio $\eta = N_{\rm HI}/N_{\rm HeII}$. (e.g. Kriss et al. 2001, Sci, 293, 1112; Fechner & Reimers 2007, A&A, 461, 847). Thereby it is possible to distinguish hard quasar radiation ($\eta < 100$) from soft radiation by star-forming galaxies ($\eta > 100$) (Haardt & Madau 1996, ApJ, 461, 20; Fardal et al. 1998, AJ, 115, 2206).

Aims: We performed a slitless spectroscopic quasar survey in the vicinity of Q 0302−003 ($z = 3.285$) and HE 2347−4342 ($z = 2.885$), two lines of sight with detectable HeII absorption. Including known quasars from the literature, seven foreground quasars can be used to study the transverse proximity effect (four near Q 0302−003 and three near HE 2347−4342). In addition to a separate analysis of the HI and the HeII absorption, we searched for

the transverse proximity effect as a fluctuation in the spectral shape of the intergalactic UV radiation field.

Results: The transverse proximity effect is generally not detected as a void in the forests (Fig. 2). Apart from the expected weakness of the effect, this is due to overdensities probably created by large-scale structure that hamper traditional searches for the proximity effect trying to link quasars to underdense regions in the forest (e.g. Rollinde et al. 2005, MNRAS, 361, 1015). However, we find that the UV radiation field in the projected vicinity of *all* foreground quasars is systematically harder than on average (Fig. 3). This effect is also visible near the central quasars in the fields (Q 0302−003 and HE 2347−4342). Due to the hard spectral energy distribution of quasars we interpret this as the proximity effect in spectral hardness acting on distances of several Mpc. We also analyzed three metal line systems towards HE 2347−4342 located near the foreground quasars and found them to be consistent with an additional ionizing contribution by the foreground quasars. The spectral hardness breaks the density degeneracy due to cosmic variance that is responsible for the frequent non-detections of the transverse proximity effect. Therefore it is a sensitive *physical* measure to reveal the transverse proximity effect even in intrinsically overdense regions or in cases where the local quasar radiation only marginally exceeds the UV background. From the transverse proximity effect of the foreground QSOs, we infer QSO lifetimes of 10–30 Myr. Please consult Worseck & Wisotzki (2006, A&A, 450, 495) and Worseck et al. (arXiv:0704.0187) for detailed results on the Q 0302−003 field and the HE 2347−4342 field, respectively.

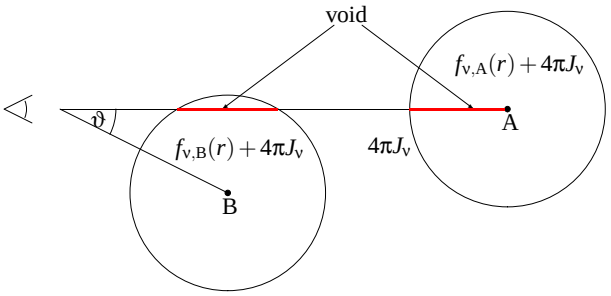

Figure 1: Illustration of the proximity effect. Quasar A and foreground quasar B locally enhance the UV background J_ν and create an underdensity in the Lyα forest with respect to the average absorption at that redshift.

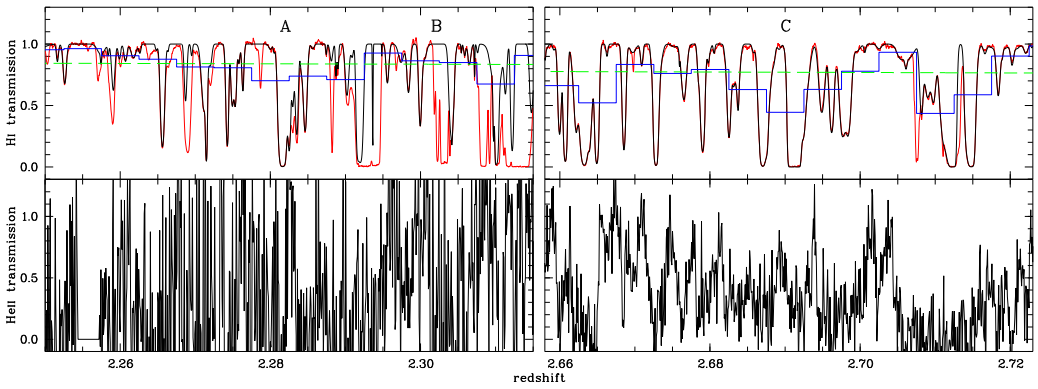

Figure 2: The Lyα forest of HE 2347−4342 in the vicinity of three foreground quasars at $z = 2.282$, $z = 2.302$ and $z = 2.690$, dubbed QSO A, B and C. The upper panels show the observed optical spectrum (red), the HI transmission (black), the mean transmission towards HE 2347−4342 (binned line) and expected mean transmission (dashed line). The lower panels display the corresponding HeII transmission. We do not detect a significant underdensity that may indicate the transverse proximity effect.

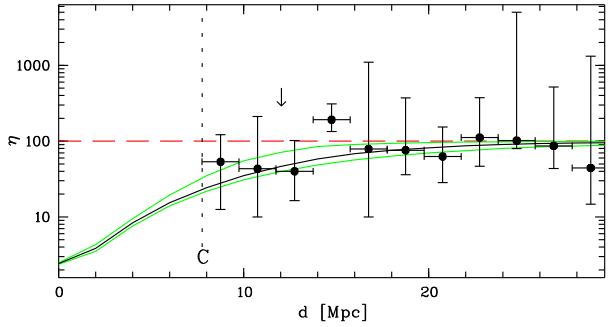

Figure 3: Binned column density ratio $\eta = N_{\rm HI}/N_{\rm HeII}$ vs. proper distance d between HE 2347−4342 and QSO C (points). The minimum separation between the two QSOs is 7.75 Mpc in the cosmological concordance model. Hard radiation corresponds to small η. The black line shows the modelled decrease of η approaching QSO C with respect to the ambient soft UV background with $\eta \sim 100$ (dashed line). Near the quasar the radiation field is harder than on average despite large small-scale fluctuations. The arrow marks a metal line system at $z = 2.7122$ that is consistent with being ionized by the UV background with an additional quasar component.

Redshifted 21cm Emission and the Reionization History

Stuart Wyithe[1], Miguel Morales[2], Avi Loeb[3] & Paul Geil[1]

[1] School of Physics, University of Melbourne, Australia
[2] Kavli Institute, Massachusetts Institute of Technology, USA
[3] Department of Astronomy, Harvard University, USA

Context: Spatial dependence in the statistics of redshifted 21cm fluctuations, and direct imaging of large HII regions promise to provide the most powerful probes of the reionization epoch. In this talk we consider the utility of both avenues.

Results: Firstly we discuss the second and third moments of the redshifted 21cm intensity distribution using a simple model that accounts for galaxy bias during the reionization process. We find that skewness in redshifted 21cm maps should be substantial throughout the reionization epoch and on all angular scales, owing to the effects of galaxy bias which leads to early reionization in over-dense regions of the IGM. We also find that the variance (or power-spectrum) of 21cm fluctuations will exhibit a minimum in redshift part way through the reionization process, when the global ionization fraction is around 50%. This minimum is generic, and is due to the transition from 21cm intensity being dominated by over-dense too under-dense regions as reionization progresses.

Examples of the evolution of the variance and skewness in redshifted 21cm intensity maps are illustrated in Figure 1. We find that the evolution of the variance and skewness in 21cm intensity maps with redshift and mean neutral fraction will probe physical quantities like the clumping of the IGM and the mass of ionizing sources. In particular, reionization scenarios with smaller values of clumping factor, or more massive (and therefore more biased) ionizing sources result in 21cm intensity maps with larger values of variance and skewness. Indeed, the variation in amplitude of the auto-correlation at fixed redshift reaches an order of magnitude over the astrophysically plausible range of minimum masses. In addition, the relative locations of minima

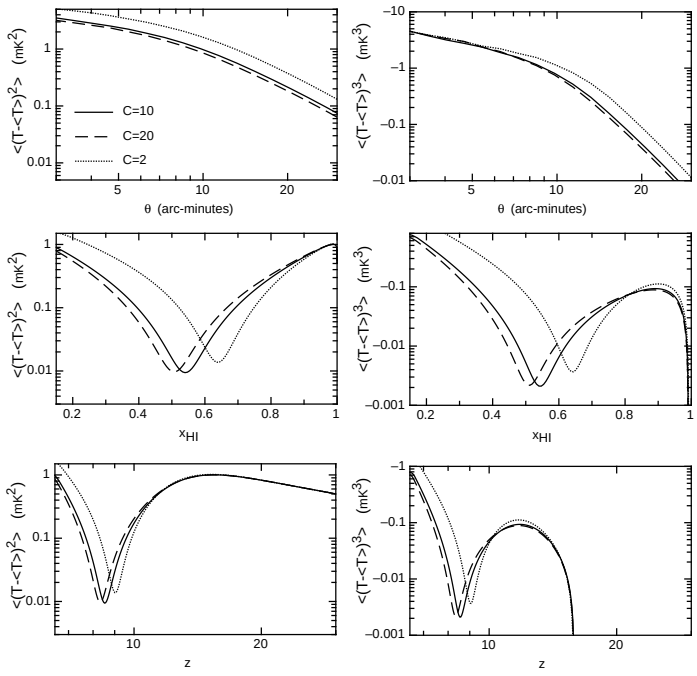

Figure 1: *Left:* Examples of auto-correlation functions, assuming sets of $(T_{\rm min}, T_{\rm ion}) = (10^4{\rm K}, 10^5{\rm K})$, $(10^4{\rm K}, 10^4{\rm K})$, $(10^5{\rm K}, 10^5{\rm K})$ and $(250{\rm K}, 10^5{\rm K})$. Here $T_{\rm min}$ and $T_{\rm ion}$ are the minimum virial temperatures for galaxy formation in neutral and ionized regions respectively. The clumping factor was chosen to be $C = 10$. The auto-correlation is plotted as a function of observed angle θ (at $z = 6.5$, *upper panel*), as a function of mean IGM neutral fraction $x_{\rm HI}$ (at $\theta = 10'$, *central panel*), and as a function of redshift (at $\theta = 10'$, *lower panel*). *Right:* Corresponding examples of skewness functions.

in variance and skewness when plotted as functions of redshift and neutral fraction can be used to distinguish between amplitudes that are increased due to large values of ionizing source mass, or small values of clumping factor. While more massive sources increase the amplitude of fluctuations at all epochs, the signature of radiative feedback is the suppression of fluctuations at epochs following, but not prior to the substantial reionization of the IGM. We therefore conclude that the detection of fluctuations in 21cm intensity should unambiguously determine the mass of ionizing sources. In summary, the details of the reionization history, including the presence of radiative feedback are encoded in the evolution of the auto-correlation and skewness

functions with redshift and mean IGM neutral fraction. The amplitudes of fluctuations are particularly sensitive to the masses of ionizing sources, and vary by an order of magnitude for astrophysically plausible models.

We discuss the detection of skewness by first generation instruments. From our simple estimates we conclude that the Mileura Widefield Array–Low Frequency Demonstrator will have sufficient sensitivity to detect skewness on a range of angular scales at redshifts near the end of reionization, while a subsequent instrument of 10 times the collecting area could map out the evolution of skewness in detail. The observation of a minimum in variance during the reionization history, and the detection of skewness would both provide important confirmation of the cosmological origin of redshifted 21cm intensity fluctuations.

We next discuss the expected cross-correlation between the distribution of galaxies and intergalactic 21cm emission at high redshifts. The early reionization of over-dense regions leads to an anti-correlation between the 21cm emission and the over densities in galaxies, matter, and neutral hydrogen. Existing Lyα surveys probe galaxies that are highly clustered in over-dense regions. By comparing 21cm emission from regions near observed galaxies to those away from observed galaxies, observations using instruments like the Mileura Widefield Array–Low Frequency Demonstrator will be able to test the generic prediction of biased reionization.

Finally, we consider the direct observation of large HII regions surrounding luminous high redshift quasars before the end of the epoch of reionization. Our approach is to implement a semi-numerical scheme to calculate the 3 dimensional structure of ionized regions surrounding a massive halo at high redshift, including the ionizing influence of a luminous quasar. We calculate mock spectra along the line-of-sight towards the high redshift quasar, and estimate the ability of forthcoming low-frequency telescopes to detect the presence of an HII region. We find that at times when the neutral fraction is $\sim 30\%$ or greater (after which the typical HII region becomes comparable to that generated by the quasar), the quasar will imprint a detectable signature that is distinct from a typical region of IGM. We find that the average level of neutral gas surrounding a single 5Mpc quasar HII region will be detectable in 1000 hours, while a detection will be possible in 1000 hours for a stack of 10 smaller 3Mpc HII regions.

The LOFAR Epoch of Reionization datacube

Saleem Zaroubi

Kapteyn Astronomical Institute, The Netherlands

LOFAR the Epoch of Reionization (EoR) project will measure the HI distribution in the Universe in the redshift range 6-11.5 within several windows of 5×5 degrees^2 with resolution of 3-5 arcminutes. The level of the expected signal is of the order of 1-10 mK. Unfortunately the signal is contaminated by a number of galactic and extra-galactic foregrounds that have a much larger brightness temperature, severe ionospheric distortions and instrument response and noise. The signal, contaminants and instrumental response will constitute the so called datacube. In this talk, I will review the simulation pipeline that we have set in the LOFAR EoR project and present results from extensive simulations of the various component of the datacube.

The main purpose of the these simulations is to test our observational strategy, estimate the data calibration accuracy one needs to reach, test the cosmological signal extraction algorithms adopted by the project and finally estimate the what we can learn from the data about the cosmological signal in the various stages of the project.

Furthermore, I discuss some of the inversion algorithm we employ for the signal extraction step and show preliminary results from applying it to simulations.

This talk is a complementary talk to the one presented by Ger de Bruyn in this meeting.

Optical properties and spatial distribution of MgII absorbers from SDSS image stacking

Stefano Zibetti[1] **& Brice Ménard**[2]

[1] Max-Planck-Institut für extraterrestrische Physik - Garching - Germany,
[2] C.I.T.A. University of Toronto - Canada

Context: Absorption line systems observed in the spectra of distant QSOs represent an invaluable source of information about the distribution and the physical properties of the gas through cosmic times. Understanding the link between these systems and their luminous counterparts (i.e., the galaxies in which they are hosted or are associated to) is a key task for the comprehension of galaxy formation and evolution.
So far such investigations required expensive spectroscopic follow-ups to identify absorbing galaxies and only allowed the analysis of small samples (N<50). The advent of the SDSS in recent years has provided the community with huge samples of absorption systems. While offering unprecedented statistical power, these samples challenge traditional analysis techniques and require new approaches in order to be fully exploited.

We use a sample of more than 2800 QSO absorbing systems detected from the MgII absorption doublet ($\lambda\lambda 2796, 2803$) in the SDSS spectra of distant QSO (Nestor et al. 2005). This sample covers the absorption redshift interval between 0.37 and 1, while the absorption strength in terms of rest-frame equivalent width of the 2796Å line, $W_0(2796)$, varies between 0.8 and 5 Å.

Aims: Our work aims at establishing possible relationships between absorbing gas properties (namely the absorption strength W_0) and the properties of the galaxies that are associated to such absorbers, in particular the galaxy luminosity and spectral energy distribution (SED) and its impact parameter. From these relationships we attempt to infer a viable physical scenario for the origins of (MgII) absorbers.

The size of our sample and the limited depth of the SDSS imaging and spectroscopy make it impossible a detailed study of individual absorbing galaxies, but enables us to apply a statistical technique (first introduced by Zibetti et al. 2005) to establish robust average relationships between galaxies and absorbers. The simple idea behind the method is the following: if absorbers are related to galaxies, on average we expect an overdensity of

galaxies around absorbed QSOs with respect to random lines of sight. While the shot noise due to random background galaxies is too high to measure this effect around individual systems, by stacking several hundreds of absorbed lines of sight the signal is strong enough to be measured (as already demonstrated by Zibetti et al. 2005). Noticeably, our method does not rely on any assumption on the number, luminosity and impact parameter of the absorbing galaxies. In practice, the images in four bands (g, r, i, and z) of the absorbed QSOs are stacked after removing the light of the QSOs, modeled as a PSF. Bright foreground sources are also masked out. The resulting smooth surface brightness distribution around the QSO center is then checked and corrected for systematic effects by comparing with a matched sample of unabsorbed QSOs. This photometric information can be used to constrain the impact parameter distribution of the absorbing galaxies, as well as their luminosity at different wavelengths. A crucial point in the analysis and a big advantage of our large sample is the possibility of splitting it according to different absorber's redshift and strength to gain insight into time evolution aspects and different physical regimes.

Results: The results of this analysis are extensively reported in Zibetti et al. (2007, ApJ, 658, 161). Here we briefly summarize the main ones. In Figure 1 the image resulting from the stacking of 600 absorbed lines of

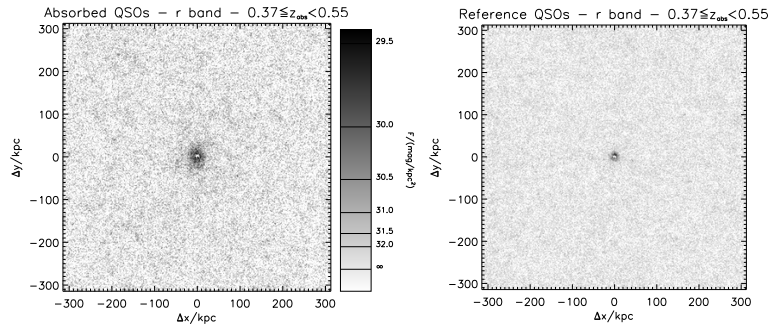

Figure 1: The stack of 600 low-redshift absorbers lines of sight (*left*) shows a clear surface brightness excess with respect to the stack of the control sample (2400 lines of sight, *right*). In both images, the light of the QSOs has been subtracted. The residuals that still remain around the unabsorbed QSOs is due to the QSO host galaxies.

sight in the lowest redshift bin (*left*) is contrasted with the stacked images

of 2400 unabsorbed ones (derived from the matched QSO control sample, on the *right*). The luminosity excess in the absorbed sample is clearly apparent. We demonstrate that the SB profile of this excess can be converted into the luminosity weighted impact parameter distribution of absorbing galaxies. Also, we compare the measured fluxes with expectations for different SED templates, as they would be observed in the stacked photometry, to infer the average luminosity and SED in different subsamples. Our main results are:
i) At $z \sim 0.4$, the average luminosity of a MgII system is 0.5 $L_g^\star$.
ii) Strong MgII absorbers ($W_0 > 1$ Å) probe galaxies with an average impact parameter $\sim$ 40 kpc and stronger systems probe smaller radii (confirming with high statistical significance the trend marginally detected by Steidel et al. 1995).
iii) While the light of weaker absorbers originates mostly from red passive galaxies, stronger systems display the colors of blue star-forming galaxies (see Fig. 2).
iv) Interestingly, no significant evolution for both impact parameter and rest-frame colors is observed from z 0.4 to z=1, but the average luminosity increases by $\sim$50%.

From these new results we argue that MgII absorbers are linked to metal-enriched gas outflows from star-forming/bursting galaxies and witness an evolutionary phase that more massive galaxies experience earlier than less massive ones, in a downsizing fashion.

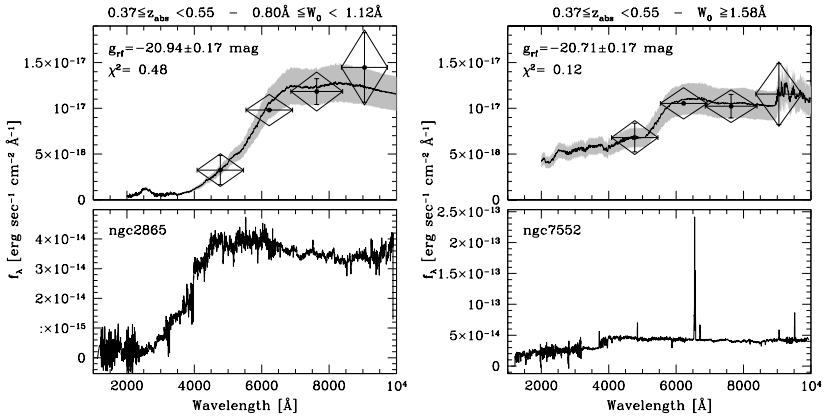

Figure 2: The best fitting SED templates (*bottom* panels) are "stacked" and compared to the observed fluxes (points, *top* panels), for low-EW (*left*) and high-EW absorbers (*right*).

Comparing gas in galaxies and DLAs

Martin Zwaan

ESO, Germany

In the local Universe we can study the gaseous properties of galaxies in detail. We know how the local cold gas reservoir is distributed amongst galaxies (The HI mass function) and how it is distributed within galaxies. At higher redshifts we only have information on cold gas measured along very thin sightlines towards bright background sources. In this talk I compare the data at z=0 with that from higher redshifts, and discuss what this teaches us about the evolution of the Universe's cold gas content.